

## TABLE OF CONTENTS

### 1. GENERAL INFORMATION

- 1.1 INTRODUCTION
- 1.2 DESCRIPTION OF OPERATION
- 1.3 SPECIFICATIONS
- 1.4 OPTIONAL EQUIPMENT

### 2. INSTALLATION

- 2.1 INTRODUCTION
- 2.2 INITIAL INSPECTION AND UNPACKING
- 2.3 POWER REQUIREMENTS
- 2.4 POWER CORDS AND RECEPTACLES
- 2.5 GROUNDING REQUIREMENTS
- 2.6 ENVIRONMENTAL REQUIREMENTS
- 2.7 INSTALLATION AND ASSEMBLY
- 2.8 REPACKAGING FOR SHIPMENT

### 3. OPERATING INSTRUCTIONS

- 3.1 INTRODUCTION
- 3.2 CONTROLS
- 3.3 MAKING A MEASUREMENT USING STANDARD COLLOID
- 3.4 SAMPLE PREPARATION
- 3.5 CHECKLIST FOR MAKING MEASUREMENTS FOR  
EXPERIENCED USER

### 4. OPERATING INSTRUCTIONS FOR USE OF AUTOMATIC TRANSFER MODULE (ATM)

### 5. THEORY OF OPERATION

### 6. MAINTENANCE

### 7. SERVICE

## 1. GENERAL INFORMATION

### 1.1 INTRODUCTION

Your new Laser Zee<sup>tm</sup> Model 500 is a sophisticated instrument for determining the electrostatic charge (zeta potential) of small solid particles dispersed in water. A mixture of such particles and water is referred to as a "colloid." Most colloids in nature have a negative charge. The magnitude of this charge (or zeta potential) determines the stability of the colloid. A stable colloid is one in which the colloid particles remain separate and distinct (dispersed). An unstable colloid is characterized by particles that gradually agglomerate. If the charge on the particles is high, the particles repel one another and the colloid is stable. If the charge is near zero, the random motion (Brownian Movement) of the particles causes them to collide and to become attached to one another. See Table 1.

In some cases, it is desirable to maximize the particle charge in order to achieve greatest stability. Paints, pharmaceuticals, and cosmetics are a few examples. In other cases, it is necessary to minimize the charge, as for example, in waste water treatment and paper manufacture. In all cases, the Laser Zee<sup>tm</sup> Model 500 can be a very effective tool in determining the proper level of chemical additives to achieve optimum control of zeta potential.

TABLE 1

<u>Stability Characteristics</u>	<u>Zeta Potential (mV)</u>
Strong Agglomeration	+ 5 to - 5
Incipient Instability	- 10 to - 30
Moderate Stability	- 31 to - 40
Good Stability	- 41 to - 60
Excellent Stability	- 61 upwards

## 1.2 DESCRIPTION OF OPERATION

Your Laser Zee<sup>tm</sup> Model 500 measures the zeta potential of colloidal particles by determining the rate at which these particles move in a known electric field. The technique is referred to as electrophoresis. Since the particles are observed with a microscope, it is common to refer to this method as micro-electrophoresis.

The colloid to be measured is placed in an electrophoresis chamber consisting of two electrode compartments and a connecting chamber. A voltage is applied between two electrodes, one located in each compartment. The applied voltage produces a uniform electric field in the connecting chamber and the charged particles respond by moving toward one or the other electrode. The direction of movement is determined by the sign of the charge --positively charged particles migrate toward the cathode (the negative electrode) and conversely, negative particles migrate toward the anode (the positive electrode). The speed of the particles is directly proportional to the magnitude of the particle charge or zeta potential.

In principle, one determines the magnitude and sign of the colloid charge by observing the speed and direction of the particle movement under the influence of the applied field. However, there is one important complicating factor. When the voltage is applied, not only do the particles move with respect to the fluid but, in addition, the fluid moves with respect to the chamber. This second effect is referred to as electroosmosis and is characterized by a movement of the fluid in one direction near the surface of the viewing chamber walls, accompanied by a return flow in the opposite direction in the center of the viewing chamber. Obviously, there must be a surface where the fluid is stationary and this surface is called the stationary layer. All measurements must be made at this stationary layer or errors due to the fluid movement will occur.

Your Laser Zee<sup>tm</sup> Model 500 provides two means for insuring that the measurements are made at the stationary layer. First, the microscope used to view the particles has a sharp depth of focus and once the microscope is focused on the stationary layer, particles above or below are out of focus and therefore not visible. (A Calibration Constant is provided which enables the operator to easily focus on the stationary layer. Its use is explained in a later section.

Once the microscope and laser are focused at the correct level, a zeta potential measurement can be made by observing the magnitude and direction of the particle movement in the presence of the applied field. Conventional instruments accomplish this by using a stopwatch to time particles between reference grid lines in a microscope eyepiece. Typically, 20 to 50 particles are timed and the results averaged to obtain one zeta potential determination. Your Laser Zee<sup>tm</sup> Model 500 is at least ten times easier to use than conventional instruments since typically only one measurement is required. The simplified measurement is made possible by a unique patented prism technique that makes the moving particles appear stationary. The prism is located inside the microscope interposed between the objective lens and the eyepiece. The prism is mounted on a galvanometer which causes the prism to repeatedly rotate a few degrees and then flip back to start another cycle. The effect of this motion is to cause the image viewed through the microscope to repeatedly scan in one direction and then reset. The rate and direction of the prism motion can be adjusted by the operator. A zeta potential measurement is made by adjusting the prism control until the apparent motion caused by the prism exactly cancels the particle velocity caused by the applied field. At this point, the particles appear stationary in the field of view, and the zeta potential is displayed on a digital readout on the front panel.

The zeta potential reading is independent of the applied voltage which is derived from a supply that can be varied from 0 to 400 volts. The electrode voltage can be displayed as a digital readout by pushing the appropriate panel buttons. Panel buttons are also provided for the digital display of the specific conductance and temperature of the sample.

The electronics is completely solid state with the exception of the laser tube and a small incandescent lamp used for reticle illumination. The design takes advantage of the latest state-of-the-art components and employs integrated circuits exclusively, in order to obtain an unusually high degree of reliability and ruggedness.

The four printed circuit boards, each with a specific group of functions, are provided with test points so that, in the unlikely event of a malfunction, a technician can easily determine which board is defective. Replacement boards are simply installed.

### 1.3 SPECIFICATIONS

Table 1-2 is a complete list of the Model 500 specifications.  
Table 1-3 contains additional information of general interest.

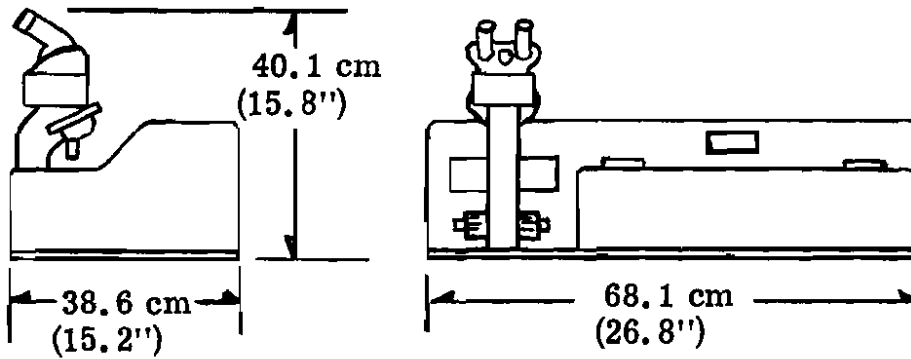
Table 1-2  
SPECIFICATIONS

<u>Readout Parameter</u>	<u>Range</u>	<u>Accuracy</u>
Zeta Potential	- 100 to + 100 mV *	$\pm 5\% \pm 1 \text{ mV}$
Mobility (Optional)	$+ 7.0 \text{ to } - 7.0 \times 10^{-4} \text{ cm}^2/\text{V-sec}^*$	$\pm 5\% \pm 0.07$
Specific Conductance		
high scale	1000 to 100,000 $\mu\text{ mhos/cm}$	$\pm 10\% \pm 100 \mu\text{ mhos/cm}$
low scale	1 to 1000 $\mu\text{ mhos/cm}$	$\pm 10\% \pm 1 \mu\text{ mhos/cm}$
Temperature	$+ 10^0 \text{ to } + 40^0$	$\pm 0.5^0 \text{ C}$
Cell Voltage	0 to 400 V	$\pm 1\% \pm 1 \text{ V}$

\*Range can be altered to customer specification.

Table 1-3  
GENERAL INFORMATION

**DIMENSIONS:**



**WEIGHT:** 20.9 Kg (46 lbs)

<b>POWER:</b>	Model 500	105 - 125 V, 60 Hz
	Model 500A	210 - 250 V, 50 Hz

Table 1-3  
GENERAL INFORMATION  
(continued)

**CONSTRAINTS ON INPUT SAMPLE:**

Minimum Particle Size	0.1 $\mu$ (0.01 $\mu$ under some conditions)
Maximum Particle Size	50 $\mu$ (500 $\mu$ with special coated chamber)
Number of Particles/cm <sup>3</sup>	10 <sup>6</sup> to 10 <sup>9</sup>
Typical Concentration for 2 $\mu$ particles	1 to 1000 ppm
Specific Conductance	1 to 100,000 $\mu$ mhos/cm
pH	3 - 10 (1 - 11 with glass chamber)
Minimum Sample Size	25 ml using syringe 100 ml using Automatic Transfer Module

Table 1-3  
GENERAL INFORMATION  
(continued)

**CHAMBER:**

Geometry	rectangular
Depth	1.5 mm
Width	15 mm
Aspect	10:1
Stationary Layer	213 $\mu$ from top (typically)
Effective Length	10 cm
Material	Acrylic (quartz optionally available)
Anode	molybdenum
Cathode	platinum (plated)
Field Strength	0 - 40 V/cm

**MICROSCOPE:**

Objective Magnification	27 X
Numerical Aperture	0.4
Depth of Focus	5 $\mu$
Working Distance	5.7 mm
Eyepiece Magnification	10 X
Overall Magnification	270 X



## **2. INSTALLATION**

### **2.1 INTRODUCTION**

This section contains all the information you will need to install your Laser Zee<sup>tm</sup> Model 500. Included are initial inspection procedures, power and grounding requirements, environmental information, installation instructions and instructions for re-packaging for shipment to another location.

### **2.2 INITIAL INSPECTION AND UNPACKING**

Your Laser Zee<sup>tm</sup> Model 500 was carefully inspected both mechanically and electrically before shipment. It should be in perfect order upon receipt. To confirm this, the instrument should be inspected for possible physical damage incurred in transit. If the instrument was damaged in transit, file a claim with the carrier. Check that you have received all of the supplied accessories listed in Table 2-1.

Unpack the instrument by opening the outer and inner boxes. Remove all the small boxes and Manual. Remove the cardboard collar. Do not attempt at this time to open the small box that has the white packing slip attached to it. Remove the instrument by grasping the microscope arm and the instrument case on the other side. Pull straight up and place the instrument on a table. If you plan to use the instrument at one location, you may want to remove the plywood pallet. This is accomplished by loosening the bolts from the underside of the base. Additional assembly information is contained in Paragraph 2.7.

Save all the packing material as you may wish to ship your unit to another location.

The various functions of the packing material are as follows:

- 1) Wooden Pallet - bolted to the instrument base plate, it prevents the instrument from sliding side to side in the carton.
- 2) Cardboard Collar - prevents the unit from moving when the container is upside down.
- 3) Plastic Covering - protects the case of the instrument from being scratched.
- 4) Stage Container - reduces the weight on the microscope arm during shipment.
- 5) Various Small Boxes - contain small items and prevents them from sliding about.
- 6) Crushed Paper - fills voids to prevent small boxes from sliding.
- 7) White Foam Corners - absorbs shock during shipment.

**Table 2-1  
PACKING LIST**

Laser Zee<sup>tm</sup> Model \_\_\_\_\_

System Serial No. \_\_\_\_\_

ATM Serial No. \_\_\_\_\_

CARTON	BOX	ITEM	QUANTITY ORDERED	QUANTITY SHIPPED	B/O	DESCRIPTION	P/N
1  LASER  ZEE <sup>tm</sup>		1	1			Laser Zee <sup>tm</sup> Measuring Unit	51059
		2	1			Operating Manual	51138
	A	3	1			Chamber, Acrylic	51066
	A	4	1			Stopper	16801
	A	5	2			6" Teflon Tubes	86509
	B	6	1			50 ml Syringe	51195
	B	7	1			Bulb Pump	51139
	B	8	1			Drain Tube	51140
	B	9	1			"Twinkle" Cleaner	
	B	10	2			Eye Pieces	77858
	B	11	1			Power Cord	17250C
	B	12	1			Temp Probe	51063
	B	13	2			Spare "O" Rings	2-022
	C	14	1			Binocular Head	77750
	D	15	1			Standard Colloid	51152
	D	16	1			Cell Cleaner	51153
	E	17	1			Spare Parts Kit	
ATM  2		18	1			Automatic Transfer Module	51096
		19	1			Power Cord	17250C
		20	7			3 Foot PVC Tubes	51141
CLEANER <sup>3</sup>		21	1			Ultrasonic Cleaner	B-220

All the items listed above serve an important function in protecting your instrument during shipment. If you have the need to ship your instrument to various locations, utilize all the packing material to insure protection for your instrument and hence maintain its operation and appearance for many years.

## 2.3 POWER REQUIREMENTS

The Model 500 can be operated from any power source supplying 105 to 125 V, 60 Hz.

The Model 500A can be operated from any power source supplying 200 to 250 V, 50 Hz.

Power dissipation is 75 W, maximum. Refer to Section 3 for the Instrument Turn-On Procedure.

## 2.4 POWER CORD AND RECEPTACLES

Figure 2-1 illustrates the standard power receptacle (wall outlet) configurations that are used throughout the world. The -PK-part number shown directly below each drawing is the number for the Model 500 power cord equipped with the appropriate mating plug for that receptacle. If the appropriate power cord is not included with your instrument, notify the nearest -PK-sales and service office and a replacement cord will be provided.

## 2.5 GROUNDING REQUIREMENTS

To protect operating personnel, the National Electrical Manufacturer's Association (NEMA) recommends that the instrument be grounded. The Laser Zee<sup>tm</sup> Model 500 is equipped with a three conductor power cable which, when plugged into an appropriate receptacle, grounds the instrument. The offset pin on the power plug is the ground connection.

## 2.6 ENVIRONMENTAL REQUIREMENTS

### 2.6.1 Operating Temperature

The electronics is designed to operate satisfactorily over the temperature range of 0° C to + 55° C. It is important, however, that the temperature of the chamber be the same as the temperature of the sample being measured. If samples are to be measured at + 20° C, then it will be most convenient to have the instrument located in a room at this same temperature  $\pm 5^{\circ}$  C.

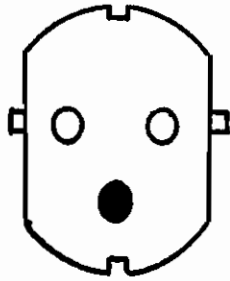
### 2.6.2 Storage Temperature

The storage temperature range of the Model 500 is  
- 40° C to + 75° C.

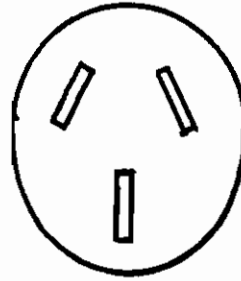
### 2.6.3 Vibration

The Laser Zee<sup>tm</sup> Model 500 utilizes a high power microscope with an overall magnification of approximately 270. Vibration caused by nearby machinery can be an annoyance unless precautions are taken. As a practical matter, vibration is usually worse on upper stories of buildings and better on the ground floor. In any case, the effects of vibration if present can usually be eliminated by placing the unit on a 2-3 inch pad of foam rubber.

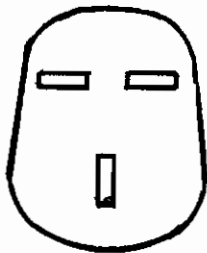
**FIGURE 2-1**



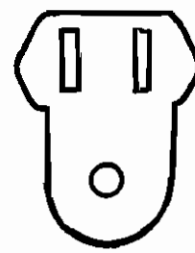
**PEN KEM P/N 51189  
"A" PLUG**



**PEN KEM P/N 51190  
"B" PLUG**



**PEN KEM P/N 51191  
"C" PLUG**



**PEN KEM P/N 51192  
"D" PLUG**

**STANDARD POWER RECEPTACLE CONFIGURATION**

## 2.7 INSTALLATION AND ASSEMBLY

Your Laser Zee<sup>tm</sup> Model 500 is a portable instrument and does not require installation. The instrument is shipped with rubber feet and is ready for use as a bench instrument. In order to protect the binocular head and eyepieces, they are packaged separately and it is necessary to unpack them and mount them in place on the microscope.

As you assemble your instrument you will notice the stage for the microscope packed in a separate box. This is done to avoid possible damage to the microscope during shipment due to the added weight of the stage. We suggest removing the stage and repacking it in its own box whenever you plan to ship the instrument to another location. The instructions for remounting, which are also contained in the packing list, are as follows:

To install the stage on the microscope:

1. Carefully remove the stage from the packing box. DO NOT pull excessively on the harness connected to the stage.
2. Rotate the objective lens one indent to the right as viewed from the normal working position.
3. Hold the stage by the end where the Automatic Transfer switch is located. The white rails on the stage base plate should be facing up and pointing toward the rear of the unit.
4. Slide the stage between the cover of the unit and the microscope arm.
5. Lower the stage onto the mounting ring of the microscope.
6. Move the stage slightly until it sits firmly in the ring.
7. Square the stage off with respect to the microscope and tighten the small knurled knob on the left hand side of the stage, below and slightly forward of the Automatic Transfer switch.
8. Return the objective lens to the original position.
9. Connect the small plug on the scope to the jack on the stage.

If you are using your instrument without the Automatic Transfer Module (ATM), you will have a connector on the stage harness which will not be used. This is the blue rectangular connector. There are no live voltages on this connector. Also on the stage harness you will find a cylindrical black connector. This is the mating connector for the temperature probe. Insert the temperature probe jack fully into the black receptacle.

## 2.8 REPACKAGING FOR SHIPMENT

The following paragraphs contain a general guide for repackaging the instrument for shipment. The unit should be packed in the original shipping container which was especially designed to protect the instrument from damage in transit. The unit should never be simply bolted to the inside of a rigid container as this provides almost no shock isolation, and damage to laser and microscope is certain to result. The unit should never be simply packed in foam or other soft material as undue stresses will be placed on the instrument case. If you do not have the original packing material or if you need other assistance, contact the nearest Pen Kem, Inc. sales and service office (see back cover for detailed information).

The detailed procedure for repacking the Laser Zee<sup>tm</sup> Model 500 is as follows:

1. Remove chamber from microscope stage, wrap in foam and put in appropriate cardboard box.
2. Remove two 6" Teflon tubes from microscope stage and put them in the same box as chamber.
3. Remove binocular head from microscope.
4. Wrap binocular head in plastic wrap and put in its own styro-foam case.
5. Fasten binocular case closed with tape.
6. Cover microscope top with tape to prevent foreign objects from falling inside.
7. Remove stage from microscope and repack in original cardboard box.
8. Put plastic cover over microscope.
9. Place Laser Zee<sup>tm</sup> Model 500 on plywood pallet. Fasten to pallet using 1/4 - 20 bolts provided.
10. Put unit and pallet into inner packing box (inside box can be left in place inside of outer box during packing. Be certain that a white foam corner is located at each bottom corner of the box.

11. Cover unit with heavy sheet of plastic provided.
12. Slip cardboard collar inside of inner box to hold down both pallet and plastic sheet.
13. Place binocular case on top of unit in box.
14. Put accessories listed in Table 2-1 in separate cardboard box and place on top of unit.
15. Fill remaining voids with newspaper or other packing material.
16. Close inner box with reinforced tape and position four additional white foam corners in place.
17. Close outer box with reinforced tape.
18. Strap outer box with nylon tape in two places to provide extra protection.



### 3. OPERATING INSTRUCTIONS

#### 3.1 INTRODUCTION

If you have just acquired your Laser Zee<sup>tm</sup> Model 500, we can understand that you are anxious to use it. The quickest way to get started is to simply follow the step-by-step instructions given in this section. However, if you haven't read the Introduction (Section 1.1) and Description of Operation (Section 1.2), it would be helpful to do that first.

The following describes the operating controls, gives a detailed procedure for making measurements using a standard colloid, notes procedures for proper sample preparation, and finally, lists an abbreviated measurement check list for the experienced user.

Make sure to use the standard colloid first before trying samples of your own choosing. If you get the right value for the standard, you then know that your instrument is in good working order and that you have understood the measurement procedure.

#### 3.2 OPERATING CONTROLS

The following paragraphs describe the location and function of all the controls on the Laser Zee<sup>tm</sup> Model 500. It will be helpful to refer to Figure 3.1 as you read the text.

##### 3.2.1 Zeta Potential (Z. P.) Control Knob

The "Z. P." control knob, located to the left of the push buttons, controls the rate and direction of the prism inside the microscope. This control is adjusted during zeta potential determinations to make the colloidal particles appear stationary.

##### 3.2.2 Voltage Control Knob

The VOLTAGE control knob, located to the right of the push buttons, controls the voltage applied to the chamber. The voltage is adjustable from 0 to + 400 volts dc.

### 3.2.3 Power Push Button

The "POWER" push button turns on the main power to the Model 500, providing that the chamber is in place on the microscope stage.

### 3.2.4 Temperature (TEMP) Push Button

When the "TEMP" button is depressed, the temperature at the tip of the thermistor temperature probe is displayed on the digital readout.

### 3.2.5 Specific Conductance (S.C.) Push Button

When the "S.C." button is depressed, the specific conductance of the sample in the chamber is displayed. (The "H.V." button must also be depressed in order to obtain a reading.)

### 3.2.6 Zeta Potential Push Button

The zeta potential of the colloid is displayed when the "Z.P." and "H.V." (see 3.2.9) push buttons are depressed and the operator has set the "Z.P." control knob so that particles appear stationary.

### 3.2.7 Voltage Push Button

When the "VOLTAGE" push button is depressed and the "VOLTAGE" control knob is adjusted (as described in 3.2.2 above), the output of the high voltage supply is displayed.

### 3.2.8 Specific Conductance Low Push Button

A specific conductance scale of 0 to 999 micromhos/cm is provided when the "S.C.," "H.V.," and "S.C. LOW" buttons are depressed. When the "S.C." and "H.V." buttons are depressed, the specific conductance scale is 0 to 99.9 thousand micromhos/cm. The high range should always be selected first so as to be sure that the conductance is within range.

### 3. 2. 9 High Voltage (H.V.) Push Button

When the "H.V." push button is depressed, the chamber electrodes are connected to the high voltage supply. The button should not be depressed until a voltage, specific conductance, or zeta potential measurement is to be made (in order to minimize heating which in time will interfere with making an accurate determination). Pushing the button a second time raises it to the "off" or elevated position. As soon as the measurement is completed, immediately return the unit to the "off" position to avoid unnecessary heating of the sample.

### 3. 2. 10 Average Push Button

Depressing the "AVERAGE" push button, when in the "Z.P." mode, results in averaging the zeta potential determinations for a 30-second period, after which a beeper sounds and the average zeta potential is displayed on the readout.

### 3. 2. 11 Substage Illumination

This control is located to the left of the push buttons on the side of the case to the right of the microscope. It is continuously adjustable to obtain a desired level of background illumination and it is used for precise focusing at the top and bottom surfaces of the chamber and for providing a background illumination to make the eyepiece reticle more visible.

### 3. 2. 12 Laser Vertical Height Adjustment (LSR ADJ)

The "LSR ADJ" control is located in the left back corner of the unit and protrudes through the top of the case. It adjusts the position of the laser beam in the vertical direction so as to illuminate only particles at the stationary layer in the chamber.

### 3. 2. 13 Microscope Focus, Coarse and Fine

This adjustment, located at the base of the microscope, consists of two parts: a coarse focus knob and a concentric inner fine focus knob graduated in 2 micron intervals. (There is also a tension adjustment which is factory pre-set; adjustment of this control is normally not required.)

#### 3.2.14 Automatic Transfer Switch

A lever located on the microscope stage assembly controls the flow of fluid through the chamber when using the optional Automatic Sample Transfer feature of the Laser Zee<sup>tm</sup> Model 500. The control has two positions: "MEASURE" and "CIRCULATE." In the "MEASURE" position, the Laser Zee<sup>tm</sup> electronics is operating and the valves controlling fluid movement are closed. In the "CIRCULATE" position, the laser and high voltage circuits are turned off, the valves controlling fluid movement are open, and if an Automatic Transfer Module is connected, the peristaltic pump contained therein is actuated. If you are not using the Automatic Sample Transfer option, leave the switch in the "MEASURE" position.

Care should be taken in operating the Automatic Transfer Switch. Undue force will eventually degrade the accuracy of the microscope focus adjustment. The control should be gripped so as to exert torque on the lever without either pushing up or down on the stage.

#### 3.2.15 Chamber Safety Interlock Switch

When the chamber is removed from the operating position on the microscope stage, a safety switch automatically disconnects power to the unit to prevent accidental exposure to either high voltage or the laser illumination.

#### 3.2.16 Inter-Ocular Spacing

The "Inter-Ocular Spacing" adjustment provides a means for accommodating differences in eye spacing from one individual to another. The adjustment is located on the binocular head between the two eyepieces.

#### 3.2.17 Left Eyepiece Focus

The "left eyepiece focus" adjustment provides a means of accommodating focus difference between the left and right eye.

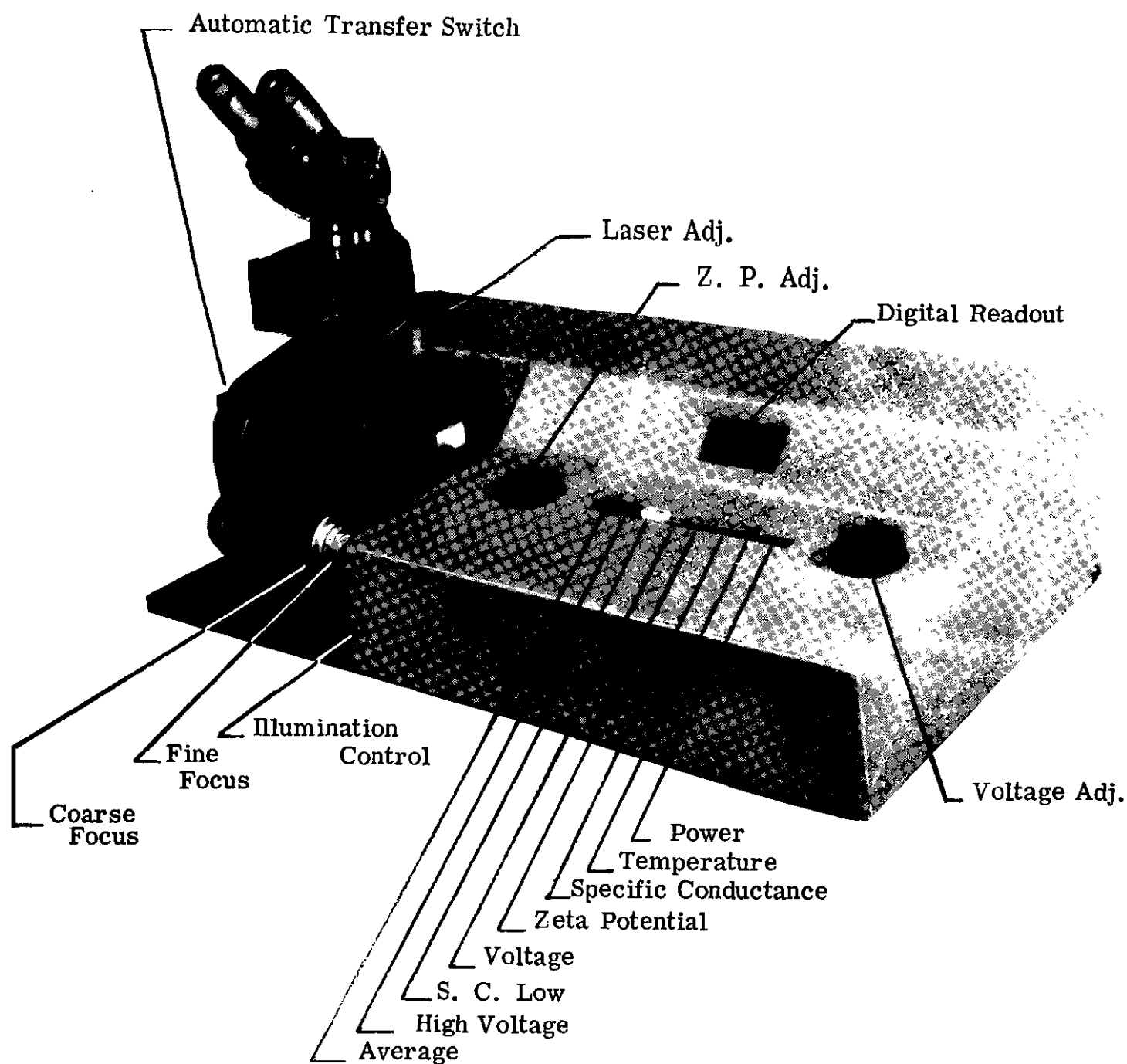


Figure 3-1: LASER ZEE<sup>™</sup> MODEL 500 CONTROLS

### 3.3 MAKING A MEASUREMENT USING THE STANDARD COLLOID

Before trying to measure a colloid of your own, it is important to first make a measurement using one of our standard colloids of known zeta potential. This will give you assurance that the instrument is working properly and that you are following the correct procedure.

There are 9 steps to making a zeta potential measurement. These steps, which will be described in subsequent paragraphs, are as follows:

- (3.3.1) Fill the chamber
- (3.3.2) Place the chamber on the microscope stage and turn the power on
- (3.3.3) Adjust the microscope for comfortable viewing
- (3.3.4) Focus at the stationary layer
- (3.3.5) Check the laser illumination of the colloidal particles
- (3.3.6) Check for zero movement with the voltage off
- (3.3.7) Measure zeta potential and specific conductance
- (3.3.8) Measure the sample temperature and correct zeta potential data for non standard temperature
- (3.3.9) Empty the chamber

You will have made your first zeta potential determination with the Laser Zee<sup>tm</sup> Model 500 if you just follow the detailed step-by-step instructions on the next few pages. You will then be ready to apply this new skill.

#### 3.3.1 Fill the Chamber

For the time being, we are going to fill the chamber using only the syringe. Later we will tell you how to do this automatically if you have the optional Automatic Transfer Module.

1. First, rinse the syringe clean using distilled or deionized water.
2. Next, fill the syringe with 25 mL of the standard colloid which was supplied with your instrument.
3. Place the chamber on a convenient flat surface. Connect the syringe to the fitting on the top of the cathode compartment (the one having a flat top on

the inside) and fill the chamber until the anode compartment (which has the inverted funnel on the inside top surface) is approximately one half full. (The syringe should be held high so that it is above the chamber during filling.)

4. Withdraw fluid back into the syringe until air begins to bubble up into the cathode compartment.
5. Slowly fill the chamber mid-section and anode compartment again. This time, keep filling the chamber until the fluid just overflows the fitting at the top of the anode compartment. At this point, carefully put the stopper on the anode fitting. There should be no air in the anode compartment as this can cause movement of the fluid by expansion or contraction of the air which in turn will give erroneous results. The chamber is now filled.

### 3.3.2 Place the Chamber on the Microscope Stage and Turn the Power On

1. Depress the "Voltage" push button. All others should be in the up position. Set the "Automatic Transfer Switch" in the "Measure" position.
2. Place the chamber on the microscope stage. Align the guide pins on the chamber base to the mating holes on the microscope stage assembly. Slide the chamber toward you using both side protrusions on the chamber base plate.

(Note: The Laser Zee<sup>tm</sup> Model 500 will not turn on unless the chamber is in place on the stage. This is a safety feature designed to protect the user from the potential hazards of reflected laser light and high voltage.)

3. Depress "Power" push button.
  - . Set voltage control for a readout of approximately 150 volts on the display panel.

### 3.3.3 Adjust the Microscope for Comfortable Viewing

1. Turn the substage illuminator to maximum brightness.
2. If you find you do not need to wear glasses, extract the eye shields on the binocular eye pieces. They will eliminate stray room light and make viewing more comfortable. If you do need glasses, leave eye shields in the retracted position. If you use eye-glasses, it may be necessary to reduce room ambient lighting to limit the amount of stray light and create a comfortable viewing situation.
3. Adjust interocular spacing for most comfortable viewing with both eyes simultaneously. Record this setting for future reference in Table 3.1.
4. Rotate the top of the Coarse Focus knob away from you so as to lower the stage to stop.
5. Next, rotate the fine focus control in the opposite direction to slowly raise the microscope stage. The first surface to come into focus will be the outside top surface of the chamber. As you continue to raise the stage (about 5-1/2 more turns on fine focus knob), you will observe the inside top surface of the chamber. Finally, after 5-1/2 more turns, you will observe the bottom inside surface. Make sure that you can identify these three surfaces. Repeat Steps 4 and 5 and this time stop when you have precisely focused on the top inside surface.
6. Close your left eye and adjust the fine focus for the sharpest image using your right eye.
7. Close your right eye and adjust left eye piece focus adjustment for best image in left eye. Record this setting for future reference in Table 3.1.

TABLE 3.1

Name	Interocular Spacing	Left eyepiece focus



#### 3.3.4 Focus at the Stationary Layer

The stationary layer is found by first focusing on the top inside surface of the cell, and then turning the fine focus knob toward the operator (counter clockwise) an amount determined by the calibration constant of the cell. This calibration constant is marked on each cell and is in the range of 200 to 250  $\mu\text{m}$  (microns), typically 213  $\mu\text{m}$ .

1. In step 3.3.3, you have already set the fine focus of the microscope to focus on the top surface. Check this again using the minute imperfections and scratches on the top inside of the chamber. Record the setting of the fine focus adjustment.
2. Note the calibration number on the cell. Add this constant to the number recorded above to arrive at the location of the stationary layer.
3. Turn the fine focus knob toward you to the setting determined above, remembering to add 200  $\mu\text{m}$  to the reading when you pass zero. (One full revolution of the fine focus knob moves the cell 200  $\mu\text{m}$  vertically.)
4. As an example, let us say that the top of the cell corresponds to a reading of 160  $\mu\text{m}$  and the calibration constant for the cell is 213. The stationary layer is therefore at  $160 + 213$  or 373  $\mu\text{m}$ . You will therefore turn the fine focus knob toward you, raising the microscope stage one full revolution (200  $\mu\text{m}$ ) and then adding an additional 13  $\mu\text{m}$ . The fine focus knob will now read 173  $\mu\text{m}$ .

Error may be introduced if the stationary layer is not re-defined prior to making each measurement, and instead the chamber is simply replaced on the stage and a zeta potential measurement is made immediately. The size of the error source may be estimated by using both procedures and comparing the difference in results.

### **3.3.5 Check the Laser Illumination of Colloidal Particles**

1. Set the substage illumination for minimum brightness.
  - Rotate "LSR ADJ" control to produce best image of particles in the microscope. Particles should appear as bright dots of red light; many having a small ring around them.
2. The particles should be uniformly bright in the central part of the viewing area. If the bulk of the particles is to the far right or left, then the mirror inside the Laser Zee<sup>tm</sup> needs to be adjusted. This mirror is set at the factory and does not ordinarily require field adjustment. However, if the unit is operated on an uneven table, or if the unit has been subjected to rough handling in shipment, an initial adjustment may be required. (For adjustment, see Section 7.)
3. Increase the substage illumination level until the grid is clearly visible but do not increase the illumination so much that the colloidal particles disappear.

### **3.3.6 Check for Zero Movement with the Voltage Off**

If there are no thermal convection currents and no fluid leaks, the colloidal particles will be stationary in the absence of an applied electric field. The purpose of the following test is twofold: to verify that the particles are indeed stationary with no applied field, and more importantly, to give the operator practice and confidence with the Zeta Potential control knob.

To make this test, follow the steps listed below:

1. Depress the "Z. P." push button.
2. Adjust the "Z. P." knob for a readout of approximately -20.0 mV. Note that the particles appear to move to the right a distance of about two grid lines, are then re-set to where they started, and that this action continues indefinitely. Now adjust the "Z. P." knob for a readout of approximately + 20.0 mV. Note that the action is now reversed from right to left.

3. Adjust the "Z.P." knob until the readout is 00.0 mV. Note that the particles on the average have no net movement to the right or left but individually do exhibit some random or Brownian motion.
4. It is important, in making measurements with the Laser Zee<sup>tm</sup>, to concentrate on the net movement of the particle "cloud" and not individual particles. To accomplish this, make a habit of staring at a grid intersection near the center of the microscope field of view. Relax and try to judge the net movement of all the particles within your peripheral vision.
5. While staring at a grid intersection, slowly turn the "Z.P." knob to the right until you first observe a slight net movement of the particle cloud to the right. When you first detect some net movement, stop and write down the number which is displayed on the readout.
6. Next turn the "Z.P." knob to the left until you first note a perceptible movement of the particle cloud to the left. Write down the number displayed on the readout.
7. With a little practice, the difference between the two numbers recorded in Steps 5 and 6 should be less than 6 mV and the average value should be approximately zero (± 0.5 mV).
8. The difference in these two readings is caused by the Brownian motion of the particles which has the effect of producing a "dead band" within which no net movement of the particle cloud can be detected with the eye.
9. The effect of the dead band on the accuracy can be minimized by making measurements in much the same way as one would balance a bridge circuit. Rotate the knob first one way and then the other so as to produce a noticeable net movement in each direction. Decrease the magnitude of the knob rotations and then split the difference. In this manner you should be able to get a reading of "00.0 mV" (± 0.5 mV).
10. If you are not able to get a zero reading, you may have one of the following problems:

- There is a leak somewhere.
- There is an air bubble somewhere.
- The fluid in the cell is either very hot or cold and the cell has not yet reached equilibrium.

11. If the reading is within  $\pm 0.5$  mV, continue with the measurement of zeta potential.

### 3.3.7 Measure Zeta Potential and Specific Conductance

Here is the part you have been patiently waiting for:

1. Depress the "H.V." button which connects the high voltage supply to the electrodes in the chamber.

Note that the particles appear to move as soon as the "H.V." button is depressed. With the standard colloid, the particles will move to the left. This standard has a negative charge and therefore the particles move toward the anode. Although the anode is on the right hand side of the stage, the particles appear to move to the left because the microscope reverses the image.

2. Adjust the "Z.P." knob as before to make the particle cloud appear stationary. Since the standard colloid is negatively charged, it will be necessary to rotate the "Z.P." knob to the right to reach this null condition. Turn the knob a little beyond the null point until you sense a net movement to the right. As before, rotate the knob back and forth to produce a barely perceivable motion in each direction and then split the difference. Stare at the grid and not individual particles. If you start looking at individual particles, you will become confused each time the prism resets to start a new scan. If you have trouble at first, try reducing the chamber voltage to 50 volts. You should always make the measurement as quickly as possible to avoid heating the contents of the chamber. You should usually be able to make the measurement within 3 to 5 seconds. Record the number displayed on the readout, in mV.
- YOU HAVE NOW MADE YOUR FIRST ZETA POTENTIAL DETERMINATION.**

3. Depress the "S.C." button and record the specific conductance. If the measured value is less than 1000  $\mu$ mhos/cm (a readout of "01.0"), you should change scale by pushing the "S.C. LOW" button which will give you a readout range of zero to 999  $\mu$ mhos/cm.
4. Release the "H.V." button as soon as the zeta potential and specific conductance measurements have been completed. You will find that the faster you operate, the better the reproducibility of your results and the less often you will have to clean the chamber and electrodes.
5. NOTE: While making zeta potential measurements you will observe that not all of the particles travel at exactly the same speed. Therefore, when you have the zeta potential knob set properly, some particles appear to move to the right and some to the left. The effect is very much like looking out of the car traveling down the middle lane of a three lane superhighway. If the car on your right is moving just a little slower than you, he appears to be moving backwards. On the other hand, a car on your left side may be moving just a little faster than you and thus appears to be moving forward. In both cases, the movement is judged not relative to the road, but relative to the vehicle containing you, the observer. In your instrument, the prism inside the microscope provides the moving frame of reference just as the car did in the above example. Particles traveling just a little faster than average appear to go one way, the ones a little slower than average appear to go the other way.

Sometimes the particles will appear to move pretty uniformly and therefore the measurement can be made easily. On other occasions, there will be quite a variation in speed and the measurement will be correspondingly more difficult. There is absolutely nothing wrong with the instrument when this occurs. In fact, it is usually a strong indication that there is something wrong with the process you are trying to control, for it indicates that the particles have not come into equilibrium and exhibit a wide distribution of zeta potential. This condition can usually be corrected by the appropriate addition of electrolytes.

### 3.3.8 Measure the Sample Temperature and Correct Zeta Potential Data for Non-Standard Temperature

Where accuracy is important, zeta potential and specific conductance should be corrected to a standard reference temperature. The measured value of zeta potential and specific conductance will be found to increase at a rate of approximately 2% per degree centigrade. The Laser Zee<sup>tm</sup> is calibrated to give the correct value only at 20° C. If your sample is not at 20° C, you can correct the data according to the actual temperature at which the measurement was made.

To accomplish this correction:

1. Place the temperature probe into the container which holds the test colloid.
2. Depress the "Temp" button and record readout. (All readings are relative to 20° C so that a readout of + 5.0 corresponds to a temperature of + 25.0° C).
3. Calculate a corrected Z. P. using the following formula:

$$\text{Z. P.}_{(\text{corrected})} = \text{Z. P.}_{(\text{measured})} \times (1 - .02T)$$

where T = temperature readout

Suppose in our case the measured Z. P. was 40.0 mV and the temperature readout was +5.0:

$$\begin{aligned} \text{Z. P.}_{(\text{corrected})} &= -40 \times (1 - .02 \times 5) \\ &= 40 \times (1 - .1) = 36 \text{ mV} \end{aligned}$$

4. Similarly, the specific conductance (S.C.) readout would be corrected in the same way and in the above example would be reduced by the same 10% factor.

5. Compare your measurement of zeta potential and specific conductance with the stated values printed on the label of the Standard Colloid.  
If your values are not within the range given on the label, try the measurement again. If you still are having trouble, check the expiration date on the colloid to make sure it is still useful as a standard.  
If you cannot resolve your difficulty, please contact PEN KEM, INC. We are always interested in helping you get the most out of your instrument.

#### 3.3.9 Empty the Chamber

It is important that the colloid not be left in the chamber any longer than necessary. Typically, you will finish your measurements in less than one minute from the time you fill the chamber. If the colloid is left too long in the chamber, you will have to clean it more often and you will not get the same level of precision.

To remove the chamber from the microscope stage, it is important that you be most careful. Use both hands. Push the protrusion on the sides of the chamber with your thumbs, away from you so as to disengage the pins from the stage assembly. Then, slide the chamber assembly to the left off the stage.

Remove the cap from the anode fitting and decant, tilting the chamber as necessary to drain cathode compartment.

After chamber is empty, connect syringe to cathode compartment fitting and flush chamber with 50 ml of demineralized water.

### 3.4 SAMPLE PREPARATION

Experience has shown us that a large proportion of the problems in making meaningful zeta potential measurements result from the sample preparation method. At this point, having made an accurate measurement of a Standard Colloid, you are ready to make measurements on colloids of more direct interest and importance to you. Keep in mind, however, that your ability to obtain meaningful zeta potential data may be affected by the following considerations.

1. Temperature
2. Agitation
3. Contamination
4. Bacterial Action
5. pH
6. Dissolved Gases
7. Solids concentration too low
8. Solids concentration too high
9. Particle Size
10. Availability of Adequate Sample Volume
11. Presence of Solvents
12. Viscosity and dielectric constant of suspending medium.

All of these factors are discussed in the paragraphs below.

#### 3.4.1 Sample Temperature

It is customary to take all data at room temperature (approximately 20° C). In Section 3.3.8, we discussed a procedure whereby the data can be corrected to compensate for deviations in sample temperature from the reference temperature of 20° C. If your process takes place at a temperature much different than 20° C, you may want to consider the impact of this when you interpret your zeta potential data.

#### 3.4.2 Sample Agitation

Samples may need to be agitated and re-dispersed prior to measurement. A conventional magnetic stirrer may be adequate. Sometimes ultrasonic energy or a high shear mixer (e.g., Waring Blender) is necessary to break up aggregates that can form during storage of the sample.



#### 3.4.3 Sample Contamination

Make sure samples are stored in inert containers such as polyethylene plastic. When not being used, samples should be sealed so as to prevent exposure to air.

#### 3.4.4 Bacterial Action

Bacterial action often causes, with time, a gradual decrease in the zeta potential. This effect can be minimized by making the measurement as promptly as possible, or by storing samples in air tight containers and keeping them in a refrigerator until the measurement can be made.

#### 3.4.5 pH

The zeta potential of almost all colloidal materials exhibit some dependence on the pH. Since pH can change with time, for example by absorption of CO<sub>2</sub> from the air, it is important to measure pH to achieve high levels of reproducibility.

#### 3.4.6 Dissolved Gases

If you are working with fluids that contain large quantities of dissolved gases, you may have some problems with gas bubbles forming on the inside of the chamber. This is particularly true if the sample was originally colder than the temperature of the room where you are working. You can eliminate these problems by placing the sample in a filtering flask and subjecting the fluid to a vacuum of approximately 15" Hg for about 30 seconds. This should de-aerate the water sufficiently so that bubbles will not form during measurement.

#### 3.4.7 Solids Concentration - Too Dilute

If the sample is too dilute, you may not have enough particles in the field of view at one time to get a good average reading. You can improve this situation by using the "Average" feature of your instrument. Proceed with the measurement exactly as before, except:

1. Depress the "Average" button subsequent to pressing the "H. V." button.

2. Instead of trying to null the movement of the particle cloud, concentrate on one particle at a time, selecting a new one every 3-5 seconds. After approximately 30 seconds, a beep will be heard and the average zeta potential of the particles tracked during that period will be displayed on the readout.

If the concentration is too low, it may be desirable to increase the concentration. If you are preparing the sample from its component parts, you can simply add more solids. Evaporation is not a suitable technique since it changes the ionic concentrations, and the zeta potential of colloidal particles is strongly dependent on its ionic environment.

#### 3.4.8 Solids Concentration - Too Concentrated

If the sample is too concentrated, the image quality will be poor and it will be difficult or impossible to recognize individual particles. You will see only a haze. One must use care in diluting a sample. Always dilute the colloid either with its own "mother liquor" or a synthetic one. For example, a highly concentrated latex paint can be centrifuged, following which a small portion of the original colloid can be added to the clear supernate. For other samples, it may be more appropriate to filter the sample instead of centrifuging it. In any case, it is important that whatever preparation is undertaken, it does not change the ionic environment of the colloidal particles.

#### 3.4.9 Particle Size

The dark-field laser illumination system enables zeta potential measurements of colloidal particles as small as 100 Å. It is, of course, much easier to view these extremely small particles if they have a high index of refraction relative to the suspending material. Sometimes it is necessary to wait in a darkened room to give the eyes a chance to dark-adapt (about 15 minutes) before trying to measure the smallest particles.

The upper limit on particle size is perhaps 50 $\mu$  ; in such a case it is easier to work with particles which have a specific gravity close to that of the suspending medium to avoid large sedimentation rates. Naturally, the sedimentation velocity does not directly affect zeta potential readings since the settling is in the vertical direction and we measure electrophoretic velocity in the horizontal direction. However, there is sometimes a

more subtle effect. If the colloid contains particles of a wide range in particle size, the larger particles will naturally settle out of the field of view first. If the larger particles have a different zeta potential than the small ones (as may be true of paper industry fibers in comparison to fines), the user may find that his measured value of zeta potential depends upon the length of time elapsed between filling the chamber and making the measurement.

\*

It is usually preferable to filter all samples to remove particles larger than say 10 - 20  $\mu$ m, unless these particles are of particular interest. Such filtration will normally eliminate any problems due to settling.

#### 3.4.10 Availability of Adequate Sample Volume

The Laser Zee<sup>tm</sup> Model 500 chamber requires about 25 ml of fluid to fill completely. If you are limited to smaller sample volumes, contact the factory for assistance.

#### 3.4.11 Presence of Solvents

Certain solvents present in the suspending medium may in time attack the plexiglass chamber. For this reason, you should never let samples stand for an appreciable length of time in the chamber. A quartz chamber is optionally available. Contact factory for details.

#### 3.4.12 Viscosity and Dielectric Constant of Suspending Medium

The Laser Zee<sup>tm</sup> Model 500 is calibrated to read zeta potential directly provided that the sample (at 20<sup>o</sup> C) has a viscosity of 1 cp and a dielectric constant of 80.1. If your sample differs from these values, you can calculate a corrected zeta potential from the following equation:

$$Z.P. (\eta\epsilon) = \frac{\eta}{\epsilon} \left( \frac{80.1}{1.0} \right)^2 Z.P. (1, 80.1)$$

where:  $\eta$  is the viscosity in centipoise  
and  $\epsilon$  is the dielectric constant of your sample

NOTE: To convert the zeta potential parameter to mobility, divide number displayed by 14.1. That is, a readout of -14.1 mV corresponds to a mobility of -1.0 cm<sup>-4</sup> volt<sup>-1</sup> sec<sup>-1</sup>.

### 3.5 CHECKLIST FOR MAKING MEASUREMENTS (FOR EXPERIENCED USER)

#### 3.5.1 Filling the Chamber

Rinse with Water. Fill syringe with 25 ml of sample. Inject fluid through cathode compartment. Fill anode compartment partially. Pull back until bubbles form at cathode. Refill slowly until full and place cap on anode fitting.

#### 3.5.2 Installing the Chamber on the Stage

Depress "Voltage." Other buttons remain in the up position. Install chamber on stage using both hands. Depress "Power." Set voltage to 150 volts.

#### 3.5.3 Adjusting Microscope for Comfortable Viewing

Turn up substage illumination. Position eye shields. Set interocular distance and left ocular to predetermined settings. Focus on top inside surface of chamber.

#### 3.5.4 Focus at the Stationary Layer

#### 3.5.5 Checking Laser Illumination

Adjust vertical height of laser if necessary.

#### 3.5.6 Checking for Zero Movement with Voltage Off

Depress "Z.P." push button. Adjust "Z.P." control knob left and right in decreasing amounts until particle cloud is stationary. Check that reading is  $0 \pm 0.5$  mV.

#### 3.5.7 Measuring Zeta Potential

Depress "H.V." push button. Adjust "Z.P." control knob until particle cloud is stationary. Read zeta potential on display. Depress "S.C." push button. Read specific conductance. If less than 1000  $\mu$ mhos/cm, depress "S.C. LOW" and read again. Release "H.V." push button.

#### 3.5.8 Empty Chamber

See Chapter 3.4.

## 4. OPERATING INSTRUCTIONS FOR USING AUTOMATIC TRANSFER MODULE

### 4.1 INTRODUCTION

Up to now, you have been filling the cell by hand, using the syringe. If you have the Automatic Transfer Module, we will now show you how to do this automatically.

The Automatic Transfer Module (ATM) was designed to simplify the task of collecting zeta potential data so that the instrument could more readily be used for production control applications. The unit contains a four way selector valve to allow the operator to circulate four separate fluids through the cell. It contains a second valve to change the direction of flow in the cell. Finally, it provides a peristaltic pump for circulating the fluids.

### 4.2 Automatic Transfer Module Controls

The controls on the Automatic Transfer Module are illustrated in Figure 4.1. They are as follows:

1. Sample Select Switch
2. Flow Direction Switch
3. Power Switch
4. Line Select Switch

### 4.3 Setting Up the ATM

- 4.3.1 Place the ATM directly to the left of the Laser Zee<sup>tm</sup>.
- 4.3.2 Set the line selector switch to the appropriate voltage and check that the correct value fuse is in place.
- 4.3.3 Connect fluid ports at rear of ATM as follows (using 3 PVC tubes each 3 feet long).

- Port 1. Leave disconnected in order to provide air inlet.
- Port 2. Connect to 1 liter flask of demineralized water.
- Port 3. Connect to a small flask containing a colloid of interest. Flask should be kept stirred using magnetic stirrer or some other appropriate means.
- Port 4. Same as Port 3.

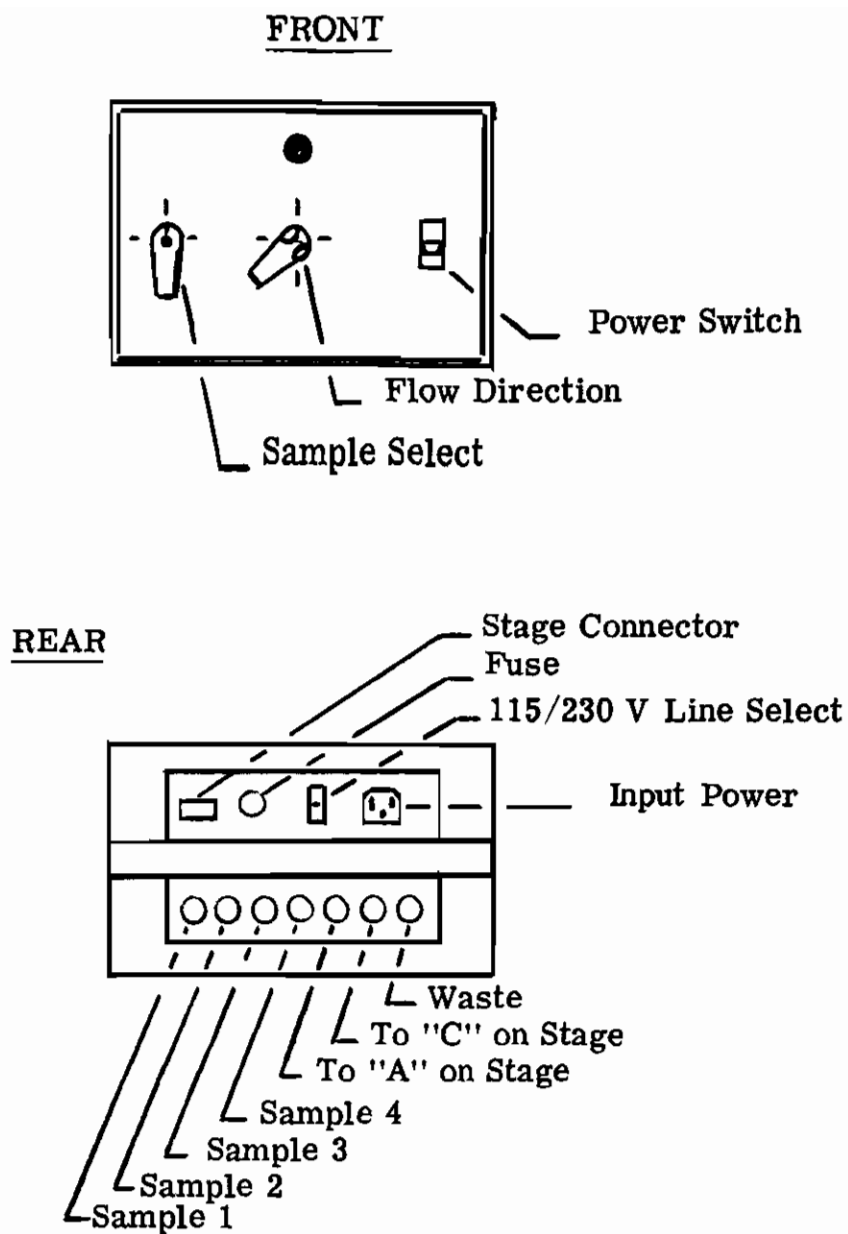


Figure 4-1: AUTOMATIC TRANSFER MODULE CONTROLS

- 4.3.4 Connect ports labeled "A" and "C" on ATM to respective ports on Automatic Transfer Stage (ATS) on microscope. Use PVC tubes 3 feet long.
- 4.3.5 Connect port labeled "Waste" to an appropriate disposal container using a 3 foot long PVC tube.
- 4.3.6 Plug connector on Laser Zee<sup>tm</sup> labeled "ATS Power" into mating connector on back of ATM.
- 4.3.7 Make sure the Automatic Transfer Switch is set to the "Measure" position.
- 4.3.8 Plug power cord in back of ATM into suitable three conductor outlet. If the three conductor outlet is not available, use an appropriate adapter. Make sure that the grounding lead is connected to an appropriate ground.
- 4.3.9 Set the power switch on the front panel of the ATM to the "on" position (panel lamp should now be on).

#### 4.4 Making Measurements with the Automatic Transfer Module

The procedure for making zeta potential measurements is the same one you used previously with a test colloid, except that you will now fill and empty the chamber automatically. To set up for automatic sample transfer, you must first connect the cathode compartment of the cell to the matching port on the ATS using one of the 6 inch teflon hoses. Next connect the anode compartment of the chamber in a similar manner.

To fill the chamber, follow the steps outlined in Table 4-1. To empty the chamber, follow the sample sequence of steps as in Table 4-1 except that in Step 5, the "Sample" switch should be set to Position 2 (water). This leaves the chamber filled with demineralized water when you are through with the measurements.

**TABLE 4-1**  
**STEPS FOR FILLING OR EMPTYING CHAMBER**

Step	ATM		ATS	Instructions
	Switch Positions Flow	Sample	Switch Positions Measure/Circulate	
1	Normal	1 (Air)	Circulate	Continue until bubbles appear at anode.
2	Normal	2 (Water)	Circulate	Circulate for 30 seconds
3	Reverse	2 (Water)	Circulate	Continue for 30 seconds
4	Reverse	1 (Air)	Circulate	Continue until first bubbles appear at cathode and then proceed immediately to Step 5
5	Normal	3 (Colloid) (Note: Both switches should be moved simultaneously)	Circulate	Continue until air is eliminated from anode chamber and anode tubing
6	Normal	3 (Colloid)	Measure	You are now ready to measure zeta potential



## 5. THEORY OF OPERATION

This section will give you a better understanding of zeta potential and the techniques employed in the design of the Laser Zee<sup>tm</sup> Model 500.

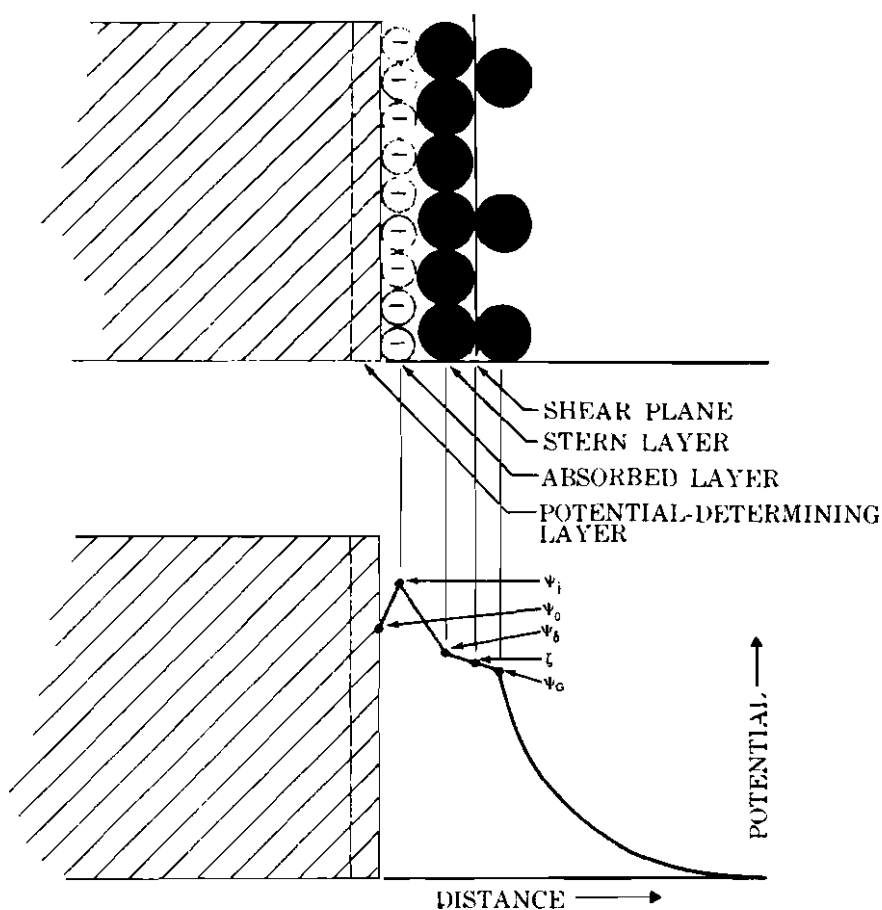
Included in this section is an I&EC reprint of "Colloidal Dispersions, Electrokinetic Effects and the Concept of Zeta Potential," by Paul Sennett and J. P. Olivier, which describes the basic concepts of zeta potential; and a reprint of "A New Technique for Microelectrophoretic Measurements," by Philip J. Geotz and John G. Penniman, which describes the details of the measuring technique used in the Laser Zee<sup>tm</sup> Model 500.



# Colloidal Dispersions, Electrokinetic Effects and the concept of ZETA POTENTIAL

PAUL SENNETT

J. P. OLIVIER



PAUL SENNETT     J. P. OLIVIER

*The colloid chemistry of lyophobic systems is, in fact, the surface chemistry of the dispersed phase, and colloidal dispersions can be understood on this basis. We are concerned with reviewing the electrical aspect of liquid / solid interfaces, and its relation to the stability and behavior of lyophobic colloids*

In present day industrial technology it is common to deal with dispersions of a solid in a liquid, or with emulsions of two immiscible liquids. Although a system is said to be a dispersion when it consists of a homogeneous continuous phase that contains a discontinuous second phase, a dispersion may exist in three distinct conditions depending upon the degree of subdivision of the discontinuous phase. For example, during the hydraulic transport of a coarsely ground limestone through a pipeline, we are able to determine the technologically important physical properties of the system from the bulk properties of the separate phases and by application of appropriate laws of mechanics and hydraulics; chemical composition of the phases, as such, is unimportant. If, however, the same limestone-water mixture is subjected to grinding to reduce the particles to submicron size, the system takes on characteristics unpredicted by the laws that previously applied; it may behave as a semisolid paste or as a free-flowing liquid, depending upon the presence of trace amounts of certain dissolved electrolytes that have no discernible effect on the original mixture. Further reduction of particle size to atomic dimensions, say by dissolving with hydrochloric acid, will yield a system with a third type of behavior—that characteristic of liquid phases.

The coarse particles in water might be called a gross dispersion, if the term mixture is regarded as inadequate; the system of fine particles is termed a colloidal dispersion, or more specifically, a sol or suspension; the third system consists of a molecular or ionic dispersion, although strictly speaking it is a one-phase system. It is the systems characterized by a degree of subdivision intermediate between gross and molecular that are of special interest to many because of their unique properties; it is the study of such systems that has led to development of the discipline of colloid science.

Colloidal systems have been the subject of rather intensive investigation for more than a century (the colloidal condition was recognized by Selmi as early as 1845). But not until the past few decades has anything like an adequate basis for theoretical development been available. Even today, nomenclature of the subject tends to reflect its long history as an observational science. Some terms reflect inaccurate hypotheses or experimental limitations; their meanings are sometimes misunderstood. For instance, we might refer to a particular substance as a colloid, but should realize that a colloidal state of matter, as distinguished from the crystalline state, does not exist as was once thought. Properly, the term "colloid" should be used with reference to a whole colloidal system.

Historically, two major classes of colloidal systems have been recognized; these are lyophilic and lyophobic colloids. Gelatin, starch, gums, some synthetic polymers, and similar materials that show such a marked affinity for water or other appropriate solvent that they form spontaneously a colloidal sol when mixed are classed as lyophilic colloids. Liquid dispersions of small solid or liquid particles produced by mechanical or chemical means are termed lyophobic colloids.

Because these terms imply an interaction with the solvent that may not actually exist, some workers prefer the terms "reversible" and "irreversible" colloids in place of lyophilic and lyophobic, respectively.

Lyophilic colloids, according to present day knowledge, are essentially true solutions and perhaps are better described as macromolecular colloids; the class also includes association colloids such as micellar solutions of surface active agents.

The primary property of lyophobic colloids that sets them apart is their great sensitivity to electrolytes; addition of small amounts of soluble salts to such dispersions will generally cause the particles to clump together, or flocculate. Lyophilic colloids, being true solutions, are insensitive to electrolytes and do not flocculate in the same sense, although they may be precipitated by high salt concentrations.

The classical, and to a great extent current, definition of the colloidal state is in terms of size alone; the lower limit is generally taken to be in the neighborhood of 10 to 50 Å., and the upper size limit, in the older literature, as 0.1–0.2 micron. The lower size limit at which we differentiate between a colloidal particle and a dissolved molecule is understandably vague, but the upper size limit is annoyingly arbitrary in that it was chosen because it represented the smallest particles visible with the light microscope. More recent authors have considered the colloidal range to extend to the region of 1-micron size but, again, this is an artificial limit corresponding roughly to the maximum size of particle that will stay in suspension for a reasonable time.

Dispersions of particles smaller than 1 micron are commonly considered sols, whereas those in which the particles are larger than 1 micron are considered suspensions. While the terms sol and suspension are useful to convey an idea of particle size, it is undesirable to thus separate suspensions (and most emulsions) from colloid science because of their degree of subdivision, as is frequently implied. Emulsions and suspensions may exhibit colloid properties and can be so treated.

How, then, should we define the colloidal size range? So that our definition will apply to systems having certain characteristics in common, it must distinguish colloidal dispersions from true solutions on the one hand, and from boulders in a lake on the other. We do this indirectly by defining a colloidal dispersion as one in which the discontinuous phase is subdivided into units that are large compared with simple molecules, but small enough so that interfacial forces, as well as inertial forces, are significant in governing system properties.

Some of the properties commonly associated with colloids, such as Brownian motion, diffusion rates, and light scattering phenomena, are direct functions of particle size. But the behavior of the system, as regards its stability or rheology for instance, is a function of the nature, as well as extent, of the particle-fluid interface. The above definition is therefore an operative one based on the macroscopic properties of a dispersion; it perhaps reflects the bias of the authors, because in practical situations, usually the bulk properties must be controlled.

The properties of colloidal dispersions, therefore, may be changed in two ways: by effecting a change in particle size distribution and hence interfacial area through crystal growth, by comminution, or by fractionation into differing size ranges; and by changing the nature of the interface by adding electrolytes or surface-active agents.

The extent of interface between a dispersed particle of given shape and the surrounding continuous phase is proportional to  $d^2$ , where  $d$  is a characteristic linear dimension of the particle; the inertia or mass of the particle increases with  $d^3$ . As a result, the ratio of interfacial to inertial forces varies with  $d^{-1}$ —hence the rapid appearance of colloid properties as a dispersion is made finer. This relation is shown in Figure 2. The diagram illustrates that particle shape is a large factor in any such relationship. The value of  $d$  below which interfacial effects become significant may be said to represent the upper colloidal size limit.

But more than size and shape must be considered with regard to inertial forces: the effective mass of the dispersed particles will also be determined by their density relative to the dispersing medium. If the density difference is small, then interfacial forces can be important up to large particle sizes. For example, if we attempt to mix clean polystyrene beads of about 1-mm. diameter with pure water, the beads tend to cling together and float to the surface in spite of their slightly higher density. The surface of the plastic resists being wet by the water, and the effective mass of the particles plus attached air is not great enough to overcome this resistance.

The extent of interface in a given dispersion is often a fixed quantity; any changes in the bulk properties of the system must then be brought about by changing the character of the interfacial region. In the example quoted above, the addition of a trace of an appropriate surfactant to the water allows the plastic to be completely wetted, and the beads will deflocculate and sink. As another example, a moist, crumbly mass of kaolin clay may be transformed into a free-flowing liquid by the addition of a fraction of a per cent of an alkali polyphosphate and resolidified by a trace of calcium

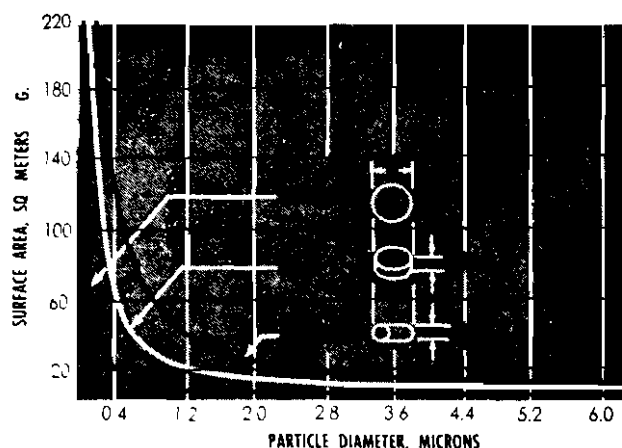


Figure 2. Variation of surface area with particle size. Note that 1-micron spheres, 4-micron disks; and 7-micron cylinders should be equally colloidal according to our definition

chloride. Observations such as these illustrate that interfacial forces do indeed control the behavior of even coarse colloidal dispersions, and that these forces are very susceptible to alteration.

The colloid chemistry of lyophobic systems is, therefore, the surface chemistry of the dispersed phase. The size of colloidal particles is an incidental quantity except insofar as it affects the degree to which surface forces are manifested. Although this point of view was adopted by Freundlich by 1909 (34), the historical emphasis on particle size persisted. Only in relatively recent years has colloid science, in its broader aspect of surface chemistry, received widespread application.

### Historical Development

The phenomena referred to collectively as electrokinetic effects pertain to the liquid flow that occurs along a solid/liquid interface as a result of an applied potential gradient, and conversely to the potential developed when a liquid is made to flow along an interface. Reuss (82), in 1808, observed that when a potential difference was maintained across a porous plug of wet clay or sand separating two portions of water, a flow of water occurred from one side of the diaphragm to the other. This phenomenon, now called electroosmosis, is almost always observed when an e.m.f. is applied to electrodes located on opposite sides of a porous diaphragm immersed in water or other liquid. If the liquid flow is not restricted, it will continue as long as a potential difference is maintained; if the flow is restricted, a pressure will build up until it is sufficient to cause a back-flow through the diaphragm that exactly balances the electroosmotic flow.

Quantitative measurements of electroosmosis were first made by Wiedemann (108) about 1850 to determine the relation between pressure, flow, and applied potential. Equilibrium pressure was found to be proportional to applied voltage and independent of dimensions of the diaphragm for a given system; mass flow rate with no pressure-drop was proportional to the current applied, and was also independent of diaphragm dimensions.

About 10 years later, Quinke (78) reasoned that because a porous object essentially consists of a mass of fine capillaries, electroosmosis should occur in a single capillary tube; this was indeed the case. Quinke also discovered that when a liquid was forced to flow through a capillary tube or porous diaphragm, a potential difference was created; this is the converse of electroosmosis, and the e.m.f. developed is called the streaming potential. He further showed that the liquid flow in electroosmosis is not necessarily in the same direction as the current flow. These facts led to the hypothesis that the observed effects were caused by the presence of electrically charged layers of opposite sign at the solid/liquid boundary. An applied voltage would therefore cause a relative displacement of the charged layers; the liquid, being free to move, thus flowed in a direction dependent on the sign of the charge it carried.

This hypothesis also explained the streaming potential as the result of a charge displacement caused by the

forced flow of liquid along the solid surface.

A third manifestation of the electrokinetic effect was investigated in 1880 by Dorn (27), who noted that when suspended particles are forced to move through a liquid in response to gravitation, a potential gradient is generated in the direction of movement. This phenomenon, variously called the Dorn effect, sedimentation potential, centrifugation potential, or migration potential, can also be qualitatively explained by this hypothesis.

The development of the theory of the electric double layer dates from 1879 and the work of Helmholtz (47), who postulated that formation of such a layer was of general occurrence at a phase boundary. He related mathematically the velocity of electroosmotic flow to charge separation in the double layer; the flow was shown to depend on an "electrokinetic potential" that corresponded to the potential drop across the layer of charge contained in the moving liquid.

At about this time, Schulze (89, 90) showed that certain colloidal sols (the lyophobic colloids) were rendered unstable and flocculated by the addition of electrolytes, and that multivalent ions had a disproportionate effect in this regard. In 1892, Linder and Picton (60) made the important observation that the particles in a colloidal sol migrate under the influence of an electric field, indicating that they are electrically charged with respect to the dispersion medium. Determination of the sign of the particle charge from the direction of its movement now made it clear that the flocculating effect of electrolytes was determined by the valency of the ion of opposite charge to the sol. This generalization is now called the Schulze-Hardy rule.

Hardy (45) and Burton (14) demonstrated that the stability of lyophobic sols is closely related to their mobility in an electric field; thus, the dependence of colloid stability on the degree of particle charge was established. Migration of particles in colloidal suspension in response to an applied electric field was first called cataphoresis, but the more general term electrophoresis is now preferred.

The assumption that the particle charge was created by the presence of an electric double layer, as proposed to account for electroosmotic flow and streaming potential, received further support from the extensive investigations of Perrin (73). He showed that the effectiveness of electrolytes in decreasing electroosmotic flow depended on the valency of the ion of opposite charge to the surface; hence the effect is completely analogous to the Schulze-Hardy rule.

By the beginning of the twentieth century, results of the investigations of Schulze, Linder, Picton, and others had aroused great interest in electrokinetic phenomena, for these methods seemed to provide a way of investigating the structure and properties of the electric double layer. Stability of colloidal sols could now be qualitatively explained in terms of a coulombic repulsion, but the origin of the surface charge and its quantitative relation to the concentration and valency of dissolved ions were yet to be explained before the problem of stability could be attacked in detail.

The experimental methods currently used for determining electrokinetic zeta potential are summarized in Table I. These are described later in this article.

### Theory of Electrokinetic Effects

Since the initial work of Helmholtz, theoretical interpretation of electrokinetic effects in terms of double-layer structure has received more detailed consideration from many investigators; results show that a rigorously quantitative treatment presents many difficulties not yet completely overcome. Useful approximations to exact expression of the relationships may be derived, however, as the basic factors are easily visualized.

Consider, for example, a solid in contact with an aqueous electrolyte solution. According to the double-layer hypothesis, the solid (by mechanisms to be considered later) will acquire a certain charge density localized in the plane of its surface; thus, a difference in

TABLE I. METHODS OF DETERMINING ELECTROKINETIC POTENTIAL

Method	Medium	Phase	Measurement
Electrostatic potential	Solid	Solid	Electrostatic potential
Streaming potential	Liquid	Liquid	Streaming potential
Electroosmosis	Liquid	Liquid	Electroosmosis
Pressure	None	None	Pressure
Velocity	Liquid	Liquid	Velocity

electrical potential between the surface and the bulk solution will be produced. Because the system as a whole is electrically neutral, the surface charge must be exactly balanced by an opposite excess charge in the liquid phase. Because of coulombic attraction the counterions will tend to concentrate in the vicinity of the solid surface, while ions of similar charge are repelled.

If no other force were operating, the potential drop across the double layer from the solid surface through the layer of counterions would be sharp. However, the ions in solution are subject to diffusional forces arising from the thermal agitation of the molecules constituting the liquid; thus the abrupt concentration gradient that would otherwise exist is dissipated to some extent. Our model of the double layer therefore involves an immobile surface-charge layer and a diffuse layer of counterions distributed in the adjacent solution according to some equilibrium function; this results in a more or less gradual decrease in potential with increasing distance from the surface.

A theoretical treatment of the structure of the double layer relating the distribution of the dissolved ions and the potential gradient near the surface to the composition of the aqueous phase was first performed by Gouy (41, 42), and independently by Chapman (15). These detailed considerations, and the modifications proposed by Stern (95) and Grahame (44) need not be introduced.

**Electroosmotic Flow.** To account for electrokinetic phenomena, it is only necessary to assume that the diffuse region of the double layer (the Gouy layer) is at least in part mobile—i.e., free to move with the liquid phase. We will say, therefore, that a shear plane may exist in the diffuse double layer at some unknown distance from the solid surface. When an external electric field is applied tangentially to a fixed surface, the mobile portion of the diffuse double layer will flow because of the forces acting on the excess ionic charge contained within it. A constant flow rate will be reached when the force exerted by the external field on the counterions (hence, on the liquid as a whole) is exactly balanced by the frictional forces arising from the viscosity of the liquid. We shall show, following Kravt (57), that a quantitative relation between the electroosmotic velocity of flow, the double-layer potential at the shear plane, and the applied external field may be derived without further consideration of the double-layer structure.

The double layer must satisfy Poisson's equation

$$\nabla^2\psi = -4\pi\rho/D \quad (1)$$

where  $\nabla^2$  is the Laplace operator,  $\psi$  is the double-layer potential at a point located a distance  $x$  from the surface,  $\rho$  is the net space charge per unit volume at the same point, and  $D$  is the dielectric constant of the medium. We assume that the liquid undergoes laminar flow, that its viscosity  $\eta$  and dielectric constant  $D$  are uniform throughout the mobile part of the double layer, and that the thickness of the double layer is small compared to the radius of curvature of the surface.

When an external field of strength  $E$  is applied, each volume element in a layer of liquid of thickness  $dx$  at a distance  $x$  from the surface will experience a force:

$$F_1 = E\rho dx \quad (2)$$

At the steady state, the viscous drag on the liquid layer will be contributed by adjacent layers that are moving at a different velocity. The side of the layer at a distance  $x$  from the surface will be retarded by a force given by

$$f_x = -\eta (dv/dx)_x \quad (3)$$

where  $v$  is the liquid velocity; the side at a distance  $x + dx$  from the surface will be accelerated by a force

$$f_{x+dx} = \eta (dv/dx)_{x+dx} \quad (4)$$

The net frictional force on the layer in question is:

$$F_2 = \eta (dv/dx)_{x+dx} - \eta (dv/dx)_x \quad (5)$$

At steady state, the total force on the layer is zero:

$$E\rho dx = \eta (d^2v/dx^2)dx \quad (6)$$

By substituting in Equation 6 the value of  $\rho$  given by Equation 1, and by recognizing that for a plane surface

$$\nabla^2\psi = (d^2\psi/dx^2) \quad (7)$$

we obtain

$$-\frac{ED}{4\pi} \frac{d^2\psi}{dx^2} = \eta \frac{d^2v}{dx^2} \quad (8)$$

This must be integrated over the whole liquid from the shear plane to infinity. The first integration yields

$$-\frac{ED}{4\pi} \frac{d\psi}{dx} = \eta \frac{dv}{dx} + C$$

and  $C$  is zero from the boundary condition that

$$(d\psi/dx)_{x=\infty} = 0; (dv/dx)_{x=\infty} = 0$$

The second integration yields

$$-(ED/4\pi)\psi = \eta v + C'$$

From the conditions that at  $x = \infty$ ,  $\psi = 0$  and  $v = v_e$  (the electroosmotic velocity), and at the shear plane,  $v = 0$  and  $\psi = \zeta$ , we obtain the classical expression

$$v_e = DE\zeta/4\pi\eta \quad (9)$$

Within the framework of our assumptions, therefore, electroosmotic flow caused by a given applied voltage gradient should indeed be determined by the potential at the boundary between the fixed and mobile parts of the double layer, as had been indicated by Helmholtz. In many textbooks we find the relation expressed by Equation 9 derived on the basis of a parallel plate capacitor model of the double layer and we might be misled to assume that this model constitutes an approximation in the derivation; the derivation given here shows that the same result is obtained on the basis of a diffuse double layer of unspecified form with the capacitor model representing the limiting case of zero diffusion. Consequently the zeta potential, as determined by experimental measurements, can by itself tell us nothing about the structure of the double layer. On the other hand, the zeta potential represents a real physical quantity accessible to experimental determination (at least to a first approximation), and therefore any theoretical consideration of the structure of the double layer and its relation to soluble electrolytes must account for its magnitude and variation.

The electroosmotic velocity given by Equation 9 is not the quantity ordinarily determined experimentally; usually, volume rate of liquid flow, or equilibrium counterpressure developed by the liquid, is determined as a function of the applied field. In all the expressions given for electrokinetic effects, c.g.s. units are implied. The practical unit of voltage must be divided by a factor of 300 to obtain potential in e.s.u.—for example, the right side of Equation 9 must be divided by  $9 \times 10^4$  if  $E$  and  $\zeta$  are expressed in practical units (volts per centimeter and volts, respectively).

If we consider the case of electroosmotic flow in a capillary of uniform cross sectional area  $A$ , then, using Equation 9, the expression for volume flow rate is:

$$V_e = Av_e = ADE\zeta/4\pi\eta \quad (10)$$

This equation is an approximation in that it assumes that all the liquid moves with the velocity  $v_e$ , whereas the mobile part of the double layer near the shear plane moves more slowly than  $v_e$ . Equation 10 may only be applied, therefore, when the thickness of the double layer is much smaller than the capillary diameter. This condition holds for capillaries larger than 1-micron diameter.

We may eliminate the area  $A$  by use of Ohm's law

$$E = i/\lambda \quad (11)$$

where  $\lambda$  is the specific conductance of the liquid and  $i$  is the current passing through the capillary. Substitution of Equation 11 in Equation 10 gives

$$V_e = D\zeta i/4\pi\eta\lambda \quad (12)$$

which is useful because  $i$  and  $\lambda$  are easily measured.

We must now consider whether Equation 12 is applicable to the electroosmotic flow in porous plugs. A rigorous treatment of the question has been given by Von Smoluchowski (106), and the following might be called a more intuitive version of his reasoning.

Assuming that a porous plug can be represented by a parallel combination of capillaries, each of nonuniform cross section, we may proceed in the following way. First, we examine a single capillary of insulating material with a nonuniform cross section. At any arbitrary location  $x$  on the capillary axis, the rate of liquid flow across the whole cross-sectional area  $A_x$  is:

$$(V_e)_x = A_x E_x D\zeta/4\pi\eta$$

where  $E_x$  is the local electric field (which is everywhere parallel to the insulating walls). At another location a distance  $dx$  from the first, we have

$$(V_e)_{x+dx} = (A_{x+dx} E_{x+dx} D\zeta)/4\pi\eta$$

If the liquid is incompressible, we have the requirement

$$dV_e/dx = 0$$

Hence, for Equation 12 to be applicable at any point:

$$d(AE)/dx = 0$$

This latter condition is met, for it is the requirement that Ohm's law (Equation 11) applies to the system at every point—i.e., the electric current also flows as if it were an incompressible liquid. Therefore, Equation 12 is valid for a capillary of arbitrary and nonuniform cross-sectional area. It also applies to any parallel combination of such capillaries, as the total volume rate of flow and the total applied current are given by summing the respective contributions of each capillary; the condition that the pore diameter be large compared to the double-layer thickness must, as with Equation 10, be observed.

**Electroosmotic Pressure.** When the electroosmotic effect is measured in terms of the counterpressure required to obtain zero rate of flow through the capillary or porous plug for a given applied field, the zeta potential may be calculated by realizing that the electroosmotic pressure  $P_e$  must cause a reverse flow of liquid in the capillary or porous plug exactly equal to the volume transported by electroosmosis.

With a capillary of uniform circular cross section, the backflow is given by Poiseuille's equation.

$$V_e = \pi P_e r^4/8\eta l \quad (13)$$

Equating Equations 12 and 13, we obtain

$$P_e = (2D\zeta li)/(\lambda\pi^2 r^4) \quad (14)$$

where  $r$  is the radius and  $l$  the length of the capillary. Or, by making use of Equation 11:

$$P_e = (2DE\zeta)/\pi r^2 \quad (15)$$

The product  $El$  corresponds to the total applied potential.

With a porous plug, the counterflow is not directly given by Equation 13, but it may be expressed by

$$V = KPA/\eta L \quad (16)$$

where  $A$  is the area and  $L$  the length of the diaphragm, and the constant  $K$  is determined experimentally by measuring flow rate as a function of pressure with no applied field. By use of Equations 12 and 16 we find

$$P_e = (D\zeta Li)/(4\pi\lambda_p KA) \quad (17)$$

where  $\lambda_p$  is now the specific conductance of the liquid-filled diaphragm. The quantity  $L/\lambda_p A$  is therefore the electrical resistance across the plug and hence

$$P_e = DE\zeta/4\pi K \quad (18)$$

where  $E$  is now the total applied potential.

The expressions derived above for the electroosmotic

effect state that flow rate will be proportional to applied current, and counterpressure proportional to applied voltage, but both are independent of capillary or diaphragm dimensions; this agrees with the experimental findings of Wiedemann (108), referred to above.

**Streaming Potential.** The streaming potential  $E_s$  is the voltage difference developed between the ends of a capillary tube or porous diaphragm through which liquid is forced to flow by an applied pressure difference  $P$ . An expression relating  $E_s$  to  $P$  and the zeta potential may be derived for laminar flow through a circular capillary of uniform diameter, where the diameter is much greater than the thickness of the double layer.

Liquid flow through the capillary carries with it the mobile part of the double layer and its contained charge. A potential difference in the direction of liquid flow is thus established and a reverse flow of electricity through the liquid will occur. At the steady state, the charge transported by the moving double layer per unit time will be balanced by the current conducted through the liquid. Equilibrium potential difference is therefore:

$$E_s = il/\lambda\pi r^2 \quad (19)$$

where  $r$  is the capillary radius;  $l$ , its length;  $\lambda$ , specific conductance of the liquid; and  $i$ , the electric current.

Velocity of flow in the double layer is not constant; it varies from zero at the shear plane to a maximum value at the capillary axis. The liquid velocity at a distance  $x$  from the shear plane (measured along a radius) is:

$$v_x = P(2rx - x^2)/4\eta l \quad (20)$$

The volume of liquid with a velocity  $v_x$  is represented by a hollow cylinder of radius  $(r - x)$  and thickness  $dx$ ; volume rate of flow in this cylindrical layer will be

$$2\pi(r - x)v_x dx = dV = \frac{2\pi P}{4\eta l} (2rx - x^2)(r - x)dx \quad (21)$$

and the rate of charge transport will be

$$i = \int_0^r \rho dV \quad (22)$$

Substituting Equation 1 and Equation 21 in Equation 22, and assuming  $x$  is negligible with respect to  $r$ , we obtain

$$i = \frac{PD r^2}{4\eta l} \int_0^r x \frac{d^2\psi}{dx^2} dx \quad (23)$$

If Equation 23 is solved by partial integration and if boundary conditions are applied such that at  $x = 0$ ,  $\psi = \zeta$ ; and at  $x = r$ ,  $\psi = 0$ ,  $d\psi/dx = 0$ , then

$$i = (PD r^2 \zeta)/4\pi\eta\lambda \quad (24)$$

Using Equation 19 and rearranging terms, we obtain the final expression for streaming potential:

$$E_s = PE\zeta/4\pi\eta\lambda \quad (25)$$

A more general derivation of Equation 25 shows that it is also applicable to a porous plug (57, page 204).

**Electrophoresis.** The phenomenon of electrophoresis is essentially the converse of electroosmosis in that the solid is not fixed in position as part of a diaphragm, but is free to move; the suspending liquid as a whole is stationary. In either case, forces acting on the double layer as a result of an applied potential gradient produce a relative movement; therefore, the electrophoretic velocity is given by the same expression.

$$v_E = DE\zeta/4\pi\eta \quad (26)$$

As with electroosmosis, shape and size of the particles have no effect on the resulting velocity, provided that the double layer is thin compared to the dimensions of the particle. Unfortunately, this condition is not so easily met for finely divided colloidal dispersions such as sols, and the problem of the appropriate correction factors for Equation 26 is still not completely solved.

**Corrections for Deviations from Theory.** In the preceding analyses, assumptions have been made that affect the validity of the derived expressions to varying degrees, and under certain circumstances, can destroy their usefulness even as first-order approximations.

The assumption of laminar flow in the liquid represents a condition that is easily met in practice; deviations would be likely only in streaming potential measurements at such high pressures that turbulent flow occurs.

Constancy of the viscosity coefficient  $\eta$  and the dielectric constant  $D$  are assumed because experimental and theoretical information concerning their variation is lacking at the present time. Further work in this area might well show that the concept of a shear plane separating mobile and immobile parts of the double layer represents an approximation to a region of more or less rapidly changing viscosity near the solid surface caused by the high concentration of ions of like charge. If such a relation could be developed, the equation for electrophoretic velocity would require solution of

$$v_E = \frac{E}{4\pi} \int_0^\psi \frac{D}{\eta} d\psi \quad (27)$$

Equation 9, basic to all electrokinetic phenomena, is derived for a mathematically plane surface (Equation 7), a condition seldom encountered; little error is introduced in many practical situations, however, because the thickness of the double layer, seldom exceeding  $10^{-5}$  cm. and usually closer to  $10^{-6}$  to  $10^{-7}$  cm., is small compared to the capillary or particle dimensions. In electrophoresis of the smallest sol particles, the assumption of a plane surface must be discarded and account taken of the curvature of the double layer.

The expression for electroosmotic flow (Equation 10) also requires that the double-layer thickness be negligible compared to pore dimensions. It assumes that flow in the double layer occurs at the same velocity as in the bulk liquid, whereas it actually is somewhat slower. For fine capillaries—e.g., 1-micron diameter—and dilute electrolytes ( $\cong 10^{-5}N$ ) where the double-layer thickness is of the order of  $10^{-5}$  cm., Equation 10 would lead to values of  $\zeta$  about 10% too low. To correct the equation, we need an analytical expression for double-layer potential as a function of distance from the surface.

Implicit in the derivation of Equations 12 and 25, which describe electroosmosis and streaming potential, respectively, is the requirement that the electrical resistance of the systems be determined by  $\lambda$ , the specific conductance of the liquid phase; this ignores the contribution of surface conductance to the current flow. The specific conductance of the surface is greater than that of the bulk liquid because of the higher concentration of ions in the double layer; conductance along the surface may be of the same order of magnitude as through the



bulk liquid in the case of dilute solutions. In Equations 11 and 19,  $\lambda$  should be replaced by the total specific conductance:

$$\lambda_T = \lambda + (2\lambda_s/r) \quad (28)$$

where  $\lambda_s$  is the specific surface conductance and  $r$  is the capillary radius. This correction can only be made in the case of uniform capillaries (57, page 206). As no valid correction for surface conductance applicable to porous plugs is presently available, accurate values of zeta potential from experiments on porous plugs can only be obtained if the surface conductance is negligible.

Conditions for the application of Equation 26, both in electroosmosis and in electrophoresis, are that the double layer be thin compared to particle dimensions (electrophoretic retardation effect), and that the surface (and bulk solid) conductance be so small that the external

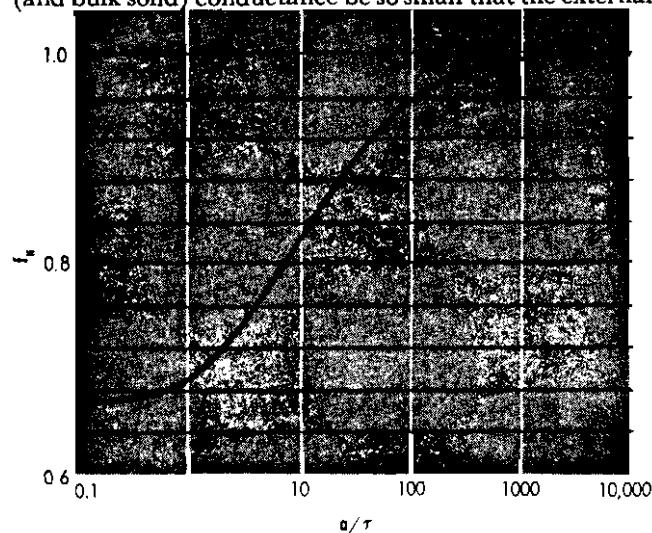


Figure 3. Correction factor for ratio of particle radius to double-layer thickness, for spherical particles

applied field is not disturbed (relaxation effect). Surface conductance reduces electrophoretic velocity by distorting the electric force-field. An approximate correction has been worked out for this effect (48).

Henry (48) has also solved the electrophoretic equations for any ratio of the particle size to double-layer thickness. His solutions are limited, however, to spheres and cylinders. His derived equation has the form

$$v_E = f_H (DE\xi/4\pi\eta) \quad (29)$$

The retardation factor  $f_H$  is a function of  $a/\tau$ , where  $a$  is the particle radius and  $\tau$  is the double-layer thickness. For spherical particles,  $f_H$  varies from  $2/3$  to 1 (Figure 3). The thickness of the double layer is given by

$$\tau = \left( \frac{DkT}{8\pi e^2 \sum n\nu^2} \right)^{1/2} \quad (30)$$

where  $e$  is the electronic charge and  $n$  is the concentration of ions of valency  $\nu$  in the bulk liquid. Equation 29 is strictly valid only for  $\xi \leq 25$  mv.

Calculation of the relaxation correction poses a difficult mathematical and theoretical problem, and a satisfactory solution has not been reached. Overbeek's calculations (57, page 211) indicate that the relaxation effect may be small in the case of 1-1 electrolytes for all values of  $a/\tau$ ; for values of  $a/\tau$  greater than  $10^2$ , both the retardation and relaxation corrections are small, and

Equation 26 can be used directly. When  $a/\tau$  has values in the range 0.1 to 100 and multivalent electrolytes are involved, both corrections may be large; the zeta potential then calculated can be seriously in error.

#### Ion Distribution in the Double Layer

The above discussion shows that electrokinetic phenomena can be described accurately by merely assuming the presence of a double layer of charge at the solid/liquid interface, provided that the double layer occupies a negligible portion of the system in question. When this condition does not prevail, further analysis will require a specific description of the double-layer structure—i.e., an expression for potential in the double layer as a function of distance from the solid surface. Such a situation will arise in any theoretical consideration of the stability of colloidal dispersions. In order to flocculate, colloidal particles must approach each other, collide, and adhere; during this process, the distance between the particles will decrease to values not only comparable to, but less than the double-layer thickness.

The formation of a double layer requires that the solid surface be charged. We can recognize three mechanisms by which this potential is developed:

—The crystal lattice of the solid may contain a net positive or negative charge arising from interior defects or lattice substitutions; the net charge is therefore compensated by an equivalent ionic charge at the surface. In contact with water, the compensating ions dissociate to form the counterions of the double layer. This type of double-layer formation, while generally uncommon, is important in describing the behavior of certain ion exchanging minerals, such as the zeolites, and clay minerals, such as montmorillonite (103). Solids that contain ionizable groups at their surface, such as sulfonated organic polymers, may also be considered as belonging to this class, which is characterized by a surface charge density that is a fixed quantity independent of the concentration of ions in the surrounding liquid.

—In the case of sparingly soluble ionic solids dispersed in water, an equilibrium exists between the ions making up the surface of the crystal and these same constituent ions in solution, where their concentrations are determined by the solubility product for the material. The potential of the solid will thus be fully determined by a thermodynamic (adsorption) equilibrium, in accord with a Nernst equation. Using colloidal AgI as an example we have:

$$\psi_0(\text{AgI}) = A + (RT/F) \ln C_{\text{Ag}^+}$$

$$\text{or} \quad \psi_0(\text{AgI}) = B - (RT/F) \ln C_{\text{I}^-} \quad (31)$$

where  $A$  and  $B$  are constants,  $\psi_0$  is the potential of the solid surface with respect to the bulk liquid,  $F$  is the Faraday charge, and  $C$  is the concentration (activity) of the particular ion in solution. Thus, if excess silver ions are added to the solution,  $\psi_0$  will become more positive; addition of excess iodide ions will make  $\psi_0$  more negative. At some point the potential will be zero, and the concentration of silver or iodide ions at this point is called the zero point of charge concentration. In general, we may express the potential of the solid by

$$\psi_0 = (RT/\nu F) \ln (C/C_0) \quad (32)$$

where  $\nu$  is the valency and  $C_0$  is the zero point of charge concentration;  $C_0$  does not necessarily correspond to the equivalence point, because one of the ions is usually more strongly adsorbed by the solid than the other. If it is the anion that is selectively adsorbed, then the solid will acquire a negative potential with respect to the solution at the equivalence point. The value of  $C_0$  can be accurately determined by electrokinetic experiments as it corresponds to zero movement, and no corrections need be applied. The potential-determining ions for

a given solid are usually apparent from its chemical composition. For most metallic oxides and hydroxides,  $H^+$  and  $OH^-$  ions are potential-determining. Solids of this class are characterized by having the potential at the solid surface fixed by the concentration of potential-determining ions and independent of the presence of other indifferent electrolytes; that the surface charge, however, will be increased by the addition of indifferent electrolytes will be shown later.

—A third mechanism by which the surface charge may originate or be affected is the adsorption of specific ions from the solution. Specific ions may be strongly adsorbed, or chemisorbed, by formation of a surface complex or compound—for example, the tri(poly)phosphate anion complex with aluminum sites on the kaolinite surface (63). Adsorption may also be aided by hydrogen bond formation or by the London dispersion (van der Waals) forces, particularly in the case of large organic molecules or ions. The adsorption mechanism is seldom responsible for the entire surface charge or potential of a solid surface (except for potential-determining ions); it is frequently a complicating factor in the other mechanisms. In some cases, the extent of adsorption, or even the adsorption isotherm of specific ions on the solid surface, may be determined from analytical measurement (57, page 161).

In general, those ions that increase the potential of the solid surface by their presence are effective as "peptizing," "stabilizing," or "deflocculating" agents for the system. The term "dispersing agent," although commonly used in industry, should be avoided, for a colloidal sol or suspension does not necessarily cease to be a dispersion when it is flocculated.

The formation of an electric double layer is easily imagined in the case of a charged surface in contact with an aqueous electrolyte solution; the ions in the solution will respond to the field of force near the interface by taking up new positions until a distribution is reached that represents an equilibrium between thermal and electrostatic forces. The analysis of the distribution, while it resembles the Debye-Huckel theory of strong electrolytes (20), was carried out about a decade earlier by Gouy (41, 42) and independently by Chapman (15).

**Gouy-Chapman Model.** Analysis of the double layer according to the model of Gouy and Chapman involves several assumptions. The charge on the solid surface is considered to be uniformly distributed; the ions making up the diffuse layer are considered as point charges; and the solvent is a structureless medium whose only influence is through its dielectric constant.

A basic requirement of the space charge in the double layer is that Poisson's equation be satisfied (Equation 1). The distribution of ions in the potential field is given by a Boltzmann relation analogous to the barometric formula.

$$n_i = n_{i0} \exp(-v_i e \psi / kT) \quad (33)$$

where  $n_i$  is the concentration and  $v_i$  the valency (including sign) of ions of kind  $i$  at a point where the potential is  $\psi$ ,  $n_{i0}$  is the bulk concentration,  $e$  is the electron charge, and  $k$  is the Boltzmann constant.

The space charge density  $\rho$  is the net sum of the positive and negative ion concentrations.

$$\rho = \sum v_i e n_i \quad (34)$$

Equations 1, 33, and 34 give the differential equation

$$\nabla^2 \psi = -\frac{4\pi}{D} \sum v_i e n_{i0} \exp\left(-\frac{v_i e \psi}{kT}\right) \quad (35)$$

that describes the variation of  $\psi$  with location in the double layer. For simplicity, the surface is assumed to be a plane, and Equation 35 integrates to give

$$\frac{d\psi}{dx} = -\left(\frac{8\pi n k T}{D}\right)^{1/2} \left[ \exp\left(\frac{v e \psi}{kT}\right) - \exp\left(-\frac{v e \psi}{kT}\right) \right] \quad (36)$$

where  $v$  is now the valency of the ion of charge opposite to that of the surface and  $n$  is its bulk concentration.

A second integration gives the final expression

$$\kappa x = \ln \frac{\left[ \exp\left(\frac{v e \psi}{2kT}\right) + 1 \right] \left[ \exp\left(\frac{v e \psi_0}{2kT}\right) - 1 \right]}{\left[ \exp\left(\frac{v e \psi}{2kT}\right) - 1 \right] \left[ \exp\left(\frac{v e \psi_0}{2kT}\right) + 1 \right]} \quad (37)$$

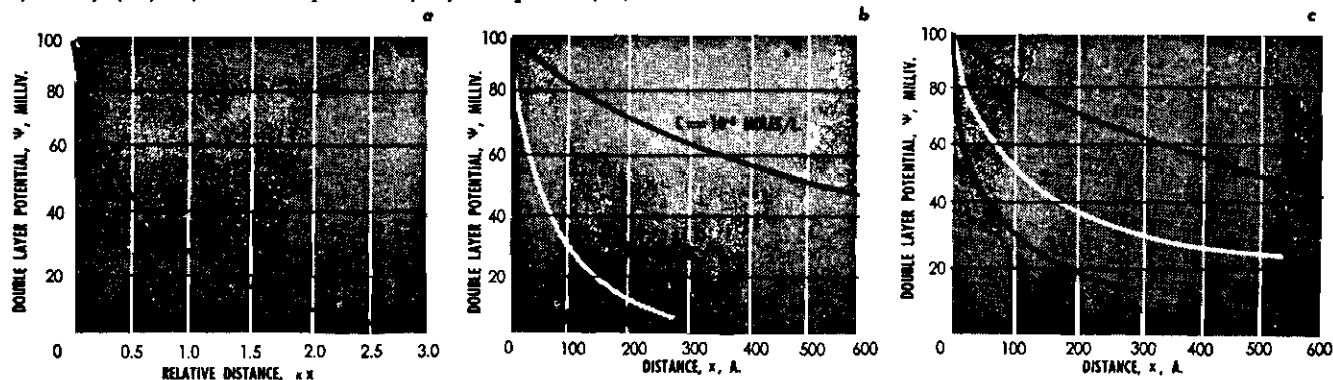
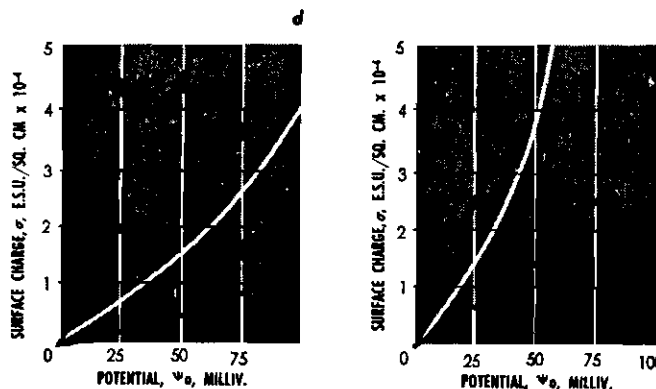


Figure 4a. A representation of Equation 37 for monovalent counterions and an arbitrary  $\psi_0$  of 100 mv. At a distance  $x$  equal to the double-layer thickness,  $\kappa x = 1$ ,  $\psi$  has decreased to roughly less than a third its maximum value. Figure 4b. Effect of monovalent electrolyte concentration, for  $\psi_0 = 100$  mv. (Equation 37). Added electrolyte compresses the double layer, so that  $\psi$  approaches zero more rapidly; the degree of compression is linear with  $(n)^{1/2}$ . Figure 4c. The marked effect of counterion valency is shown where  $\psi_0$  is 100 mv., electrolyte concentration is  $10^{-6}$  moles/liter. Value of  $v$  is indicated on the lines (Equation 37). Figures 4d and 4e. It is shown that the surface charge is proportional to  $(n)^{1/2}$  for a given value of  $\psi_0$ , and that  $\psi_0$  is inversely proportional to  $v$  at a given charge density (Equation 41). Figure 4d is for monovalent electrolyte concentrations. Figure 4e is for 0.1 mole/liter electrolyte, with values of  $v$  indicated



where  $\kappa = (8\pi v^2 e^2 n / DkT)^{1/2}$  (38)

The function  $\kappa$  is the reciprocal of the double-layer thickness (Equation 30).

A relation between the surface charge density  $\sigma$  and  $\psi_0$  can be obtained from Equation 36, for the electro-neutrality of the system requires that

$$\sigma = - \int_0^\infty \rho dx \quad (39)$$

Using Equation 1 we can integrate the above expression

$$\sigma = \frac{D}{4\pi} \int_0^\infty \frac{d^2\psi}{dx^2} dx = - \frac{D}{4\pi} \left( \frac{d\psi}{dx} \right)_{x=0} \quad (40)$$

and insertion of Equation 36 gives

$$\sigma = \sqrt{\frac{DnkT}{2}} \left[ \exp\left(\frac{ve\psi_0}{2kT}\right) - \exp\left(-\frac{ve\psi_0}{2kT}\right) \right] \quad (41)$$

For surfaces of fixed potential, Equation 37 describes how  $\psi$  decreases from its initial value  $\psi_0$  with increasing distance from the surface at any given concentration of indifferent electrolyte. For surfaces of constant charge, however,  $\psi_0$  will depend on electrolyte concentration (Equation 41); once it is determined, Equation 37 will apply.

The effect of electrolyte concentration and valency on the value of  $\psi$  as a function of  $x$  or  $\sigma$  is shown in Figure 4.

In spite of the assumptions made, the Gouy-Chapman analysis of the double layer has been useful in developing an understanding of colloid stability. But in the study of electrocapillary effects, this model leads to a double-layer capacity that is much too high—i.e., the surface charge density  $\sigma$  given by Equation 41 is too large at high electrolyte concentrations or high potentials. The reason for this is made clear if we consider the situation at a surface having a potential of 200 mv. in a 0.1N monovalent electrolyte solution. By Equation 33 the electrolyte concentration near the surface should be 300N, which is impossibly high. Because we know that  $\psi_0$  can be even greater than 200 mv., the difficulty must lie in the assumption of point charges; one way around this difficulty was developed by Stern (95).

**Stern Theory.** Stern recognized that the error caused by neglect of the finite ionic size was important only in the immediate vicinity of the surface; in fact, the first layer of ions at the surface is usually sufficient to decrease the potential to values low enough so that the Gouy-Chapman model becomes reasonable. Stern proposed that the counterions could be considered as divided between a diffuse layer of point charges and an immobile surface layer of thickness  $\delta$  able to contain a certain maximum number of counterions per square centimeter. A Langmuir-type adsorption equilibrium is assumed between the ions in solution and those in the Stern layer, where the adsorption energy is divided into electrical and van der Waals contributions. The electric potential at the Stern layer is indicated by  $\psi_\delta$ , and the van der Waals energy by  $\phi$ . The adsorbed charge per unit area is then given by

$$\sigma_s = \frac{n\sigma_m}{n + A \exp\left(-\frac{ve\psi_\delta}{kT} + \phi\right)} \quad (42)$$

where  $\sigma_m$  is the charge corresponding to a monolayer of counterions and  $A$  is a frequency factor (57, page 133). Total charge density at the surface is then

$$\sigma = \sigma_s + \sigma_G \quad (43)$$

where  $\sigma_G$  is the charge density corresponding to the Gouy model when  $\psi_0$  is replaced by  $\psi_\delta$ . The total surface charge is also given by

$$\sigma = (D'/4\pi\delta) (\psi_0 - \psi_\delta) \quad (44)$$

if we assume that the Stern layer comprises a molecular condenser with a dielectric constant  $D'$ . The complete expression for the Stern model of the double layer is

$$\frac{D'}{4\pi\delta} (\psi_0 - \psi_\delta) = \frac{n\sigma_m}{n + A \exp\left(-\frac{ve\psi_\delta}{kT} + \phi\right)} + \left(\frac{DnkT}{2\pi}\right)^{1/2} \left[ \exp\left(\frac{ve\psi_\delta}{2kT}\right) - \exp\left(-\frac{ve\psi_\delta}{2kT}\right) \right] \quad (45)$$

If we have an estimate of  $D'$ ,  $\delta$ , and  $\sigma_m$ , the double layer can be described for surfaces governed by Equation 32 for  $\psi_0$ . Investigations of double-layer capacity in electrocapillary effects (44) show that  $D'$  has a value in the range 3–6 and that  $\delta$  is of the order of  $5 \times 10^{-8}$  cm.;  $\sigma_m$  can be estimated from hydrated ionic radii. For surfaces of constant charge, the left side of Equation 45 becomes a constant—i.e.,  $\psi_0$  and  $\psi_\delta$  decrease equally for a given change in concentration.

The Stern model, while still a crude picture of what we may imagine to be a complex situation, does display most of the properties of the double layer that have been inferred from experimental observations of double-layer capacity. This model also helps to explain the origin of the zeta potential calculated from electrokinetic effects.

In the theory of the electrokinetic effects, we introduced the concept of a shear plane located at some distance from the surface, but did not at that point indicate the reason. For a large class of surfaces, an absolute value of  $\psi_0$  can be obtained with Equation 32. Because  $\psi_0$  changes by 57 mv. per decade of concentration change, and because 6 or 8 decades are not unreasonable for a material such as AgI,  $\psi_0$  may have values up to several hundred millivolts. The corresponding values of  $\zeta$ , however, are much smaller (57, page 231); therefore, the shear plane must be located at a distance  $x$  corresponding to  $\psi = \zeta$ . The concept of a shear plane in the Gouy layer is somewhat of a contradiction of the model, however. The Stern theory provides a model in which a shear plane is already conceptually present. It is probable that  $\zeta$  corresponds more or less closely to  $\psi_\delta$ ; a rigorous test of such a correlation is difficult, for it is difficult to obtain good electrokinetic data on reproducible surfaces under conditions such that  $\zeta$  may be calculated with reasonable certainty.

An extension of the Stern model has been proposed by Grahame (44). Although both anions and cations can be adsorbed by forces other than electrical—i.e., chemical or van der Waals—anions are the less strongly hydrated; Grahame therefore postulates that the nonelectrical forces are chiefly operative for anions, which become adsorbed with loss of their hydration shells. By this model, the Stern layer is in turn divided into two parts: a

relatively thin surface layer (of variable occupancy) of strongly adsorbed anions whose centers of charge lie in a plane (inner Helmholtz plane) at a distance  $x_i$  from the surface, followed by a Stern layer (outer Helmholtz plane) of hydrated counterions whose centers of charge lie in a plane at a distance  $\delta$  from the surface and whose concentration is given by the Stern theory (Equation 42). The Gouy-Chapman model is then used for values of  $x$  greater than  $\delta$ .

As thus defined, however, it would appear that when the Stern layer is highly occupied, the distance of closest approach of ions in the Gouy layer to the Stern plane should be greater than  $\delta$  because the ions are not actually point charges; it would seem reasonable that the Gouy layer limit would be more accurately located at a distance  $\delta + d_c$ , where  $d_c$  is the diameter of the hydrated cation.

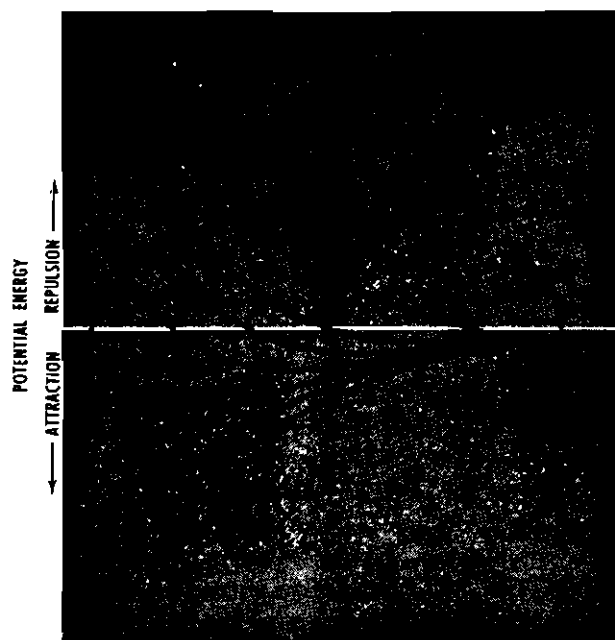


Figure 5. Net potential energy of interaction between colloidal particles. Curve 7—the attraction that exists in the absence of any repulsion. This corresponds to a high electrolyte concentration and rapid flocculation as described by Equation 47. Curves 6 to 1—show, in that order, the effect of decreasing electrolyte concentration that leads to increasing double-layer thickness, and hence, longer range repulsing forces. Curve 3—the barrier of about 15  $kT$  would impart considerable stability to the dispersion. Curve 4—slow flocculation would take place. Curve 5—flocculation would be rapid

Taking the effective anion diameter as  $d_a$  and the cation diameter as  $d_c$ , we have (for  $\psi_0$  negative)

$$\begin{aligned} x_i &= d_a/2; \delta = d_a + d_c/2 \\ x_{sp} &= d_a + d_c; x_G = d_a + 3d_c/2 \end{aligned} \quad (46)$$

where  $x_{sp}$  is the location of the shear plane and  $x_G$  locates the closest approach of diffuse ions.

Grahame's model is illustrated schematically in Figure 1, where the relative distances are in accord with Equation 46. The quantitative expression of the relationships involved depends on adsorption equilibria that are not well understood at present. One feature of the model is the activation energy required for chemisorption of ions of the same sign as the surface; another

is the possibility of eliciting an expression for the zeta potential, as the location of the shear plane seems reasonable and consistent with the model.

Of the various double-layer treatments that have been postulated, that of Bolt (9) is particularly interesting in that a variation of the dielectric constant with  $\psi$  is taken into account, as well as the effect of ionic size, polarization, and interaction. The results indicate that the original Gouy-Chapman expressions are valid for estimating particle-particle repulsion in the theory of stability, but not valid for the treatment of ion exchange equilibria.

### Stability of Colloidal Dispersions

The term stability, when applied to colloidal dispersions, is a relative term intended to express the resistance of the dispersion to change. The usual meaning is stability with respect to time, but the term could also refer to tolerance of added solutes, heat, freezing, vibration, dilution, etc. We will restrict ourselves here to reviewing briefly the theoretical aspects of the stability of dispersions toward flocculation with respect to time; we will not consider such changes as sedimentation or crystal growth through aging.

When we refer to a colloidal dispersion as deflocculated, or peptized, we imply a system in which the forces of repulsion acting to keep the particles separated exceed the forces of attraction that would cause particles to adhere on contact; in a flocculated system, the attractive forces predominate. The condition of the dispersion is not determined by a simple balance of forces, however. If this were the case, then a dispersion would either be perfectly stable or unstable, flocculating almost instantly; this is contrary to all observations.

The time for which sols are stable, or inversely, the flocculation rates of sols, is known to cover a wide range of values from years to fractions of a second. The observed range of flocculation rates indicates that even when the flocculated condition is the lowest energy state of the system (which thermodynamically is always the case) an energy barrier can exist that prevents particle to particle adhesion on contact, and that contacts can be frequent. The rate of flocculation will therefore depend on the collision frequency of the sol particles and their energy with respect to the energy barrier. Colloidal particles undergo Brownian motion and thereby diffuse and collide; they are in kinetic-thermal equilibrium with the suspending fluid. In the absence of an energy barrier, the flocculation rate will be determined solely by the collision frequency. The theory of rapid flocculation was developed by Von Smoluchowski in 1919 (57, page 278) and leads to the expression

$$N/N_0 = [1 + (t/T)]^{-1} \quad (47)$$

where  $N/N_0$  is the fraction of particles remaining per unit volume after time  $t$ . The term  $T$  is the time required for the number of particles to decrease to half the original number. Groups of adhering particles are counted as units in this expression.

The problem of slow flocculation, in which an energy barrier prevents the close approach of particles, has been summarized by Overbeek (57); by the model of diffusion

in a field of force, it is possible to show how the coagulation, or flocculation, rate is decreased by the barrier. Because colloidal particles diffuse slowly and their motion is random, the problem cannot be treated in the same way as a chemical reaction involving an energy barrier. It becomes necessary to know the total shape of the potential energy curve, rather than just its height.

Verwey and Overbeek (105) in 1948 published their now famous treatise on the interaction of sol particles having an electric double layer. Starting with a consideration of the free energy of the double layer, Verwey and Overbeek show how, on the close approach of two surfaces, the overlapping double layers interact to increase the free energy of the system, thus leading to a potential energy of repulsion. With the Gouy description of the double layer, it was possible to relate the energy of repulsion between particles as a function of their separation to the ionic makeup of the solution. The picture of the interaction was completed by a consideration of the London dispersion forces as applied to particles of colloidal size, which as an approximation

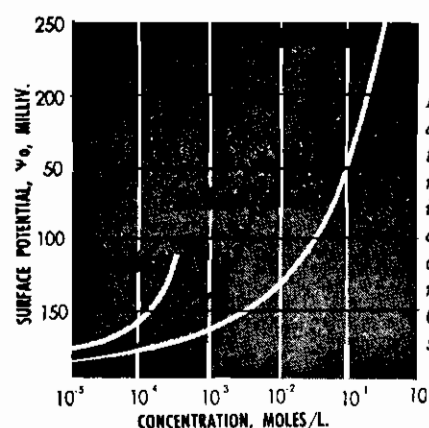


Figure 6. Electrolyte concentration necessary to produce moderately rapid flocculation. Taking  $\psi_0$  as 100 mv., concentrations of mono-, di-, and trivalent ions required are 50, 2, and 0.2 mmole./liter, respectively

leads to an attraction varying with  $d^{-2}$  for small distances, and with  $d^{-4}$  at larger separations.

Figure 5 shows schematically the net potential energy of interaction obtained by adding the two effects. Stability and flocculation of the dispersion are demonstrated by these curves, as explained in the caption.

Another feature of the curves obtained by Verwey and Overbeek is the secondary minimum occurring at relatively great distance of separation ( $\approx 200\text{\AA}$ ); in curve 4, this minimum is deep enough to trap a sizable fraction of the particles. This type of flocculation is reversible, as the particles can occasionally diffuse apart. Flocculation in the secondary minimum is shown by calculation (57, page 324) to be most probable for relatively large anisometric particles, and can account for the formation of tactoids and Schiller layers in sols of rod-like or platelike particles.

As well as accounting for the observed flocculation rates of sols at various electrolyte concentrations, the theory of Verwey and Overbeek quantitatively describes the Schulze-Hardy rule. This is illustrated in Figure 6 for particles with a platelike shape under moderately rapid flocculation conditions. The area to

the left of the curves defines the region of stability; this agrees with observations.

#### Measurement of Electrokinetic Effects

The methods for the determination of zeta potential all use the phenomena resulting from the impression of a potential or pressure gradient across the system being studied. For instance, small charged particles suspended in a system will move under the influence of an applied potential gradient; from the measurement of the resulting velocity of motion, the zeta potential may be calculated with the appropriate formula. If the particles can be held stationary, the liquid becomes the easily observed mobile phase and its flow rate can be measured and converted to zeta potential. If both liquid and particulate material are held fixed, the pressure developed may be used to calculate zeta.

Table I summarizes the presently used experimental methods for determining zeta potential that will be described in greater detail. For detailed descriptions of the various apparatus used, the references in the following sections should be consulted.

**Electroosmosis.** The apparatus for electroosmosis (Figure 7) requires that the material whose zeta potential is being determined can be formed into a capillary or a porous plug so as to constitute a system of capillaries. The porous plug is placed between two measuring electrodes connected to a high impedance voltmeter. When a potential gradient is established via the working electrodes, the electrolyte flows. If the system is kept closed, the rate of movement of the electrolyte can conveniently be observed by measuring the movement of a small bubble in the capillary and converting this to flow rate. If, during the impression of a voltage, the upper stopcocks are left open and no short-circuiting path is provided by a capillary, the electrolyte will rise in one of the tubes to an equilibrium level. The potential gradient is determined from the voltage across the measuring electrodes and their spacing.

When the rate of movement of the bubble is measured, the zeta potential may be calculated by Equation 12; when the pressure developed (as measured by the height of liquid rise) is measured, Equation 18 is used.

Electroosmosis has been used in the study of aqueous dispersions of kaolinite at various pH levels (4), of quartz in KCl solutions (84), of calcite in solutions of various salts (23, 43), and of bentonite in aqueous solutions of several salts (69).

**Streaming Potential.** The apparatus for determining streaming potential (Figure 8) is similar to that used for electroosmosis. Again, it must be possible to form the material into a capillary or a porous plug, held between two electrodes

To measure the streaming potential it is only necessary to measure the potential developed when the electrolyte is forced through the porous plug by a constant pressure. From the voltage developed, the zeta potential may be calculated by Equation 25, provided that the measuring circuit draws no current from the system.

The streaming potential setup is well suited to the determination of the zeta potential of materials such as

glass that can be formed into capillaries. It is also easily applied to coarse mineral particles such as those frequently treated by froth flotation processes (35).

Streaming potential determination for substances in aqueous electrolytes include: quartz in dodecylammonium acetate solutions (36);  $\text{Al}_2\text{O}_3$ ,  $\text{SnO}_2$ ,  $\text{Fe}_2\text{O}_3$ , and  $\text{TiO}_2$  in various electrolytes (55); corundum in solutions of surface active agents (37, 38); stainless steel in acids (59); corundum in various electrolytes (65); rutile at different pH levels with surface active agents (43); gypsum in solutions of several salts (10); barium sulfate in various electrolytes (10-13, 88); and scheelite in solutions of salts and surface active agents (70).

**Electrophoresis.** The electrophoretic separation and identification of proteins and other lyophilic colloids having an isoelectric point are a familiar and useful analytical tool in biochemistry. However, methods applicable to lyophobic systems will be emphasized here.

There are two well known methods of electrophoresis that are applied to dispersions: they involve the measurement of particle velocity either individually, by observing the particles directly with a microscope, or collectively, by measuring the velocity of a mass of particles by following the movement of a sharp concentration gradient. A third method, used by the authors and recently patented, has been termed the mass-transport method.

The measurement of the velocity of individual particles in a potential gradient is usually carried out in an apparatus such as that shown schematically in Figure 9. This apparatus consists essentially of a microscope with a calibrated reticule for the observation of the individual particles; a thin transparent cell, equipped with platinum measuring electrodes, that contains the colloidal suspension under study; zinc-zinc sulfate reversible working electrodes connected with a constant voltage supply; and a system of tubing and stopcocks for filling and cleaning the cell and electrode compartments. The platinum electrodes are used only for measuring the potential drop across the cell in which the particles are being observed; the potential gradient is developed by applying a voltage to the zinc electrodes further removed from the cell area. Platinum is not a suitable working electrode material because gas formation and polarization at the electrodes give rise to an uncontrollable variation in potential drop. Zinc or copper electrodes are generally used with aqueous systems; they must, however, be sufficiently removed from the measuring area so that ions from the electrode chambers do not have time to move to the measuring area during the experiment. Extremely small quantities of divalent ions have a marked effect on the particle mobility.

The cell itself must be transparent and thin and is frequently of rectangular cross section (1, 22, 68). A long, cylindrical cell has also been used by many workers (49, 83, 86, 97, 98) and is used in a currently available commercial instrument (112); the thin flat cell of rectangular cross section is also available commercially (99).

No matter what the cell geometry, the electrical double layer at the cell wall itself imparts a motion to the

whole suspension in the cell. The suspension moves rapidly in one direction near the wall, more slowly further from the wall, and in the opposite direction at the center of the cell. At some point in the cell there is no net motion applied to the suspension as the result of the zeta potential of the cell wall-liquid interface. It is at this point that the observed velocity of the particles in the system is equal to their electrophoretic velocity. Calculations have shown that this stationary level is located at a distance equal to 21.2% of the total cell thickness from the top (or bottom) of a wide flat cell, and at a distance equal to 14.8% of the diameter from the wall of a cylindrical cell (57, page 219).

In use, the cell is filled with the suspension under study and a known potential is applied. With an objective lens that gives a small depth of focus, the microscope is focused at the stationary level and the time for a particle to move a known distance is measured with a stopwatch. When particles of several kinds are present (each kind having its own characteristic mobility), a number of particles may be measured so that the distribution of mobility may be obtained. The results are reported as mobility cm./sec. (v./cm.) or converted to zeta potential by Equation 26.

This technique can be applied only to dilute suspensions so that the individual particles may be distinguished. The particles must also be small enough or have a density close enough to that of the suspending medium so that they will neither rise nor fall out of the stationary level under the influence of gravity while they are observed. The particles do, of course, have to be large enough to be easily seen in the microscope. An ultramicroscope or dark-field illumination may be used to extend the range of the method to finer particles.

The microscopic determination of electrophoretic mobility has been applied successfully to such diverse aqueous systems as kaolinite (34, 50, 97, 98, 104), xylene emulsions (68), proteins adsorbed on quartz particles (1), colloidal particles present in water supplies (83), cellulose and carbon black treated with various surface active agents (22), bacteria at different levels of pH (54), and normal and sickle human red blood cells (89).

In many cases, even when the particles are too small to be readily seen by use of the ultramicroscope, the migration rate of a mass of particles under the influence of a potential gradient may be measured by the moving boundary method. It is necessary in this method to form a sharp interface between a colloidal suspension and the colloid-free dispersing medium. Some of the early work on electrophoretic migration performed by Burton (14) on metal sols was carried out by this method. A simplified drawing of a moving boundary electrophoresis apparatus is shown in Figure 10.

The apparatus for moving boundary electrophoresis in its simplest form consists of a U-tube fitted with electrodes at the top of each arm of the U. Colloidal dispersion is added to the bottom of the U.

An apparatus used extensively by Tiselius (100) for the study of proteins is a more elaborate modification of the simple U-tube. In the Tiselius apparatus the cell arms

# MEASUREMENTS OF ELECTROKINETIC EFFECTS

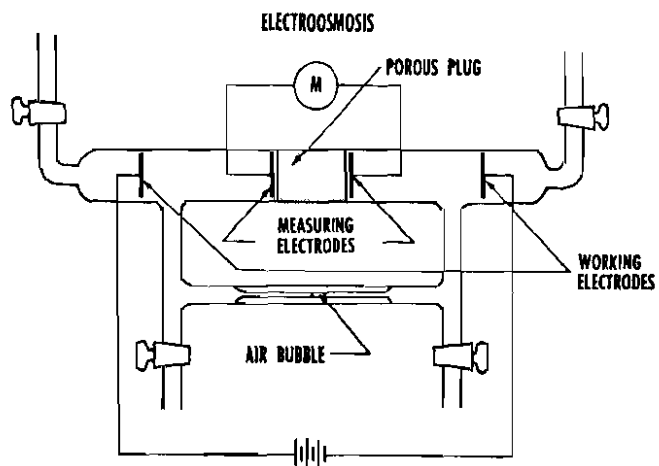


FIGURE 7

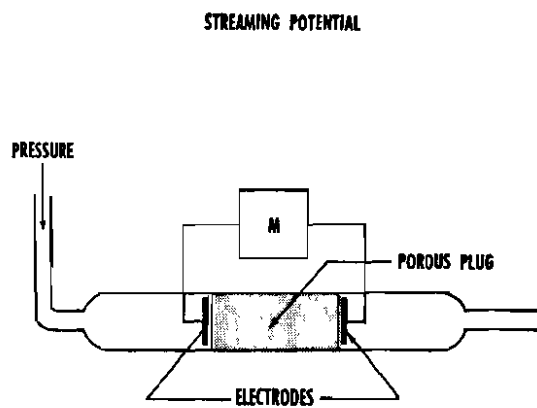


FIGURE 8

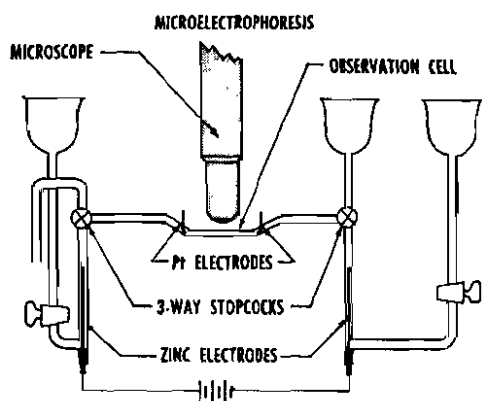


FIGURE 9

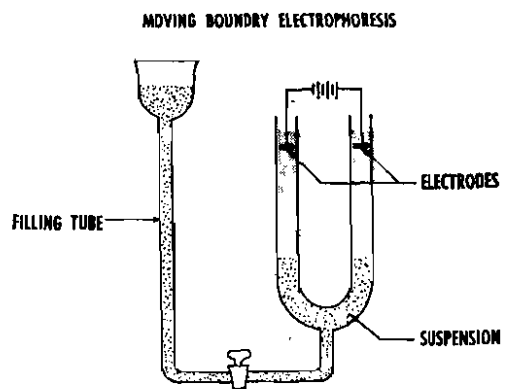


FIGURE 10

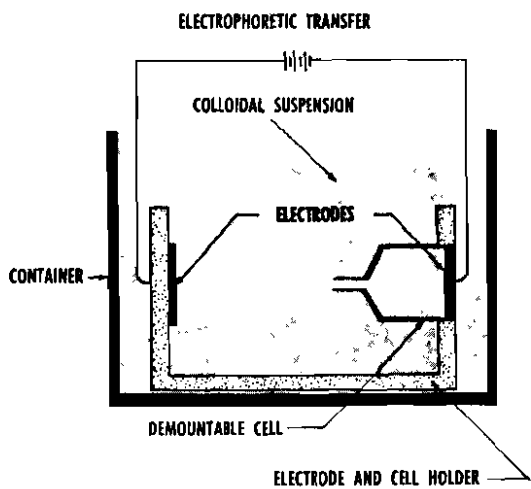


FIGURE 11

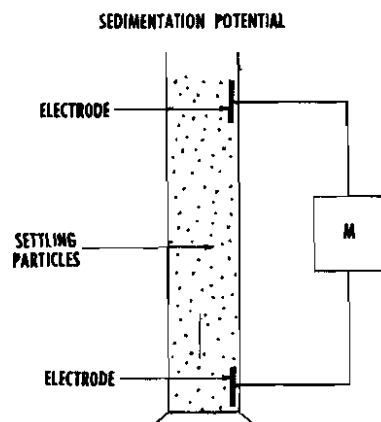


FIGURE 12



are of rectangular rather than circular cross section so that the visibility of the boundary is much improved. The boundary surface is established by sliding together the previously filled upper and lower portions of the cell; the upper portion contains the colloid-free supernatant liquid, while the lower portion contains the colloidal suspension. The boundary formed in this way is well defined. The Tiselius design also has reversible electrodes in a relatively large compartment well removed from the boundary; in this way, the colloidal dispersion is not contaminated by electrode reaction products, even in prolonged experiments. With lyophilic colloids such as proteins the Schlieren method of viewing the boundary may be used (57, page 216).

The zeta potential may be calculated from the observed mobility by Equation 26 if its limitations are observed.

The moving boundary method is suitable for almost any colloidal sol provided that a boundary can be formed that can be seen directly or observed by the use of techniques such as the Schlieren method. It is necessary to have a supernatant liquid of the same composition as the liquid in which the particles are suspended, and this can usually be obtained by the centrifugation of some of the colloidal suspension with the same composition as is placed in the bottom of the U-tube. Density of the particles must be close to that of the suspending liquid because gravitational forces must be negligible.

In addition to the initial work of Burton (14) and the later work of Tiselius (100), this technique has been used on other substances by various investigators. The systems studied include the effect of several electrolytes on platinum, gold, silver, bismuth, lead, iron, and selenium sols (14, 107); the effect of electrolytes on latex emulsions (64); and the effect of various electrolytes on arsenic trisulfide and ferric oxide sols (107). All these materials can be prepared as extremely fine particles and hence are amenable to study by this method.

A device for measuring electrophoretic velocity has been developed by the authors and is shown in Figure 11. It consists of a container filled with the suspension under study in which is immersed a bracket that supports two electrodes placed opposite each other. One electrode, shown on the left in the diagram, is completely accessible to the solution, while the electrode shown on the right is placed at the closed end of a cell that has a restricted tubular opening directly between the two electrodes. The electrode in the cell must be reversible; Ag-AgCl and zinc have both been used successfully. To measure mobility with this device, the cell and container are filled with the suspension to be studied. When a potential difference is impressed between the two electrodes, particles having an electric charge will migrate either into or out of the cell (depending on the sign of the cell electrode). After a short time there will be a change in composition of the cell contents because of the migration of the particles; the change may be determined by analysis, and from this concentration change the mobility and zeta potential of the particles can be calculated. Because kaolin has a specific gravity of about 2.58, the concentration change may be detected

by weighing the cell before and after the impression of the voltage gradient. In this case, the mobility may be calculated from the weight change by

$$v_e = \frac{\Delta W}{t} \frac{\rho_s}{\rho_s - \rho_l} \left[ \frac{1}{EAM} \cdot \frac{1}{1 - \frac{M}{\rho_s}} \right] \quad (48)$$

where the voltage gradient  $E$  is given by the current.

$$E = \frac{i}{\lambda A} \quad (49)$$

In the above equation,  $\Delta W/t$  is the change in cell weight per second,  $v_e$  is the electrophoretic mobility,  $M$  is the colloid concentration in grams per cc.,  $A$  is the area of the cell opening,  $\rho_s$  is the density of the colloid, and  $\lambda$  is the specific conductance of the suspension.

This apparatus, which we call the electrophoretic mass-transport cell, is similar in principle to the Hittorf method for determining the transference number of ions. Indeed, the Hittorf method or modifications thereof could be used to measure the zeta potential of systems that are amenable to moving boundary methods. It appears, however, to be little used.

In the measurement of the mobility of kaolin clays dispersed in water, the major difficulty preventing the use of the moving boundary or microelectrophoresis technique is gravity settling of the larger clay particles.

Kaolin clays such as those of the Georgia deposits consist of small hexagonal platelets or loosely bound stacks of platelets. The kaolin particles generally have a wide size distribution, ranging from 0.2-micron diameter platelets which may be only 0.01 micron thick or less, up to large stacks of platelets 5 or 10 microns in diameter and 30 or more microns thick. By the older definition of colloids in terms of particle size, most of a material such as this would not be so classified; however, these clays do exhibit typical colloidal behavior (such as deflocculation and flocculation) so that the zeta potential of clay systems can give considerable information about the nature of the clay surface and thus help to explain the rheology of concentrated kaolin suspensions.

The device shown in Figure 11 is especially valuable for studying kaolin-water systems or other systems containing particles large enough to preclude the use of the microelectrophoretic or moving boundary methods. With this device, the time of application of the voltage gradient is short (only a few minutes at most); therefore, most of the larger particles will still be in suspension at the end of the experiment. Although some of the larger particles may have settled out from the area between the two electrodes directly in front of the cell opening, corresponding size particles from a level of solution above the cell opening have settled into this area. Hence, little change in composition of suspension caused by particle settling can occur. A further unique property of this device is that electrophoretic mobility at a high

**AUTHOR** J. P. Olivier is Assistant Research Director, Freeport Kaolin Co., Gordon, Ga. Paul Sennett is Senior Chemist, with the same company.



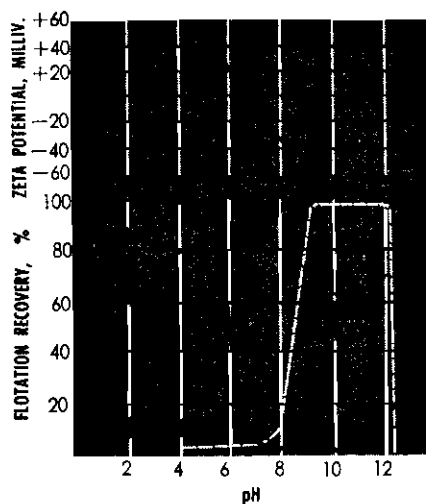


Figure 13. Flotation recovery of goethite, using anionic and cationic collectors. Note that zeta potential goes from a high positive value at low pH, through zero at a pH of 6.7, to a high negative value. All values determined in 0.0001M NaCl

colloid concentration may be measured. The instrument has been used to measure clay mobilities in aqueous suspensions containing up to 70% by weight of kaolin.

**Sedimentation and Centrifugation Potential.** The e.m.f. produced by particles falling through a suspending medium  $E_D$  (Dorn effect) may be used to calculate the zeta potential if the particles are of uniform size.

$$E_D = \frac{D\xi}{3\eta\lambda} r^2(\rho - \rho')ng \quad (50)$$

where  $r$  is the particle radius,  $(\rho - \rho')$  is the difference in specific gravity,  $n$  is the concentration, and  $g$  is the gravitational acceleration.

Where particles move by gravity through a liquid, the experimental setup shown in Figure 12 may be used for the measurement of zeta potential. Particles may also be made to move through the liquid by centrifugation (53, 87) or by ultrasonic vibration (19, 85).

Neither the sedimentation potential, centrifugation potential, nor the potential developed by ultrasonic vibration has been used extensively. Sedimentation potential has been used for measurement of the zeta potential of borosilicate glass, fused silica, silicon, fused alumina, and carborundum in KCl and BaCl<sub>2</sub> solutions (72); for quartz in KCl solutions (84); and for glass in solutions of several salts (80). Centrifugation potential has been used in the study of AgI and As<sub>2</sub>S<sub>3</sub> sols in KI and KNO<sub>3</sub> solutions (53, 87). The ultrasonic vibration technique has been used with quartz (85).

**Other Methods.** Work by Elton (29, 30) showed that if particles in a narrow size range were allowed to sediment in an ionic solution, they would settle more slowly than they would in a nonionic solvent of the same viscosity. This he attributed to a viscous drag brought about by the shearing of the electrical double layer. From measurements of the retardation of settling he was able to calculate zeta potentials in reasonable agreement with values determined by other methods. The method was applied to quartz, borosilicate glass, carborundum, and silica in aqueous KCl solutions (24, 25, 31, 32).

When a capillary containing an electrolyte is vibrated mechanically, an a.c. voltage is generated between its two ends. This phenomenon, extensively studied by Ueda, Tsuji, and Watanabe (102) and termed the "U effect" is related to the zeta potential and was used by them to measure an a.c. streaming potential of a glass capillary containing a KCl solution.

### Effects in Practical Systems

Although not always taken into account, the nature of the electrical double layer has an important influence on many practical systems. Although in many cases the technique used for its measurement gives rise to some doubts that the number obtained is valid, the zeta potential is an important characteristic property of the double layer. A review of the literature shows that many workers have made extensive investigations of the relation of zeta potential to the properties of various systems. The following paragraphs illustrate some of these.

**Flotation.** The sign and magnitude of surface charge influence profoundly the adsorption characteristics of mineral surfaces. Because the whole practice of froth flotation depends on the nature of solid-liquid and solid-liquid-gas interfaces, it is not surprising that zeta potential measurements relate to the flotation behavior of many mineral substances.

Figure 13 from the work of Iwasaki, Cooke, and Colombo (52) illustrates the close correlation of zeta potential with flotation behavior. In the flotation of oxide minerals where the collector must be adsorbed by the surface, anionic collectors should be effective on positive surfaces, and cationic collectors on negative surfaces. That this is indeed the case is shown in the bottom half of the figure where flotation recovery for a cationic collector and for two anionic collectors is plotted as a function of pH. At the zero point of charge, little collector is adsorbed and flotation recovery is nil. Above a pH of 12 the flotation efficiency falls off abruptly because of the low concentration of quaternary ammonium ions available at high hydroxide ion concentrations.

Other studies have shown similar behavior for rutile (43), corundum (66), hematite (51), and quartz (36, 38, 52). A discussion of the relationship between flotation and zeta potential is given by Aplan and Fuerstenau (3) and by deBruyn and Agar (18).

**Clarification and Filtration.** In light of the previous discussion of the influence of zeta potential on colloid stability, it is perhaps surprising that more practical research effort has not been expended on the influence of various electrolytes on the stability of colloids in water supplies and similar dilute colloidal suspensions.

In the purification of municipal water and in the cleaning up of industrial wastes, it is usually necessary to remove solids from dilute suspensions. To this end, flocculating agents such as aluminum sulfate are frequently used before a filtration, decantation, or centrifugation procedure. The effect of the trivalent aluminum is to lower markedly the zeta potential, even at low aluminum ion concentration (as noted in the discussion of the Schulze-Hardy rule); the lowering of the potential al-

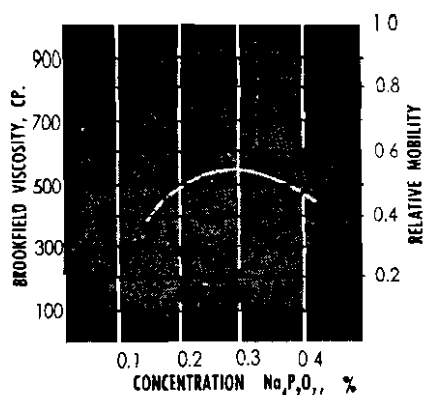
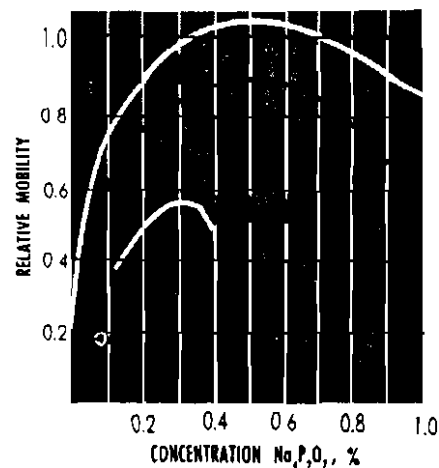


Figure 14. Mobility and viscosity of a 47.5 volume % kaolinite suspension with addition of deflocculant. Apparently, some degree of correlation exists

Figure 15. Mobility of kaolinite as a function of flocculant addition for several kaolinite concentrations, as measured by mass transport electrophoresis



lows the fine particles to gather into aggregates which are more easily removed by one of the above processes. In many cases, such as in sewage and paper mill effluents, there is appreciable lyophilic material present. Because these lyophilic colloids coat lyophobic particles, the problem of economic clarification is complicated.

In the wet processing of kaolin clays, it is necessary first to make a stable dispersion at fairly low solids so that the naturally occurring mineral may be classified by centrifugal techniques into fractions of various particle size distribution (2). As a final step in the processing, the clay must be filtered out of the dispersion so that it can be dried economically. The filtration rate of the deflocculated particles is extremely slow, so the clay-water dispersion is treated with sufficient acid to lower the zeta potential and flocculation occurs.

To obtain the maximum filtration rate, the zeta potential must be lowered to zero; under plant operating conditions, however, the clay still has a negative charge although it is well flocculated. Oakes and Burcik show a nearly linear relation of filtration rate to zeta potential reduction in a sample of Wyoming bentonite (69).

**Relationship between Mobility and Viscosity.** Einstein (28) derived an equation that relates the viscosity of a suspension of uncharged spherical particles to that of the suspending medium itself. The equation takes the form

$$\eta = \eta_0(1 + 2.5\phi)$$

where  $\eta$  is the viscosity of the suspension,  $\eta_0$  is the viscosity of the dispersion medium, and  $\phi$  is the volume fraction occupied by the spherical particles. The equation is valid under the conditions for which it was derived

Deviations might come about through

- nonspherical particles
- high colloid concentration, which gives rise to particle interference
- forces of attraction and repulsion caused by an electrical double layer on the particles

Insofar as this latter effect is reflected by the zeta potential determined from mobility measurement, the zeta potential might correlate with the flow behavior of colloids.

One of the few substances studied as to the relation of zeta potential to viscosity is kaolin clay. In terms of a

study of the influence of the double layer on viscosity, the choice is a poor one because it represents a highly complicated system; nonetheless, it is of important commercial interest.

Van Wazer and Besmertnuk (104) concluded from microelectrophoresis measurements that although low viscosity deflocculated slurries consisted of particles having a high zeta potential, other forces were the primary factor in determining consistency. Street, however, found a good correlation between viscosity at low rates of shear and zeta potential when low colloid content slurries were used (96, 97).

The authors have used the electrophoretic mass-transport cell for determining the mobility of a fine-particle kaolin clay as a function of the amount of deflocculant tetrasodium pyrophosphate added; Brookfield viscosity was also determined. The results obtained (Figure 14) show that some relationship exists between zeta potential and viscosity. Certainly no better correlation should be expected for at least three reasons:

- Clay slurries are not Newtonian; therefore, no single number describes the rheological behavior
- Kaolin particles may have a charge on the face surfaces different from that on the edge; thus nature of the floc may change as well as degree of flocculation.
- The measurements were made on a 47.5 volume % slurry, so that particle-particle interference would be expected.

The mobility of kaolinite as measured by mass-transport electrophoresis is a function of concentration, as the data plotted in Figure 15 show. In addition to particle-particle interference at higher particle concentrations, an electroosmotic effect is likely to occur when the mass-transport method is applied to highly concentrated kaolinite suspensions. The kaolinite particles are platelets about 0.2 micron thick; at 50 volume %, the space between platelets is not large compared to the double-layer thickness, and the flow is retarded.

**Soil Structure.** Soils used for agricultural purposes contain an appreciable fraction of colloidal material. This material consists of both lyophobic and lyophilic colloids, but in any case its state of flocculation profoundly influences the soil structure. The soil must be kept in a flocculated state in order that it be porous.

Calcium ion is an excellent flocculant. Organic polyelectrolytes are also effective in maintaining a flocculated soil by forming bridges between particles.

A classic example (79) of the influence of the state of flocculation on the structure of soil occurs when good agricultural land is flooded by sea water. The calcium of the naturally occurring clay minerals exchanges for the sodium of the sea water. The sodium-exchanged soil is also flocculated, but continued leaching by rain-water removes sufficient sodium so that the soil becomes deflocculated and packs into a hard mass not suitable for good plant growth. This condition can be avoided by the addition of calcium ions in the form of gypsum.

**Other Phenomena Related to Zeta Potential.** Because laundering operations consist in part of suspending dirt particles in water a correlation might be expected between charge on the particles and detergency. Work on several synthetic soils led to the conclusion by Durham (27) that there was a qualitative correlation between zeta potential and redeposition of soil, but that other factors were involved. Doscher (22) attributes detergency largely to the degree of adsorption of the surface active agents. Other workers have also investigated this relation, with varying results (26, 75-77).

The microelectrophoretic method is a useful tool to workers studying bacteria (58). It has been used to identify the nature of the surface of living bacteria by comparing their migration rates under varying conditions with those of model systems under the same conditions. James (54), for instance, showed that *Aerobacter aerogenes* had a polysaccharide surface under normal conditions, but a lipid surface when grown in the presence of crystal violet. Normal and abnormal blood cells have been studied (89).

Other phenomena are no doubt associated with zeta potential, although in many cases quantitative data are lacking. Soyenkoff (92), in an early review of the behavior of fine particles in organic liquids, concluded that electrokinetic potential was not important in oil dispersions. Later work, however, indicated that this is often not true. Reising (81) studied the appearance of several paint pigments suspended in organic oils when a 450-volt potential was impressed across a 1/50-in. gap containing the suspension. Some pigments migrated to the anode, some to the cathode, and others assumed a lines-of-force arrangement. Similar behavior was found for coal particles suspended in oil (46). Winslow (170, 171) found that certain substances such as powdered silica gel suspended in oil assumed a lines-of-force arrangement in strong electric fields. He designed an electrostatic clutch making use of the increased viscosity. Gemant (39), in a study of transformer oil, used a novel radioactive tracer technique to measure magnitude of the zeta potential of magnesium oxide, graphite, and high molecular weight fatty acid salts.

#### Direct Applications of Electrokinetic Phenomena

Electrokinetic phenomena have been or are being used directly to some extent. Any process that involves the separation of particles with differences in zeta potential

suggests itself as a likely candidate for an electrokinetic separation technique. In the field of lyophilic colloids, for instance, the electrophoretic separation of proteins and amino acids is commonplace. Except as noted below, there does not appear to have been much application to the separation of lyophobic colloids, probably because separations are more easily accomplished by other methods. Electrophoretic deposition of colloidal particles, however, has been used in several cases. Electroosmosis has also been used for dewatering.

**Separations.** A recent study by Todd and Wild (707) describes a unique separation procedure that is related in some way to the electrical character of a solid-liquid interface. Their separation procedure was applied to 1- to 30-micron particles of mineral mixtures suspended in nonconducting organic liquids. When a d.c. potential of 1750 v. was applied to the suspension across a 0.4-cm. gap, materials of the mixture would usually plate out on the electrodes. With the proper choice of liquid and surface active agent, Todd and Wild were able to separate completely such mixtures as  $\alpha\text{SiO}_2$ - $\text{MoC}_2$ , talc-aluminum oxide, and garnet- $\text{FeTiO}_3$ . In many other cases, a considerable increase in the concentration of one of the components was obtained.

**Electrophoretic Deposition.** At one time, the electrophoretic deposition of rubber latex was a common method of forming thin rubber goods. Natural rubber latex was deposited on an anode of the desired shape. This method has largely been replaced by simpler dipping techniques.

Electrophoretic deposition of paints has aroused considerable interest in recent years and is in commercial use on a limited scale. The process, while not new (76), appears to be gaining favor in the industrial application of paint film to metal parts as large as automobile bodies. The usual commercial practice is to make the metal part the anode and electrophoretically deposit the paint materials from a water emulsion. The paint system can usually be made to behave as if it consisted of particles of only a single electrophoretic mobility. If the conductivity of the paint batch is kept low, power costs are small.

Electrophoretic deposition of paint usually gives a denser and more coherent coating than is obtainable by conventional dip or spray methods. In addition, little paint is wasted—there are no sags or runs and the coating is very uniform, even over rough spots, sharp edges, and within boxed sections. A number of recent papers show the great current interest in the subject (6-8, 33, 40). For further information, see page 60 of IND. ENG. CHEM., August 1965.

**Electrical Dewatering.** Electrophoresis and the liquid counterflow, electroosmosis, suggest themselves as a means of dewatering fine particle size suspensions that are not amenable to filtration. In fact, the capillary rise phenomenon observed in 1808 by Reuss in Moscow was essentially an electroosmotic dewatering process.

In the early part of the present century Count Schwerin made extensive studies of the electrophoretic and electroosmotic dewatering of peat and clay and obtained some 50 patents on various aspects of the process.

In a clay plant of his design, the clay was made to deposit on a partially immersed rotating drum from which it could be removed by a scraping mechanism. The process was apparently more efficient than the filtration processes of the day. A good review of electrical dewatering of clay is given by Curtis (17). Stanczyk (94) made a study of the dewatering of phosphate rock slime by electrophoresis and electroosmosis (94).

An interesting application of electroosmosis for the temporary stabilization of high moisture content soils prior to excavation has been described (61, 62, 71). The process consists of driving a solid anode and a perforated cathode into the ground several feet apart; when a voltage is applied, water collects inside the cathode and may be pumped out. Removal of a small amount of water usually markedly increases bearing strength of the soil.

An electrophoretic method known as electrode-cantation (56, 93) can be used for the concentration of colloidal dispersions. In the electrode-cantation process, two electrodes are used to impress a potential across a colloidal suspension; the electrodes are separated from the bulk of the suspension by a membrane which allows the migrating colloidal particles to build up on the membrane, rather than on the electrodes. If the concentrated colloid is more dense than the suspension, it will frequently sink to the bottom in a fairly dense layer that can be removed from the system. Should the concentrated colloidal material have a tendency to stick to the membrane, it can usually be released by a momentary reversal of the current. A multicompartment cell with several membranes may be used to increase the efficiency of the separation. The process has been used for concentrating rubber latex (67).

## REFERENCES

- (1) Abramson, H. A., Moyer, L. S., Garin, H. M., "Electrophoresis of Proteins," Reinhold, New York, 1942.
- (2) Agnello, L. A., Morris, H. H., Gunn, F. A., *IND. ENG. CHEM.* **52**, 370 (1960).
- (3) Aplan, F. F., Fuerstenau, D. W., in "Froth Flotation," D. W. Fuerstenau, Ed., p. 170, American Institute of Mining, Metallurgical and Petroleum Engineers, Inc., New York, 1962.
- (4) Ballou, E. V., *J. Colloid Sci.* **10**, 450 (1955).
- (5) Benton, D. P., Elton, G. A. H., "Second International Congress of Surface Activity," Vol. 3, p. 28, Academic Press, New York, 1957.
- (6) Berry, J. R., *Paint Technol.* **27** (12), 13 (1963).
- (7) *Ibid.*, **28** (1), 24 (1964).
- (8) *Ibid.*, **28** (3), 53 (1964).
- (9) Bolt, G. H., *J. Colloid Sci.* **10**, 206 (1955).
- (10) Buchanan, A. S., Heymann, E., *Proc. Roy. Soc. (London)* **195A**, 150 (1948).
- (11) Buchanan, A. S., Heymann, E., *J. Colloid Sci.* **4**, 137 (1949).
- (12) *Ibid.*, p. 151.
- (13) *Ibid.*, p. 157.
- (14) Burton, E. F., *Phil. Mag.* **11**, 425 (1906).
- (15) Chapman, D. D., *Ibid.*, **25** (6), 475 (1913).
- (16) Crosbe and Blackwell Ltd., Brit. Patent **455,810** (Oct. 28, 1936).
- (17) Curtis, C. E., *J. Am. Ceram. Soc.* **14**, 219 (1931).
- (18) DeBruyn, P. L., Agar, G. E., in "Froth Flotation," D. W. Fuerstenau, Ed., p. 91, Am. Inst. Mining, Metallurgical, Petroleum Engs., Inc., New York, 1962.
- (19) Debye, P., *J. Chem. Phys.* **13**, 1 (1933).
- (20) Debye, P., Huckel, E., *Physik Z.* **24**, 185 (1923).
- (21) Dorn, E., *Wied. Ann.* **10**, 70 (1880).
- (22) Doscher, T. M., *J. Colloid Sci.* **5**, 100 (1950).
- (23) Douglas, H. W., Walter, R. A., *Trans. Faraday Soc.* **46**, 559 (1950).
- (24) Dulin, C. I., Elton, G. A. H., *J. Chem. Soc.* **1952**, p. 286.
- (25) *Ibid.*, **1953**, p. 1168.
- (26) Durham, K., *J. Appl. Chem. (London)* **6**, 153 (1956).
- (27) Durham, K., "Second International Congress of Surface Activity," Vol. 4, p. 60, Academic Press, New York, 1957.
- (28) Einstein, A., *Ann. Physik.* **4**, 19 (1906).
- (29) Elton, G. A. H., *Proc. Roy. Soc. (London)* **197A**, 568 (1949).
- (30) Elton, G. A. H., *J. Chem. Phys.* **19**, 1317 (1951).
- (31) Elton, G. A. H., Hirschler, F. G., *J. Chem. Soc.* **1952**, p. 2953.
- (32) Elton, G. A. H., Mitchell, J. W., *Ibid.* **1953**, p. 3690.
- (33) Finn, S. R., Mell, C. C., *J. Oil Colour Chemists Assoc.* **47**, 219 (1964).
- (34) Freundlich, H., "Kapillarchemie," 1st ed., Leipzig, 1909.
- (35) Fuerstenau, D. W., *Mining Eng.* **8**, 834 (1956).
- (36) *Ibid.*, **9**, 1365 (1957).
- (37) Fuerstenau, D. W., Modi, H. J., *J. Electrochem. Soc.* **106**, 336 (1959).
- (38) Gaudin, A. M., Fuerstenau, D. W., *Mining Eng.* **7**, 958 (1955).
- (39) Gemant, A., *J. Phys. Chem.* **56**, 238 (1952).
- (40) Gloyer, S. W., Hart, D. P., Cutforth, R. E., *Off. Dig., Federation Soc. Paint Technol.* **37**, 113 (1965).
- (41) Gouy, G., *Ann. Phys.* **7** (9), 129 (1917).
- (42) Gouy, G., *J. Phys.* **9** (4), 457 (1910).
- (43) Graham, K., Madeley, J. D., *J. Appl. Chem. (London)* **12**, 485 (1962).
- (44) Grahame, D. C., *Chem. Rev.* **41**, 441 (1947).
- (45) Hardy, W. B., *Proc. Roy. Soc. (London)* **66**, 110 (1900).
- (46) Hedrick, J. E., Andrews, A. C., Sutherland, J. B., *IND. ENG. CHEM.* **33**, 1055 (1941).
- (47) Helmholtz, H., *Wied. Ann.* **7**, 337 (1879).
- (48) Henry, D. C., *Proc. Roy. Soc. (London)* **133**, 106 (1931); *Trans. Faraday Soc.* **44**, 1021 (1948).
- (49) Hunter, R. J., Alexander, A. E., *J. Colloid Sci.* **17**, 781 (1962).
- (50) *Ibid.*, **18**, 820 (1963).
- (51) Iwasaki, I., Cooke, S. R. B., Choi, H. S., *Trans. AIME* **217**, 237 (1960).
- (52) Iwasaki, I., Cooke, S. R. B., Colombo, A. F., *U. S. Bur. Mines, Rept. Invest.* **5593**, 1960.
- (53) Jacobs, G., *Trans. Faraday Soc.* **48**, 355 (1952).
- (54) James A. M., "Second International Congress of Surface Activity," Vol. 4, p. 254, Academic Press, New York, 1957.
- (55) Johansen, P. G., Buchanan, A. S., *Australian J. Chem.* **10**, 392 (1957).
- (56) Kirk, R. E., Othmer, D. F., "Encyclopedia of Chemical Technology," Vol. 5, p. 549, Interscience Publishers, New York, 1950.
- (57) Kruyt, H. R., "Colloid Science," Vol. I, Elsevier, New York, 1952.
- (58) *Ibid.*, Vol. II, Elsevier, New York, 1949.
- (59) Levy, B., Fritsch, A. R., *J. Electrochem. Soc.* **106**, 730 (1959).
- (60) Linder, S. E., Picton, H., *J. Chem. Soc. (London)* **61**, 148 (1892).
- (61) Loughney, R., *Const. Methods and Equip.* **36**, No. 8, 70, 74, 78, 82 (1954).
- (62) Loughney, R., Hickey, W. E., *Eng. News Record* **162**, No. 15, 41, 45 (1959).
- (63) Lyons, J. W., *J. Colloid Sci.* **19**, 339 (1964).
- (64) Maron, S. H., Bowler, W. W., *J. Am. Chem. Soc.* **70**, 3893 (1948).
- (65) Modi, H. J., Fuerstenau, D. W., *Ibid.*, **61**, 640 (1957).
- (66) Modi, H. J., Fuerstenau, D. W., *Trans. AIME* **217**, 381 (1960).
- (67) Murphey, E. J., *Trans. Inst. Rubber Ind.* **18**, 173 (1942).
- (68) Neogy, R. K., *J. Indian Chem. Soc.* **31**, 291 (1954).
- (69) Oakes, P. T., Burcik, E. J., *Natl. Acad. Sci.-Natl. Res. Council, Publ.*, No. 456, 225 (1956).
- (70) O'Connor, D. J., "Second International Congress of Surface Activity," Vol. 3, p. 319, Academic Press, New York, 1957.
- (71) Olinger, W. A., "Sixteenth Annual Minerals Symposium," Univ. Minn., p. 46, Jan. 11-12, 1955.
- (72) Pearce, J. B., Elton, G. A. H., *J. Chem. Soc.* **1960**, p. 2186.
- (73) Perrin, J., *J. Chem. Phys.* **2**, 601 (1904).
- (74) *Ibid.*, **3**, 50 (1950).
- (75) Porter, A. S., "Second International Conference of Surface Activity," Vol. 3, p. 103, Academic Press, New York, 1957.
- (76) Powney, J., Wood, L. J., *Trans. Faraday Soc.* **36**, 420 (1940).
- (77) *Ibid.*, p. 57.
- (78) Quinke, G., *Pogg. Ann.* **113**, 513 (1861).
- (79) Quirk, J. P., Schofield, R. K., *Soil. Sci.* **6**, 163 (1955).
- (80) Quist, J. D., Washburn, E. R., *J. Am. Chem. Soc.* **62**, 3169 (1940).
- (81) Reising, J. A., *IND. ENG. CHEM.* **29**, 565 (1937).
- (82) Reuss, F. F., *Mem. Soc. Imperiale Natural. Moscou* **2**, 327 (1809).
- (83) Riddick, T. M., *TAPPI* **47**, 171A (1964).
- (84) Roy, C. B., *J. Indian Chem. Soc.* **38**, 903 (1961).
- (85) Rutgers, A. J., *Nature* **157**, 74 (1946).
- (86) Rutgers, A. J., de Smet, M., *Trans. Faraday Soc.* **48**, 635 (1952).
- (87) Rutgers, A. J., Nagels, P., *Nature* **171**, 568 (1953).
- (88) Ruysen, R., Loos, R., *Ibid.*, **162**, 741 (1948).
- (89) Schulze, H., *J. Prakt. Chem.* **25** (2), 431 (1882).
- (90) *Ibid.*, **27**, 320 (1883).
- (91) Seaman, G. V. F., Pethica, B. A., "Second International Conference of Surface Activity," Vol. 4, p. 277, Academic Press, New York, 1957.
- (92) Soyenko, B., *J. Phys. Chem.* **35**, 2993 (1931).
- (93) Stamberger, P., *J. Colloid Sci.* **1**, 93 (1946).
- (94) Stanczyk, M. H., Feld, I. L., *U. S. Bur. Mines, Rept. Invest.* **6451**, 1964.
- (95) Siern, O., *Z. Elektrochem.* **30**, 508 (1924).
- (96) Street, N., *Australian J. Chem.* **9**, 467 (1956).
- (97) Street, N., *J. Colloid Sci.* **12**, 1 (1957).
- (98) Street, N., Buchanan, A. S., *Australian J. Chem.* **9**, 450 (1956).
- (99) Thomas, Arthur H. Co., Catalogue No. 65, Philadelphia, Pa.
- (100) Tiselius, A., *Trans. Faraday Soc.* **33**, 524 (1937).
- (101) Todd, G., Wild, G. A., *Anal. Chem.* **36**, 1025 (1964).
- (102) Ueda, S., Tsuji, F., Watanabe, A., "Second International Conference of Surface Activity," Vol. III, p. 3, Academic Press, New York, 1957.
- (103) Van Olphen, H., "Clay Colloid Chemistry," Interscience, New York, 1963.
- (104) Van Wazer, J. R., Besmertnik, E., *J. Phys. and Colloid Chem.* **54**, 89 (1950).
- (105) Verwey, E. J. W., Overbeek, J. T. G., "Theory of the Stability of Lyophobic Colloids," Elsevier, New York, 1948.
- (106) Von Smoluchowski, M., "Graetz Handbuch Der Elektrizität Und Des Magnetismus," II, p. 385, Leipzig, 1921.
- (107) Weiser, H. B., Merrifield, P., *J. Phys. and Colloid Chem.* **54**, 990 (1950).
- (108) Wiedemann, G., *Pogg. Ann.* **87**, 321 (1852).
- (109) *Ibid.*, **99**, 177 (1856).
- (110) Winslow, W. M., *J. Appl. Phys.* **20**, 1137 (1949).
- (111) Winslow, W. M., U. S. Patent **2,417,840** (March 25, 1947).
- (112) Zeta Meter Inc. Bull. 6-61, 1720 First Ave. New York, N. Y.

# A NEW TECHNIQUE FOR Microelectrophoretic measurements

A WIDE VARIETY of instrument configurations for making microelectrophoretic measurements has evolved over the years.<sup>1</sup> The common feature of all conventional instruments has been the measurement of one particle at a time. As the time of measurement increases, however, the susceptibility to errors also increases. Some of these time-dependent error sources are: 1) Convection currents caused by heating of the sample; 2) Bubbles formed as gases come out of solution, causing changes in the location of the stationary layer; 3) Contamination of sample by diffusion of electrode reaction products; 4) Settling of particles, causing changes in particle charge distribution; 5) Changes in effective length of electrophoresis chamber due to electrode reactions; 6) Changes in location of the stationary layer, resulting from unsymmetrical contamination; 7) Errors caused by partial flocculation of particles, particularly with systems near zero charge; and 8) Changes in the chemistry of the colloid in dynamic systems that have not reached equilibrium.

Each of the above-mentioned potential error sources could be reduced if there were an effective means of taking the data much more quickly, without loss of accuracy. The purpose of this paper is to describe a method that allows the observer to measure many particles effectively and simultaneously. This is made possible by adding a key feature to the conventional instrument: a rotating cube prism inside the microscope. The rotation of the prism causes a translation of the particle image. The rate of rotation is controlled by the operator and is adjusted until the average particle motion caused by the applied field is canceled by the prism rotation. If the rotation rate is too fast, the particles

will appear to drift one way; if too slow, they will drift in the opposite direction. When the rotation rate is just right, the "particle cloud" will appear stationary. Since the operator simultaneously observes and measures many particles, the precision is the same as if ten to thirty particles were measured at once. The result is a faster generation of data, with fewer time-dependent errors.

## Theory of operation

### *Rotating prism method*

For the purposes of this description, it is assumed that the electrophoresis chamber has been filled with a colloidal dispersion and positioned relative to the stage of the microscope as schematically indicated in *Figures 1* and 2. The operator-observer adjusts the microscope to focus at the stationary layer of the chamber. An appropriately shaped laser beam provides a sheet of illumination that is adjusted to coincide with the focal plane of the

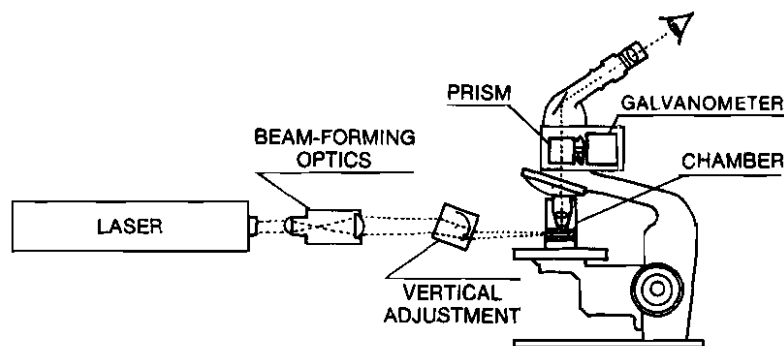


Figure 1 Diagram of light paths in the rotating prism

microscope and the stationary layer. Furthermore, it is assumed that a dc voltage is impressed across the electrodes, causing a negatively charged particle to migrate toward the anode, as indicated in Figure 2 by an arrow.

The motion of a typical particle seen by the observer in the plane of the microscope reticle consists of two velocity components. The first velocity component  $V_e$  is due to the electrophoretic movement of the particle as magnified by the microscope objective. The second velocity component  $V_p$  is a translation of the particle image caused by the rotation or scanning motion of the prism. A quantitative description of these two velocity components of the image movement of particles may be given in the following.

The electrophoretic velocity of the particle is equal to its mobility  $u$  times the electric field strength  $E$ . In turn,  $E$  may be expressed as  $V/L$  where  $V$  is the voltage applied across the electrodes, and  $L$  designates the effective length of the chamber or approximately the linear spacing between electrodes. If the magnification of the objective lens is  $M$ , the image velocity due to the electrophoretic effect is simply  $M$  times the electrophoretic velocity or

$$V_e = MuV/L \quad (1)$$

On the other hand, the velocity component due to the prism rotation may be approximated as:

$$V_p = t \frac{(N-1)}{N} \dot{\theta} \quad (2)$$

where  $t$  is the thickness of the prism,  $N$  is the prism's index of refraction, and  $\dot{\theta}$  the rotation rate of the prism.

The rotation rate of the prism may also be expressed as

$$\dot{\theta} = GS \quad (3)$$

where  $G$  is the scale factor associated with the galvanometer and associated drive circuit, and in turn

$$S = WKV \quad (4)$$

where  $W$  is equal to the voltage output of an operator-controlled adjustable potentiometer (P1),  $V$  is the voltage applied across the electrodes, and  $K$  is a constant introduced by a calibration potentiometer (P2).

The prism thus rotates at a rate equal to the product of the operator-controlled setting  $W$ , the applied electrode voltage  $V$ , and a net calibration constant  $GK$ . It should be noted, however, that although the prism rate  $\dot{\theta}$  is governed by Eqs. (3) and (4), additional circuitry is incorporated to ensure that the angle  $\theta$  never exceeds  $\pm 0.05$  rad in either direction, as required to maintain the approximation given in Eq. (2). As a result, the angle  $\theta$  can be described by a sawtooth wave-form having a peak-to-peak amplitude of .1 rad and a slope equal to  $\dot{\theta}$ .

*continued*

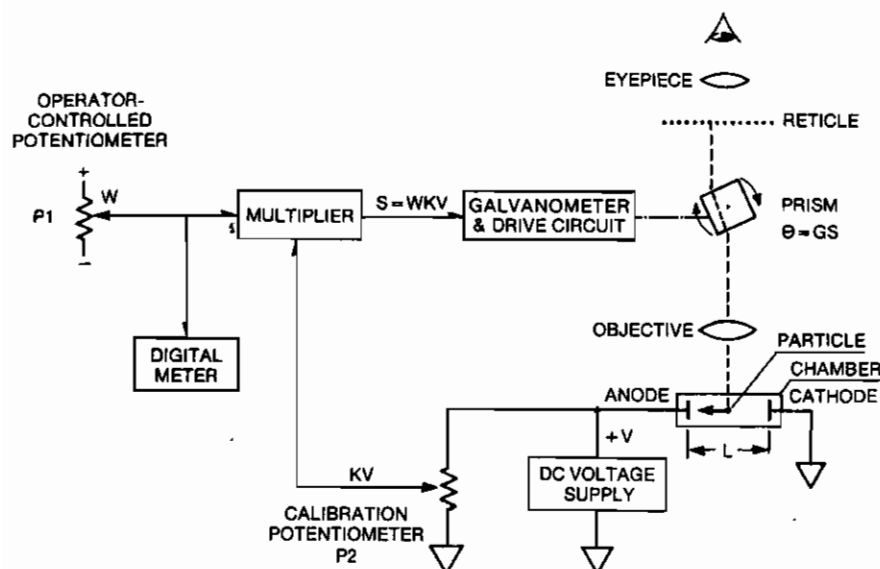


Figure 2 Schematic diagram of the rotating prism technique.

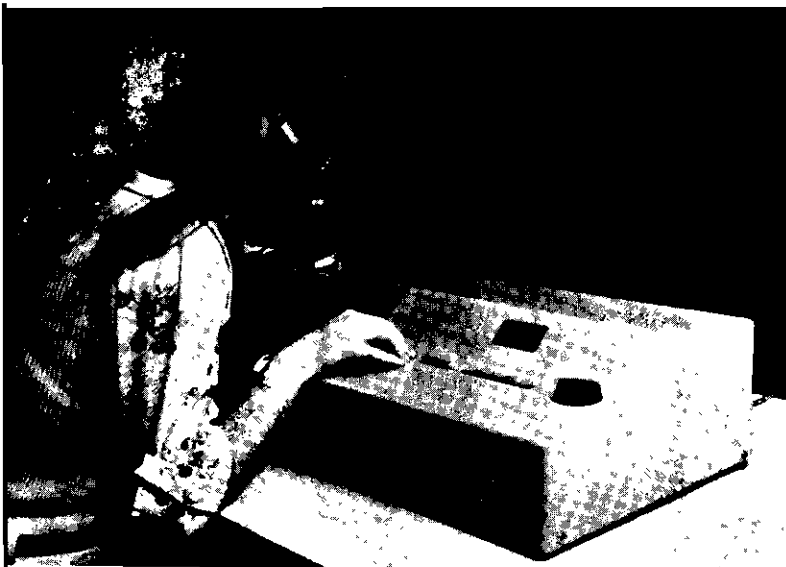


Figure 3 Model 500 semiautomatic zeta potential measuring system.

Substituting Eqs. (3) and (4) into Eq. (2) yields:

$$V_p = t \frac{(N-1)}{N} WVGK \quad (5)$$

In order to make a measurement, the operator merely adjusts the potentiometer P1 in such a manner that the image motion caused by the electrophoretic effect is just canceled by an opposite motion produced by the prism rotation. At this null condition, the particle image appears stationary with reference to the eyepiece reticle of the microscope and  $V_e = V_p$ . Stated otherwise:

$$MuV/L = t \frac{(N-1)}{N} WVGK \quad (6)$$

or

$$u = \left[ t \left( \frac{N-1}{N} \right) \frac{GKL}{M} \right] W \quad (7)$$

From Eq. (7) it is seen that the electrophoretic mobility, i.e., the quantity being measured, is directly proportional to  $W$ , the output voltage of the potentiometer P1, and that all of the parameters inside the brackets can be considered as constants. Hence, by means of the digital voltmeter, the voltage  $W$  may be displayed, thereby indicating electrophoretic mobility provided the operator has adjusted the potentiometer P1 to satisfy the null conditions of Eqs. (6) and (7). These null conditions

are satisfied, of course, when the scanning rate of the prism produces an apparent image motion equal to and opposite in direction to the electrophoretic velocity of the suspended particle as viewed by the operator through the microscope eyepiece. It will be noted that the scale factor, i.e., the bracketed term in Eq. (7), is independent of the voltage  $V$  applied across the chamber. This is extremely desirable since it is often necessary to change the voltage over a relatively wide range.

Calibration of the system described here is readily accomplished by adjustment of the calibration potentiometer P2, which in turn changes the value of  $K$ . Although Eq. (7) shows that the instrument scale factor is a function of  $t$ ,  $N$ ,  $G$ ,  $K$ ,  $L$ , and  $M$ , it is possible to calibrate the system without knowing all of these constants individually. In fact a precise calibration can be made using only an accurate scale located at the focal plane of the microscope objective, a precise measurement of the voltage  $V$ , an accurate time reference, and a measured value for the effective length of the chamber.

Finally, it is noted that for those aqueous samples where Smoluchowski's equation is valid, the zeta potential at 20°C is simply 14.2 times the mobility value. Accordingly, the system described here can be made to read out directly zeta potential, rather than mobility, by simply adjusting  $K$  by a factor of 14.2.

#### Experimental method

In order to illustrate the advantages of the rotating prism method, comparative measurements were made with and without the prism feature. All experiments were performed using a standard model 500 Laser Zee Meter™ (Figure 3). The following paragraphs describe details of the microscope, electrophoresis chamber, laser optics, electronics, and methods of data collection.

The microscope is a Nikon SU equipped with a 20X, .4 N.A. objective and two 10X eyepieces mounted on a binocular head. The prism/galvanometer assembly is installed between the body and the binocular head, thereby extending the effective tube length and producing a total magnification of 275. The working distance of 5.7 mm allows focusing from the top to the bottom of the electrophoresis chamber. Rotation of the 30-mm prism produces an equivalent particle displacement of 70  $\mu\text{m}/\text{scan}$ . The overall field of view is 650  $\mu\text{m}$  in diam. An eyepiece grid provides a fixed frame of reference for judging the motion of the particles.

The rectangular electrophoresis chamber is oriented horizontally and has a depth of 1.5 mm and a width of 15 mm. This 10:1 aspect provides a

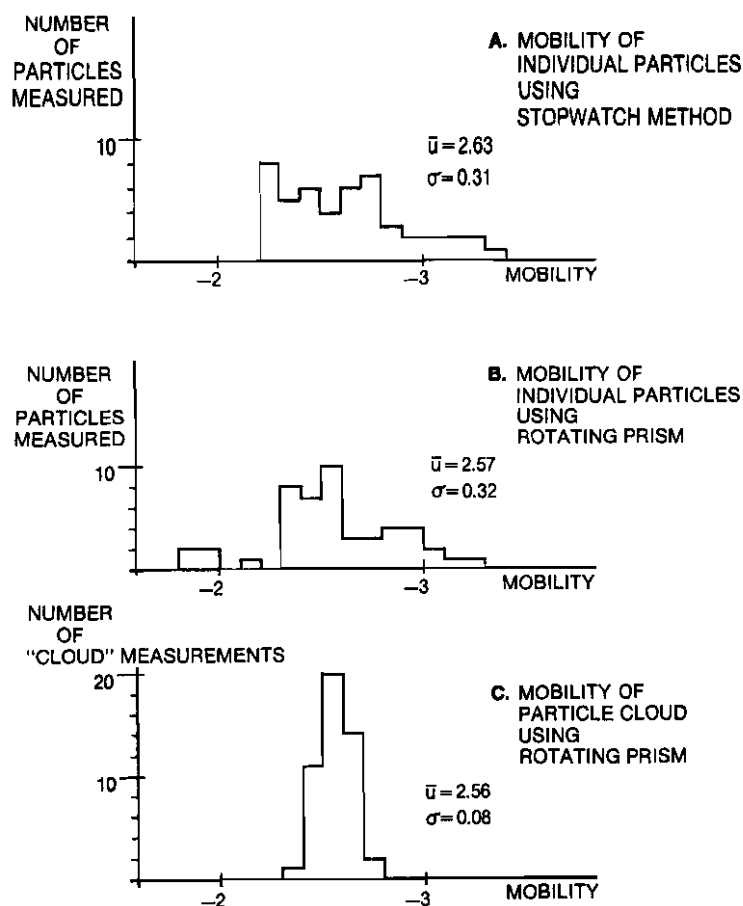


**Figure 4** Histograms of particle mobility obtained by three methods.

stationary layer located at 19.4% of the apparent depth, or typically 230  $\mu\text{m}$ . The chamber used in these experiments is fabricated from methylmethacrylate plastic; a glass chamber is also available. A nongassing molybdenum anode and a platinum cathode are used exclusively. No gassing is observed even with formaldehyde-fixed human erythrocytes suspended in .15 M saline. This blood sample is used as an independent means of calibration, in addition to the procedure described previously.

All measurements reported here were made at an applied electrode potential of 100 v, corresponding to a field strength of 10 v/cm. The field strength can be adjusted from 0–40 v/cm. The voltage was applied for a total time of 1 min or less per sample in order to minimize effects caused by diffusion of electrode products.

The chamber can be filled automatically using the automatic transfer module, an optional accessory requiring about 100 ml of colloidal dispersion per

sample. This feature is convenient where sample volume is plentiful since the rinsing and filling can be accomplished by turning appropriate valves without removing the cell from the microscope stage. Alternatively, the chamber can be rinsed and filled using a syringe, reducing the sample size requirement to about 25 ml. (It can be further reduced to about 3 ml if the sample quantity is limited.)

The Laser Zee Meter illuminates the colloidal particles horizontally through the side of the chamber by means of a 2-mw helium-neon laser. The .7-mm circular beam is compressed in the vertical direction with cylindrical lenses so that most of the laser output power is concentrated within the 5  $\mu\text{m}$  depth of focus of the microscope. The width of the laser beam just fills the microscope field of view. Very few out-of-focus particles are illuminated and a dark-field image is maintained even at a concentration of 10–200 ppm. The laser beam is polarized so the *E* vector is horizontal, thus maximizing the brightness of small particles, as observed at a 90° angle with the microscope. Particles with high refractive index as small as 150 Å are readily visible as are 0.1  $\mu\text{m}$  latex particles.

The electronics is fully solid state, with the exception of the plasma tube. By depressing suitable push buttons, a digital readout is obtained of the sample temperature, specific conductance, or the applied voltage across the chamber electrodes.

The instrument reads out zeta potential directly as calculated from Smoluchowski's equation. The unit is factory calibrated, as described previously, for aqueous fluids at 20°C. When it is more appropriate to refer to the mobility of the particle, it may be calculated by dividing the zeta potential readout by 14.2. The colloidal dispersion used for these experiments consisted of 25 ppm rutile ( $\text{TiO}_2$ ) pigment (supplied by E.I. duPont de Nemours Co.) dispersed in deionized water with 10 ppm  $\text{Na}_2\text{P}_2\text{O}_7$  and 100 ppm KCL. The mean particle size was .13  $\mu\text{m}$ .

Three separate methods for determining particle mobilities were evaluated for speed of data acquisition. In each case, six measurements were made for one filling of the chamber; the chamber was filled eight times for a total of 48 data points.

The first method is the conventional "stop-watch" technique. The prism rotation rate was set at zero. Randomly selected particles were timed over 12 eyepiece grid lines, corresponding to 221  $\mu\text{m}$ . At an applied potential of 100 v, the typical transit time was approximately 10 sec.

The second method is similar to the first except that randomly selected particles were measured by



adjusting the prism rate to make the particle appear to stop. Each particle measurement was made in 10 sec or less.

The third method utilizes the ability of the eye to judge the net movement of a whole field of particles. The prism rate control is adjusted until the cloud of particles appeared on the average to be stationary. The exact procedure for judging the null condition is discussed later. Simply stated, the null is approached first from one direction and then from the other, and an average measurement is obtained in 10 sec or less.

### *Experimental results*

Figure 4a shows a typical histogram for the  $\text{TiO}_2$  dispersion using the conventional stopwatch method. Figure 4b illustrates similar data using the rotating prism to measure individual particles. Finally, Figure 4c illustrates the technique of using the eye to average the movement of the particle cloud. Significant improvement in precision is obtained.

### **Discussion**

Figure 4a illustrates the well-known fact that individual colloidal particles normally have slightly different values of mobility. It is precisely because of this mobility distribution that the conventional stopwatch method is so slow. For example, assume that the mobility distribution in Figure 4a is normally distributed with standard deviation  $\sigma$ . One concludes that, if a single particle is measured, there is a 95% probability that the mean mobility falls within  $\pm 2\sigma$  of this one measurement. Since higher precision is usually required, one normally measures additional particles and computes a mean mobility. As with any experiment of this type, the standard deviation of the sample mean is inversely proportional to the square root of the number of samples. Many additional measurements are therefore required to make significant improvements in precision.

Figure 4b illustrates that the rotating prism can be used to collect data on individual particles in much the same way as the conventional stopwatch technique. Since the particles are still being measured one at a time, the speed of the data taking and the standard deviation associated with a single measurement are comparable to the data shown in Figure 4a.

The real benefit of the prism technique is illustrated in Figure 4c. In this case, the operator adjusts the prism control until the particle cloud as

a whole is stationary. Although the mean mobility determined in this manner is the same as in the previous two experiments, we see that the standard deviation for single 10 sec particle cloud measurements is improved by a factor of four compared to either of the previously discussed techniques for measuring single particles.

Recalling that the precision of the sample means varies inversely to the square root of the number of measurements, we conclude that it would take 16 stopwatch measurements on individual particles to achieve the same measurement precision as with a single particle cloud measurement. Put another way, we can say that the particle cloud measurement is 16 times faster than conventional techniques.

It is appropriate at this point to discuss the manner in which the operator judges when the particle cloud is stationary. First of all, the operator's eye must focus on a reference point on the eyepiece reticle. One must *not* look at individual particles or the benefits of the approach are largely lost. It sometimes takes a little practice to keep one's eye on the reticle, particularly for those operators long accustomed to making individual measurements of single particles.

The best procedure for nulling the particle cloud is as follows: with the cell voltage turned off, the prism rate is set at zero and a stationary particle cloud is observed. The cell voltage is turned on and the direction of the electrophoretic velocity of the particles is noted. The prism control is then adjusted in the appropriate direction until the net motion of the particle cloud is approximately stopped. The operator then adjusts the setting somewhat further until a barely perceptible motion is observed first one way and then the other. The magnitude of the adjustments in alternating directions is reduced slowly until the cloud appears stationary. The procedure is similar to obtaining a balance on a resistance bridge or similar instrument. After a few minutes practice, this average reading can be obtained in less than 10 sec.

The purpose in approaching the null condition first from one direction and then from the other is to eliminate the effect of a dead zone in the operator's ability to perceive a null condition. Consider first a hypothetical colloid in which all of the particles have exactly the same mobility. It is, of course, a simple matter to adjust the prism rate so the particles are stationary. On the other hand, consider a colloid with a broad charge distribution such as the  $\text{TiO}_2$  sample used in these experiments. At the null point, approximately an equal number of particles are moving in each direction. The wider the

mobility distribution curve, the more difficult it is to define the null. The operator senses that a range of values exists where no net movement of the particle cloud is observed. Approaching the null points first from one direction and then from the other helps to eliminate errors resulting from the existence of this dead zone.

### Conclusions

Accurate electrophoresis measurements can be made using the rotating prism method, and single particle measurements of mobility agree closely with values obtained using the conventional stopwatch technique. More importantly, the rotating prism method allows the operator to measure more than 10 particles simultaneously. Data are thereby attained more rapidly and consequently with less error due to time-dependent factors.

The time-dependent errors likely to be minimized by the prism method include errors resulting from convection currents, bubble formation, diffusion of electrode reaction products, changes in the effective length of the chamber, and changes in the position of stationary layer caused by contamination of the chamber surfaces. In addition, certain colloidal dispersions are difficult to measure with standard techniques and can benefit from the high rate of

data acquisition made possible with the prism method. Such dispersions include those near zero charge where the sample coagulates rapidly, making measurements difficult; those in which time-dependent changes in mobility are significant such as in adsorption-desorption studies or of chemically reactive systems; and those of high specific gravity systems which settle rapidly.

It is also evident that the rotating prism method would be ideal for high concentration systems where conventional stopwatch techniques are impossible because individual particles cannot be followed by eye between grid lines. Preliminary tests show, for example, that metal oxide particles as small as 150 Å at a concentration of  $10^{10}$  particles/cm<sup>3</sup> can be readily measured, whereas this is impossible using the conventional technique.

The prism system is easy to calibrate, requiring only a value for the effective cell length, a precision reticle, a voltage reference, and a time reference. The readout is calibrated directly in mobility or zeta potential and is independent of changes in the applied cell voltage.

### Reference

1. *Surface and Colloid Science*, edited by E. Matijevic (Wiley, New York, 1974), Vol. 7, pp. 81-99.

## 6. MAINTENANCE

A minimum of maintenance is required for the Laser Zee<sup>tm</sup> Model 500. Maintenance is limited to three areas:

1. The Chamber
2. The Microscope
3. General Cleaning and Care of Unit.

### 6.1 CLEANING AND MAINTAINING THE CHAMBER

DO NOT attempt to dismantle the chamber other than to remove the anode compartment. Any additional dismantling of the chamber may result in leaks which will cause error in measurement.

The cathode electrode is platinum-plated and requires no maintenance. It should never be cleaned with an abrasive cleaner.

The anode electrode is composed of molybdenum which oxidizes with use. The fact that it oxidizes and turns black does not indicate that it should be cleaned. In fact, the electrode can become totally blackened by oxidation without any degradation in data accuracy. The best way to determine when to clean the electrode and whether the viewing chamber is too dirty for proper measurement is to check the calibration with a Standard Colloid as follows.

- 6.1.1 Fill the chamber with the standard colloid and adjust the microscope so as to focus at the top stationary layer. Measure the zeta potential and record. Adjust the microscope to focus at the bottom stationary layer. The bottom stationary layer is located by finding the bottom inside of the chamber and then rotating the fine-focus control on the microscope away from you (clockwise) an amount equal to the calibration constant of the chamber. Measure the zeta potential and record. The difference in measured zeta potential as recorded at the top and bottom stationary layer should not exceed 3 mV. If it does exceed 3 mV, the chamber requires cleaning.

A difference greater than 3 mV between measurements at the top and bottom stationary layers indicate that the surface charge of the top and bottom insides of the chamber

has changed due to contamination. This usually results from settling out of particles which changes the surface charge on the bottom due to their physical presence. Ultrasonic cleaning, as prescribed below, will restore the surfaces to equal charge so that equal results should be obtained at the top and bottom stationary layers. While we have incorporated an anode cleaning step into the cleaning procedure below, it is not always required. If the average of top and bottom results in out-of-specification for the standard colloid, then the anode should also be cleaned.

Another indication of when the chamber should be cleaned occurs when air bubbles tend to occlude on the walls. This condition may be visually apparent, or perceived through difficulty in reaching zero charge with no applied potential. The air bubbles are sticking to contaminant which must be ultrasonically removed.

#### 6.1.2 To Clean the Chamber

1. Empty the chamber and then remove the four screws which hold the anode compartment in place. Put the anode compartment aside. Clean the anode electrode with the abrasive cleaner supplied and wipe with damp cloth.
2. Mount anode compartment in place again using the same four screws. If the "O" ring is deformed, replace it with a spare from the accessories kit. Be careful to seal joint properly with the "O" ring.  
NOTE: DO NOT overtighten the four screws. Tighten the screws until the compartment is snug against the clear top plate.
3. Fill the chamber with the non-abrasive liquid cleaner, supplied by Pen Kem, Inc., diluted with 5 parts tap water to 1 part cleaner. Immerse the chamber in an ultrasonic bath. Include a small amount of the cleaner in the fluid of the ultrasonic bath. Turn on the ultrasonic cleaner and let it run for 15 minutes.

4. After 15 minutes, flush out the cleaning solution and rinse the chamber with at least 500 ml of tap water using a hand pump. Be certain that all the detergent has been removed from the chamber.
5. Rinse the outside of the chamber under running tap water. Dry the outside of the chamber with a soft cloth, taking care not to scratch the area where the laser beam enters the chamber. Make sure that this area is clean and free from water marks. If this area is not clean, the laser will not produce a clear particle image.
6. Rinse the inside of the chamber several times with demineralized water using a syringe. Let the chamber stand for several hours while filled with demineralized water. This will allow the chamber to return to an even temperature after uneven heating while in the ultrasonic bath and will ensure that all trace of the cleaning solution has been removed.

## 6.2 THE MICROSCOPE

- 6.2.1 The microscope used on the Laser Zee<sup>tm</sup> Model 500 is a high quality optical instrument. As with any precision optical device, a certain amount of care and cleaning is essential to maintain a factory-like operation.
- 6.2.2 Do Not force the microscope stage into the stop at the end of its travel. If forced, it will tend to loosen the precision gearing mechanism and cause excessive backlash.
- 6.2.3 The adjustable STOP ring, concentric with the coarse and fine focus knob is not used in the operation of the Laser Zee<sup>tm</sup> Model 500. It is factory set and should not be touched.
- 6.2.4 Periodically, remove the eye cups of the eyepieces by twisting slightly and then pulling. Clean the lens of the eyepieces using ordinary eyeglass lens tissue. Also clean end of objective lens with lens tissue.
- 6.2.5 Periodically clean the microscope with a damp cloth, particularly the Automatic Transfer Stage base plate where the chamber is normally positioned.

## 6.3 GENERAL CLEANING AND CARE OF UNIT

- 6.3.1 Occasional cleaning with a damp cloth will keep your instrument in top notch condition. Wipe away any spills, particularly around the microscope area. Clean the sub-stage illuminator and the area around it.
- 6.3.2 A coating of a light furniture wax on the case will keep it looking like new. However, take care not to spray any fluid near the hole in the case where the laser beam emerges. Any fluid spray there may coat the optics inside with a misty film.

## 7. SERVICE

7.1 In the remote event that a problem in in the operation of the instrument occurs, follow the Troubleshooting Procedure (7.1.1) to determine the faulty module. When you request a replacement of parts, please refer to the paragraph in the Troubleshooting Procedure that tells you about the replacement of the part.

7.2 The following items are contained in the Service section of the Manual.

1. Troubleshooting Procedure
2. Replaceable Parts Kit
3. Vendor List
4. Schematics

## ALIGNMENT OF LASER BEAM AND MIRROR

On occasion, it may become necessary to realign the laser beam, particular if the instrument has been subjected to stress during shipment.

Problem 1: There may be poor particle definition, that is, the particles illuminated by the laser are not truly in focus.

Problem 2: It may be that only a partial illuminated field exists when viewed through the Binocular Head. Steps 3 and 4 below are concerned only with Problem 1 and may be ignored if only the mirror requires adjustment.

### To Check Alignment

1. Fill the cell with a standard colloid and put in place on stage.
2. Plug unit in and depress "Pwr" and "S. C. " buttons. All others are released.
3. Observe that laser beam is shaped as shown in Figure 1 when viewed at output of height prism, using a piece of paper (see Fig. 2).
4. Beam should appear symmetrical as shown in Figure 1. If it is not, raise or lower optical telescope slightly, loosen single hex screw near base of telescope. Telescope is located between laser and optical platform.
5. After alignment of telescope, check to see if mirror is properly adjusted. The laser beam should intercept the center of the objective lens. Alternately loosen and tighten the two screws which mount the mirror to the right angle bracket. DO NOT overtighten these screws.
6. For final alignment of laser beam, view through binocular head and adjust mirror until the total viewing area is full of illuminated particles. From time to time, it may be necessary to adjust the height prism during adjustment of mirror.



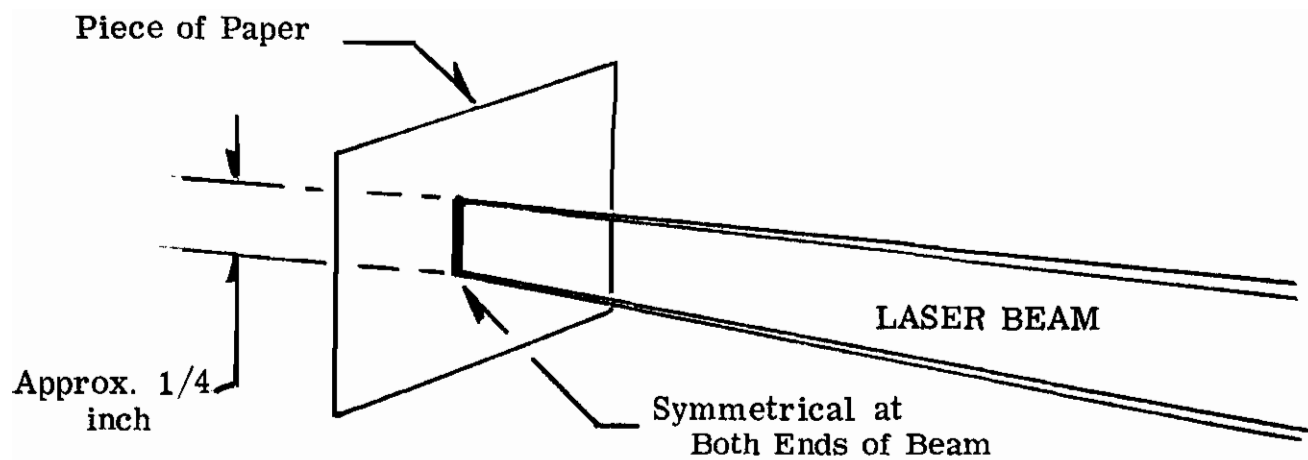


FIGURE 1

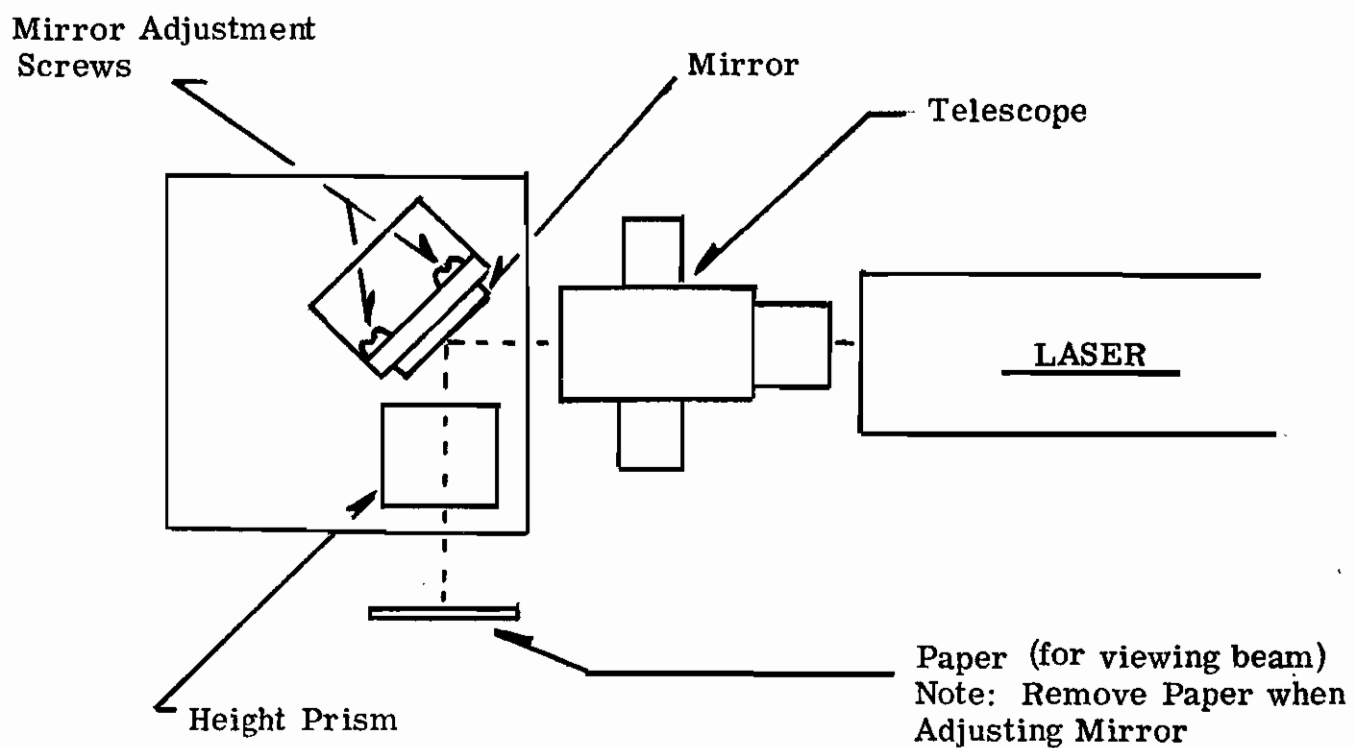


FIGURE 2

LASER ZEE METER<sup>TM</sup>  
TROUBLESHOOTING PROCEDURE  
for

MODEL 500

1. Before starting the following troubleshooting procedure, verify that there is in fact a problem with the Laser Zee Meter (LZM) by using the Functional Test provided.
2. The following paragraphs represent a step by step method of isolating a malfunction so that corrective action can be taken. If the problem is located on either the Analog, Digital, or Switch Module return the defective card to PEN KEM for repair or replacement. If the problem is found on the Mother Board or associated Electronics Chassis, PEN KEM or its authorized agent will either supply replacement parts, recommend a local supplier, or exchange the complete Electronics Chassis depending upon the individual circumstances.

The LZM must be recalibrated if the Analog card is replaced. It must also be recalibrated if any of the following Mother Board components are replaced: R1-R3, R7-R8, R12, R15-R20, R24, R25, R29-R33, R35 and R37. It is not likely however, that any of these resistors will ever fail in normal use.

When a defective part has been replaced, repeat the troubleshooting procedure from the beginning to verify that there are no additional problems.

3. In order to perform the following troubleshooting, the following equipment is required:
  1. Multimeter - Simpson Model 260 or equivalent 20K OHM/volt meter.
  2. Oscilloscope - 10MHZ Bandwidth, .5v/cm Sensitivity.
4. Since troubleshooting requires working with voltages as high as 500 volts, only an experienced technician should undertake such service. Logic levels referred to in text as "1" or "0" are defined as follows:

logic 1	+2.0 to +5.3 volts DC
logic 0	0 to +1 volts DC

It will also be convenient to make a notation to the left of each step number as to whether or not the unit passed that particular test.

5. Unplug power cord from power outlet.
6. First check main power fuse located at rear of instrument. (On early units this requires cover to be removed and fuse is on right side of electronics chassis).
7. If fuse is good, loosen four screws holding cover to base plate. Unplug temperature sensor and electrode connectors if present and then lift case straight up and put aside.
8. Rotate voltage control knob( immediately to right of power switch) fully CCW.
9. Plug power cord in wall outlet.
10. Fill cell with tap water.
11. Plug thermistor plug into mating connector on LZM.
12. Depress "POWER" and "VOLTAGE" buttons on LZM; release any other buttons..
13. Verify that laser is operating.

#### CAUTION

Never look directly into laser beam or its reflection from a specular surface. Do not interpose any object such as a watch crystal in the laser beam path as the reflected light is potentially harmful to the eyes. For this reason an interlock switch is provided which automatically turns unit off whenever cell is removed from its normal position on the microscope.

2  
2/6/74

14. If laser is operating turn laser off using switch on laser power supply and proceed to step 15. If laser is not operating proceed as indicated below.
- 14.1 Check that switch on Laser Power Supply is "ON". If it is, use Multimeter to verify that voltage of 120 VAC  $\pm$  10% is present between pins 2 and 4 of terminal strip on right hand side of electronics chassis. Numbering of pins is from left to right.

#### CAUTION

Do not use a meter which operates off AC power for tests in step 14 unless you are positive that both the inputs are isolated from the line.

- 14.2 If voltage is present across pins 2-4 and laser is not operating remove laser and its associated power supply and return to PEN KEM for replacement.
- 14.3 If voltage is not present between pins 2 and 4 check that input line voltage of either 120 VAC or 220 VAC is present between pins 2 and 5. If voltage between pins 2 and 5 is not correct, check fuse and fuse wiring.
- 14.4 If voltage is correct between pins 2 and 5 check that voltage across pins 2 and 6 is 120 VAC. If it is proceed to 14.5. For units working from input line voltages of 120 VAC there should be a jumper from pins 5 to pin 6. For units working from 220 VAC input power, auto transformer T3, as shown in schematic 51053, reduces line voltage to 120 VAC. If voltage between pins 2 and 6 is not 120 VAC check variac and associated wiring.
- 14.5 If voltage between pins 2 and 5 is 120 VAC, check operation of "POWER" switch. First unplug main power cord and then unplug two-conductor plug from power switch to Motherboard. Check continuity of switch using Multimeter.
- 14.6 If Power switch is good, check operation of microswitch on microscope stage. This can be done by removing connector from left hand side of Electronics Chassis and checking continuity between pins D and F. Microswitch is normally open and closes when cell is in position under microscope.
- 14.7 If microswitch is good and 120 VAC is still not present between pins 2 and 4, wiring in electronics unit must be defective and can be checked out using schematic and wire list provided.
- 14.8 After repairs replace any connectors removed previously and repeat paragraphs 8 through 13.

15. Preliminary Tests of Mother Board

- 15.1 Verify that red lever switch at right front corner of Mother Board is in "NORMAL" position.
- 15.2 Connect one side of multimeter to Test Point 3 (TP3) on Mother Board (M.B.). Unless otherwise stated all measurements are made with respect to this terminal.
- 15.3 TP 1 on M.B. measures less than +10 VDC. If not, variac is probably defective. Unplug LZW power cord and isolate problem using schematic before applying power again.
- 15.4 Rotate Voltage Control Knob (to right of push buttons on LZW) slowly clockwise checking that voltage at TP 1 increases uniformly up to at least +400 VDC. If operation is erratic then variac is probably defective. If voltage reaches only 200 volts then either C1 or C2 on M.B. or associated components are defective. Before trying to troubleshoot this circuitry turn Voltage Control Knob fully CCW and then 1/8 turn CW. This insures that voltages in high voltage power supply will be approximately 50 V and therefore less dangerous.
- 15.5 Set same Voltage Control Knob for reading of +100 VDC at TP 1 ( $\pm 5$  VDC).
- 15.6 Test Point voltages on Mother Board should measure as follows. Record actual measured values in right hand column.

Test Point	Minimum Value (VDC)	Maximum Value (VDC)	Measured Value
2	+14.7	+15.3	
4	-14.7	-15.3	
5	+4.7	+5.3	
6	+1.2	+2.8	
7	-9.0	-15.0	
8	+1.0	+3.0	
9	+1.0	+3.0	
10	+1.5	+1.5	

- 15.7 If above test point voltages are within specification, skip to step 16.
- 15.8 If any of the above test point voltages are out of specification, remove first the Digital and then Analog card from its socket. If removal of one card or the other eliminates the problem, then that card has a short circuit and must be replaced.
- 15.9 If removal of both cards does not solve the problem, then troubleshoot various circuits using Mother Board Schematic and Electronics Wiring Diagram.

## 16. Troubleshooting the Z.P. Mode of Operation

- 16.1 Depress "Z.P." and "POWER" pushbuttons on LZM and release any other buttons.
- 16.2 Verify that voltage at TP 1 on Mother Board is still 100 VDC +5V and adjust Voltage Control Knob if necessary.
- 16.3 Using Z.P. Control knob (located immediately to left of push buttons on LZM), verify whether readout can be set to approximately "+25.0" and "-75.0". Also check that the reading can be made to vary continuously between these two limits as the Z.P. Control Knob is rotated. If these conditions are met, skip to step 16.22.
- 16.4 If difficulty is experienced with only one digit position, exchange the bad readout device with one that was previously working. If the same digit position is still not operating, the Digital Card is defective and should be returned for replacement. If the same readout device is not operating, only the readout need be replaced.
- 16.5 If the decimal point is in the wrong position check that pin 15 is at logic 0. If not, remove Digital Card. If pin 15 is now at logic 0 then Digital Card is defective. If pin 15 is not at logic 0 check operation of U1 on Mother Board. Logic levels should be as follows:
- |    |        |         |
|----|--------|---------|
| J3 | pin 6  | logic 0 |
| J3 | pin 12 | logic 0 |
| J3 | pin 17 | logic 0 |
| U1 | pin 2  | logic 1 |
| U2 | pin 1  | logic 1 |
- 16.6 Set Z.P. Control Knob so as to provide +1 VDC at TP 3 on Analog Board. If this is accomplished skip to step 16.8.
- 16.7 If +1 VDC can not be provided, check operation of R4, R5, R6 and R26 on Mother Board, the connection through Switch Board from pin 16 to pin 9, and finally the connection from pin 9 of Switch Board to pin 16 of Analog Board.
- 16.8 Observe waveform at TP 5 on Analog Board using scope. Waveform should appear as in Figure 1. Period between pulses should be .75 m sec +.25 m sec. If measurement is within specification, skip to step 16.11.

16.9 Remove Digital Card. If waveform at TP 5 is now correct, Digital Card is defective and must be replaced.

16.10 Voltages on Analog Card Connector should be as follows:

Pin	Minimum Value (VDC)	Maximum Value (VDC)
19	+14.7	+15.3
20	-14.7	-15.3
22	+4.7	-5.3

If these voltages are not correct check for open connections from power supplies to pins 19, 20 and 22. If voltages are correct and unit failed to pass test 16.8 then Analog Card is defective and must be replaced.

16.11 If pulses are being generated in accordance with step 16.8 then readout should be between -20 and -50. If it is skip to step 16.18.

16.12 If readout is not between -20 and -50 then check that +5 VDC +.3 VDC appears at pin 22 of Digital Card and ~~that~~ pin 18 measures 0 VDC +.1 VDC. If not check for open circuits on Mother Board.

16.13 Using scope check that pulse signal described in step 16.8 appears at pin 3 of Digital Card. If not check Mother Board for open circuit from pin 8 of J1 to pin 3 of J2.

16.14 Check that sign of readout is minus. If it is skip to 16.16.

16.15 If sign is positive check that TP4 on Analog Card is logic 0. If it is not, remove Digital Card. If TP4 still is not at logic 0, Analog Card is defective and must be replaced. If TP 4 and pin 20 of J2 both logic 0 then Digital Board is defective.

16.16 The following voltages should be obtained on Digital Card connector J2:

pin 1	logic 1
pin 2	logic 0

If voltages are correct skip to step 16.18.



16.17 If logic levels in step 16.16 are not correct, remove Digital Card. Using Multimeter, determine resistance to ground (TP 3 on M.B.) from pins 1 and 2 of J2.

pin 1	greater than 100 K
pin 2	less than 10

If values are correct and step 16.16 failed then Digital Board is defective. If values are incorrect, check operation of Switch Card; it is probably defective.

16.18 Set Z.P. Control Knob so as to provide -1 V at TP 3 on Analog Module.

16.19 Observe waveform at TP 5 on Analog Board using scope. Time between pulses should be .5 to 1 m sec. If this condition is not met, Analog Board is defective.

16.20 If Readout on LZM is between +20 and +50 repeat setp 16.3, otherwise proceed.

16.21 If Readout on LZM is minus, check that TP4 on Analog Board is logic 1. If not remove Digital Card. If TP 4 still is not logic 1, Analog Card is defective. If TP 4 and pin 20 of J2 both are logic 1 then Digital Board is defective.

\* 16.22A ( See Below)

16.22 Adjust Z.P. Control Knob for readout of approximately "-75.0" +2.0.

16.23 Prism located ~~inside microscope objective~~ rotates slowly about 6° left to right... (viewed from operating position) and is reset approx once a second... If this condition is met skip to step 16.33.

16.24 Observe waveform at TP 2 of Analog Card. Waveform appears as in Figure 2 with a peak to peak amplitude of 8 - 12 V, and a period of 10 - 16 seconds. If these conditions are met skip to step 16.28.

16.25 Measure voltage at TP 1 of Analog Card. Voltage measures same as TP 9 on Mother Board as recorded in step 15.6. If not, check continuity from pin 1 of J1 to pin 9 of J3 through Switch Card to pin 15 of J3 to TP 9 on Mother Board.

16.26 Measure voltage at pin 9 of J1. It should measure ~~Q+ or -~~ .1VDC and +5.3 VDC. If not check operation of Switch Card.

\* 16.22A Loosen thumbscrew and remove binocular head of microscope.

8  
2/6/74

- 16.27 Remove Analog Board and measure resistance to ground (pin 3 on M.B.) from pin 4 of J1. If it is greater than 10 KOHM and unit failed test described above in step 16.24 then Analog Board is defective. If less than 10 K look for short on Mother Board or Switch Board.
- 16.28 Remove Analog Board if present and measure resistance from pin 10 of J1 to ground (TP3 on M.B.). Resistance should be 40 OHMS  $\pm$ 5. If so skip to step 16.30.
- 16.29 Unplug connector from left side of Electronics Assembly. Measure resistance of galvanometer by connecting Multimeter to pins A and C of cable plug. Resistance should be 30 OHMS  $\pm$ 10. If resistance is greater than this check for a broken wire. If galvanometer itself is open circuit (an unlikely situation) order a replacement from PEN KEM. If circuit does measure 30  $\pm$ 10 plug connector back into electronics assembly and check for open or shorts on M.B.
- 16.30 Observe waveform at pin 5 of J1. Waveform appears as shown in Figure 3 with a peak to peak amplitude of 1V  $\pm$ .3V.
- 16.31 If waveform measured above is satisfactory but prism still does not move, shaft may be frozen. Check for this by turning prism gently with fingers.
- 16.32 If no waveform was present during step 16.30 and unit passed step 16.28, the Analog Board is defective.
- 16.33 Observe Waveform at TP 2 on Analog Board using scope. Waveform appears as in figure 2.
- 16.34 Set lever switch at right front corner of Mother Board to "Calibrate" position.
- 16.35 Sawtooth waveform stops when next reset to positive limit. If sweep does not stop skip to step 16.37.
- 16.36 If sweep stops, depress "Average" button. Sweeps starts, makes one complete sweep, and stops again. If unit does this, skip to step 16.38.
- 16.37 Remove Digital Board. Sweep observed at TP 2 is stops. Ground pins 12 and 13 of J2 and sweep starts. If these conditions are met and steps 16.35 or 16.36 failed, then Digital Board is defective. If unit fails step 16.37 check operation of U2. If U2 is good then Analog Card is defective.

16.38 Approximately 30 to 50 seconds after average button was depressed in step 16.36 a "beep" is heard and the LZM readout is approximately "-75.0"  $\pm$ 5.0.

16.39 Set lever switch back to "NORMAL".

## 17. Troubleshooting Voltage Readout Mode

- 17.1 Depress "Voltage" and "Power" push buttons on LZM. All other buttons are released. Make sure lever switch at right front corner of Mother Board is set to "NORMAL".
- 17.2 Adjust Voltage Control Knob so as to produce a reading of 100 VDC  $\pm 2$  VDC at TP 1 on Mother Board as measured with Multimeter.
- 17.3 LZM display should read "+100"  $\pm 5$ . If it does, skip to step 18.
- 17.4 No decimal point should be displayed on readout. If one is present check voltages on Mother Board at points listed below.

J3	pin 12	logic 0
J3	pin 17	logic 1
U2	pin 2	logic 1
U2	pin 1	logic 0
J2	pin 15	logic 1
J2	pin 10	logic 0

- 17.5 TP 1 on Analog Board should measure +7.5 VDC  $\pm 2$  VDC. If it does skip to step 17.7.
- 17.6 If TP 1 does not measure +7.5 VDC  $\pm 2$  VDC, check voltage at junction of R24 & R25 on Mother Board. It should be +7.5v  $\pm 2$ v. If it is, check continuity to pin 10 of J3, through switch board to pin 9 of J3, and finally across Mother Board to pin 1 of J1.
- 17.7 Test that pin 9 of J1 measures logic 0. If not, check continuity of logic 0 signal from pin 1 of J3 through switch assembly to pin 11 of J3 across Mother Board to pin 9 of J1.
- 17.8 Test that pin 15 and pin 17 of J1 are both logic 1. If not test that pins 2 and 4 of U2 on Mother Board are at logic 0. If they are U2 is defective and must be replaced.
- 17.8 Voltage at pin 2 of Analog Card should measure the same as voltage at TP 8 on Mother Board as recorded previously in step 15.6. If not check continuity from TP 8 to pin 14 of J3 to pin 8 of J3 across Mother Board to pin 2 of J1.

- 17.10 Voltage at TP2 of Analog Card should measure  $\approx .2$  to  $\approx .4$  VDC and voltage at TP 3 should be the same as TP 2. If they are not the same check continuity of signal from TP 2 to pin 4 of J1 to pin 22 of J3 to pin 7 of J3 and finally across Mother Board to pin 16 of J1.
- 17.11 If TP 2 and TP 3 are correct but readout is still not correct, Analog Card is defective.

## 18. Troubleshooting the S.C. Readout Mode

- 18.1 Depress "S.C.", "S.C.Low", "H.V.", and "POWER" push buttons. All other buttons are released.
- 18.2 Adjust Voltage Control Knob so as to produce a reading of  $+100 \text{ VDC} \pm 2 \text{ VDC}$  at TP 1 on Mother Board as measured with Multimeter.
- 18.3 For most tap water samples the LZM Display should read between  $+100$  and  $+800$  and if it does skip to step 18.12.
- 18.4 If decimal point is in wrong position check voltages on Mother Board at points listed below.
- |    |        |         |                          |
|----|--------|---------|--------------------------|
| J3 | pin 6  | logic 1 |                          |
| J3 | pin 12 | logic 1 | if not check Switch Card |
| J3 | pin 17 | logic 0 |                          |
| J2 | pin 10 | logic 1 | if not replace U2 on     |
| J2 | pin 15 | logic 1 | Mother Board.            |
- 18.5 Measure voltage on TP 1 of Analog Board. It should be the same as the voltage on TP 10 on Mother Board as recorded previously in step 15.6. If it is not, check continuity from TP 10 to pin 19 of J3, through Switch Board to pin 9 of J3 and finally to pin 1 of J1.
- 18.6 Measure voltage at pin 20 of J3. Voltage at this point should be approximately equal to  $4 \text{ mv}$  times the S.C. (in  $\mu\text{mhos/cm}$ ) of the water used as a sample. For example, a water sample of  $300 \mu\text{mhos/cm}$  would produce a voltage at pin 20 of approximately  $+1.2 \text{ VDC}$  ( $4\text{mv} \times 300 \mu\text{mhos/cm}$ ). If voltage is between  $.4 \text{ VDC}$  and  $3.2 \text{ VDC}$  proceed to step 18.9.
- 18.7 If voltage at pin 20 is not correct, set Voltage Control Knob so as to produce a reading of  $25 \text{ VDC} \pm 2 \text{ VDC}$  at TP 1 on Mother Board.
- 18.8 Remove cell from microscope stage, unplug electrode connector from LZM, remove electrodes stoppers from cell and lay electrodes on insulated surface so that they do not touch one another. Plug electrode connector back into LZM and put cell back in place on microscope. Measure voltage on anode (red lead). It should be  $25 \text{ VDC} \pm 2 \text{ VDC}$ . Turn LZM off. Measure resistance from cathode (black lead) to ground. The resistance should be  $1000 \text{ OHMS}$ . Turn power back on. If either of these two tests fail, check wiring of Electronic Unit using schematic provided.

When repairs, if any, are complete, remove cell from microscope, unplug electrode connector, install electrodes again in cell, plug electrode connector back into LZM, and put the cell back in place on microscope. Next, set Voltage Control Knob to again produce 100 volts at TP 1 on Mother Board.

- 18.9 Measure voltage at pin 2 of J1. It should be the same as at pin 20 of J3. If not check continuity from pin 20 of J3 through Switch Card to pin 8 of J3 to pin 2 of J1.
- 18.10 Voltage at TP 2 and TP 3 on Analog Card should be the same. If not, check continuity from pin 4 of J1 to pin 22 of J3 through Switch Assembly to pin 7 of J3 to pin 16 of J1.
- 18.11 Voltage at pin 9 of J1 should be 0 to +.5 VDC. If it is not, check pin 11 of J3. If pin 11 does not measure 0 to +.5 VDC then Switch Card is defective.
- 18.12 Release "S.C. LOW" button on LZM. Decimal point on readout should move two places to right. If it does skip to step 18.14.
- 18.13 If decimal point in wrong position check voltages on Mother Board at points listed below:
- |    |        |         |                          |
|----|--------|---------|--------------------------|
| J3 | pin 6  | logic 0 | if not check Switch Card |
| J2 | pin 10 | logic 0 | if not replace U2 on     |
| J2 | pin 15 | logic 0 | Mother Board             |
- 18.14 Readout is less than "+01.0" (1000 u mhos/cm). If it is not, remove Switch Card as it is defective.
- 18.15 Depress "S.C. LOW" again. Release "H.V." push button.
- 18.16 Readout on LZM should be "+.000"  $\pm$ .002. If it is not, replace Analog Card.

## 19. Troubleshooting Temperature Mode of Operation

19.1 Depress "TEMP" and "POWER" push-buttons on LZM and release any other buttons.

19.2 Set Voltage Control Knob fully CCW.

19.3 LZM display ready approximately "+05.0" +5 which corresponds to  $25^{\circ}\text{C} \pm 5^{\circ}\text{C}$ . This assumes that thermistor is at normal room temperature. If readout is correct, LZM should be operating correctly and troubleshooting procedure is completed. If you are still having difficulty, contact PEN KEM or its authorized sales agent for further help.

19.4 If decimal point is in wrong position check that logic levels are as follows:

J3	pin 12	logic 0	If not replace
J3	pin 17	logic 0	Switch Card.
J2	pin 10	logic 0	If not replace Us on
J2	pin 15	logic 0	Mother Board.

19.5 If readout is not correct, measure TP 11 on Mother Board. Voltage should be between +0.0 and +1.6 VDC. If it is skip to step 18.11.

19.6 If voltage at TP 11 is not correct, unplug thermistor from LZM. Resistance values on plug should measure as follows:

	$20^{\circ}\text{C}$	$25^{\circ}\text{C}$	$30^{\circ}\text{C}$
tip to sleeve	7,496	6,000	4,834
ring to sleeve	37,300	30,000	24,270

If values at room temperature ( $20 - 30^{\circ}\text{C}$ ) are outside these limits then thermistor probe is defective.

19.7 Turn LZM off by releasing "POWER" switch. Using Multimeter, measure resistance from thermistor socket on LZM to ground (TP 3 on M.B.). Values on socket should be as follows:

tip to ground	17.K to 19K OHMS
ring to ground	5.5 K to 6.5K OHMS

If measurements outside these limits check for open or short circuit in wiring.



19.8 Turn LZM on again by depressing "POWER" switch.

19.9 Voltages at various points should be as follows:

ring contact of thermistor socket	-3.0 to -3.8VDC
pin 2 of U3 on M.B.	-3.0 to -3.8VDC
TP 11 on M.B.	-6.5 to -8.5VDC

If first two voltages measured above are not equal then U3 is defective.

19.10 Plug thermistor into socket on LZM.

19.11 Measure voltage at T.P. 1 on Analog Card. It should read +7.5VDC  $\pm$  .2VDC. If not, the switch assembly is defective.

19.12 Voltage at TP 2 and TP 3 should be equal in value. If not, check switch card for continuity between pin 22 and pin 7.

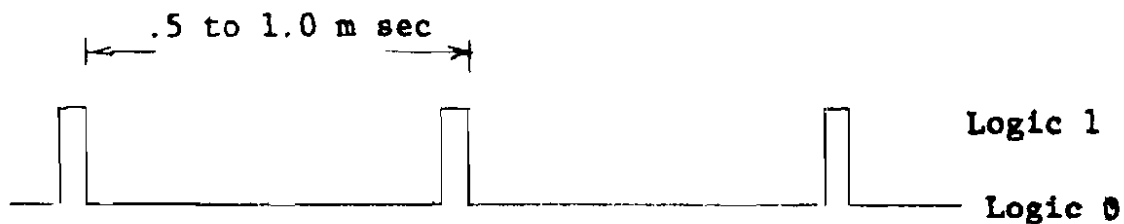


FIGURE 1  
Waveform at TP 5 on Analog Card.

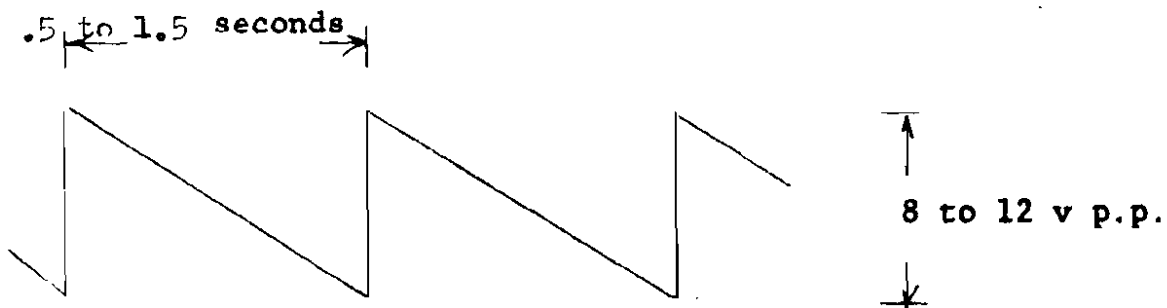


FIGURE 2  
Waveform at TP 2 on Analog Card.



FIGURE 3  
Waveform at Pin 5 of J1.

PEN-KEM  
211 CLEVELAND DRIVE  
CHOTLA-CN-HUDSON, N.Y. 10520

MODEL 500- REPLACEABLE PARTS LIST

ASSEM. REF. DESIG.	PEN-KEM P/N	QUAN./ ASSEM.	DESCRIPTION	MANUF.	MANUF. P/N
A1	51CC1-40000	1	BOARD ASSY:ANALOG- MODEL 400 ONLY	PENKIM	F410A1C3-1
A1	*****	2	C:FXD POLY CARB. 0.01 UFF	72528	ACR15C-811
A1	*****	1	C:FXD POLY CARB. 2.5 UF	ACTPA	CM05E0471
A1	*****	1	C:FXD MICA 470 Pf	72136	F410A1C3-1
A1	*****	0	C:FXD POLY CARB. 0.01 UFF	72928	CSR13E685
A1	*****	5	C:FXD TA 6.8 UF	56289	CSR13E685
A1	*****	0	C:FXD TA 6.8 UF	56289	CSR13E685
A1	*****	0	C:FXD TA 6.8 UF	56289	CSR13E685
A1	*****	0	C:FXD TA 6.8 UF	56289	CSR13E685
A1	*****	1	C:FXD MICA 100 Pf	72136	CM05E0471
A1	*****	18	C:FXD CER 0.01 UF	55275	CK068X1C3
A1	*****	0	C:FXD CER 0.01 UF	55275	CK068X1C3
A1	*****	0	C:FXD CER 0.01 UF	55275	CK068X1C3
A1	*****	0	C:FXD CER 0.01 UF	55275	CK068X1C3
A1	*****	0	C:FXD CER 0.01 UF	55275	CK068X1C3
A1	*****	0	C:FXD CER 0.01 UF	55275	CK068X1C3
A1	*****	0	C:FXD CER 0.01 UF	55275	CK068X1C3
A1	*****	0	C:FXD CER 0.01 UF	55275	CK068X1C3
A1	*****	0	C:FXD CER 0.01 UF	55275	CK068X1C3
A1	*****	0	C:FXD CER 0.01 UF	55275	CK068X1C3
A1	*****	0	C:FXD CER 0.01 UF	55275	CK068X1C3
A1	*****	1	C:NOT USED	55275	CK068X1C3
A1	*****	0	C:FXD CER 0.01 UF	55275	CK068X1C3
A1	*****	0	C:FXD CER 0.01 UF	55275	CK068X1C3
A1	*****	0	C:FXD CER 0.01 UF	55275	CK068X1C3
A1	*****	0	C:FXD CER 0.01 UF	55275	CK068X1C3
A1	*****	0	C:FXD CER 0.01 UF	55275	CK068X1C3
A1	*****	0	C:FXD CER 0.01 UF	55275	CK068X1C3
A1	*****	0	C:FXD CER 0.01 UF	55275	CK068X1C3
A1	*****	0	C:FXD CER 0.01 UF	55275	CK068X1C3
A1	*****	0	C:FXD CER 0.01 UF	55275	CK068X1C3
A1	*****	0	C:FXD CER 0.01 UF	55275	CK068X1C3
A1	*****	0	C:FXD TA 6.8 UF	56289	CSR13E685
A1	*****	5	DIODE: SI SWITCHING	01295	IN914
A1	*****	0	DIODE: SI SWITCHING	01295	IN914
A1	*****	2	DIODE: SI SWITCHING	01295	IN3595
A1	*****	0	DIODE: SI SWITCHING	01295	IN3595
A1	*****	0	DIODE: SI SWITCHING	01295	IN914
A1	*****	0	DIODE: SI SWITCHING	01295	IN914
A1	*****	0	DIODE: SI SWITCHING	01295	IN914
A1	*****	4	TSTR: SI FET	01295	2N4857
A1	*****	0	TSTR: SI FET	01295	2N4857
A1	*****	0	TSTR: SI FET	01295	2N4857
A1	*****	0	TSTR: SI FET	01295	2N4857
A1	*****	5	R:FXD COMP 100K OHM 5% 1/4W	01121	RCR07G1C4JS
A1	*****	0	R:FXD COMP 100K OHM 5% 1/4W	01121	RCR07G1C4JS
A1	*****	2	R:FXD COMP 22K OHM 5% 1/4W	01121	RCR07G223JS
A1	*****	1	R:OPTIONAL TRIM	01121	RCR07G223JS
A1	*****	1	R:OPTIONAL TRIM	01121	RCR07G223JS
A1	*****	1	R:FXD COMP 10 OHM 5% 1/4W	01121	RCR07G1C4JS
A1	*****	0	R:FXD COMP 100K OHM 5% 1/4W	01121	RCR07G1C4JS
A1	*****	1	R:FXD COMP 36K OHM 5% 1/4W	01121	RCR07G363JS
A1	*****	7	R:FXD COMP 1K OHM 5% 1/4W	01121	RCR07G1C2JS

REF. DESIG.	PEN-REM P/N	QUAN./ ASSEM.	DESCRIPTION	MANUF.	MANUF. P/N
R10	*****	4	R:FXD COMP 10K OHM 5% 1/4W	01121	RCR07G1C3JS
R11	*****	2	R:FXD COMP 220K OHM 5% 1/4W	01121	RCR07G224JS
R12	*****	6	R:FXD COMP 4.7K OHM 5% 1/4W	01121	RCR07G472JS
R13	*****	2	R:FXD MET FLP 10K OHM 1% 1/8W	11502	RN60C1CC2
K14	*****	1	R:NOT USED		
R15	*****	1	R:FXD MET FLP 1K OHM 1% 1/4W	11502	RN60C1CC1
R16	*****	1	R:NOT USED		
R17	*****	0	R:FXD COMP 1K OHM 5% 1/4W	01121	RCR07G1C2JS
R18	*****	0	R:FXD COMP 1K OHM 5% 1/4W	01121	RCR07G1C2JS
R19	*****	0	R:FXD COMP 10K OHM 5% 1/4W	01121	RCR07G1C3JS
R20	*****	0	R:FXD COMP 10K OHM 5% 1/4W	01121	RCR07G1C3JS
R21	*****	0	R:FXD MET FLP 10K OHM 1% 1/8W	11502	RN60C1CC2
R22	*****	0	R:FXD COMP 10K OHM 5% 1/4W	01121	RCR07G1C3JS
R23	*****	2	R:FXD COMP 47K OHM 5% 1/4W	01121	RCR07G473JS
P24	*****	0	R:FXD COMP 100K OHM 5% 1/4W	01121	RCR07G1C4JS
P25	*****	0	R:FXD COMP 4.7K OHM 5% 1/4W	01121	RCR07G472JS
R26	*****	0	R:FXD COMP 22K OHM 5% 1/4W	01121	RCR07G223JS
K27	*****	0	R:FXD COMP 1K OHM 5% 1/4W	01121	RCR07G1C2JS
R28	*****	0	R:FXD COMP 4.7K OHM 5% 1/4W	01121	RCR07G472JS
R29	*****	0	R:FXD COMP 220K OHM 5% 1/4W	01121	RCR07G224JS
K30	*****	1	R:FXD COMP 470K OHM 5% 1/4W	01121	RCR07G474JS
R31	*****	0	R:FXD COMP 1K OHM 5% 1/4W	01121	RCR07G1C2JS
R32	*****	0	R:FXD COMP 100K OHM 5% 1/4W	01121	RCR07G1C4JS
R33	*****	0	R:FXD COMP 1K OHM 5% 1/4W	01121	RCR07G1C2JS
R34	*****	0	R:FXD COMP 47K OHM 5% 1/4W	01121	RCR07G473JS
P35	*****	0	R:FXD COMP 1K OHM 5% 1/4W	01121	RCR07G1C2JS
K36	*****	0	R:FXD COMP 4.7K OHM 5% 1/4W	01121	RCR07G472JS
R37	*****	1	R:FXD MET FLP 100K OHM 1% 1/8W	11502	RN60C1CC3
R38	*****	1	R:NOT USED		
R39	*****	1	R:NOT USED		
K40	*****	1	R:NOT USED		
P41	*****	0	R:FXD COMP 4.7K OHM 5% 1/4W	01121	RCR07G472JS
P42	*****	0	R:FXD COMP 4.7K OHM 5% 1/4W	01121	RCR07G472JS
TP1	*****	5	TEST JACK: WHITE: RECTANGULAR	74970	105-11C1-001
TP2	*****	0	TEST JACK: WHITE: RECTANGULAR	74970	105-11C1-001
TP3	*****	0	TEST JACK: WHITE: RECTANGULAR	74970	105-11C1-001
TP4	*****	0	TEST JACK: WHITE: RECTANGULAR	74970	105-11C1-001
TP5	*****	0	TEST JACK: WHITE: RECTANGULAR	74970	105-11C1-001
U1	*****	4	IC:LIN. UP. AMP.	01295	LM741CN
U2	*****	2	IC:DUAL VOLTAGE TRANSLATOR	12040	DM88CC
U3	*****	0	IC:DUAL VOLTAGE TRANSLATOR	12040	DM88CC
U4	*****	1	IC:LIN. OP. APP.	12040	LM30EH
U5	*****	3	IC:PREC. COMP.	12040	LM311H
L6	*****	0	IC:LIN. UP. AMP.	12040	LM741CN
U7	*****	1	IC:UP. APP. CURRENT	12040	LH0002CH
U8	*****	0	IC:PREC. COMP.	12040	LM311H
U9	*****	4	IC:QUAD, 2-INPUT NAND	01295	SN74CCN
L10	*****	0	IC:QUAD, 2-INPUT NAND	01295	SN74CCN
U11	*****	0	IC:LIN. OP. APP.	01295	LM741CN
U12	*****	0	IC:LIN. UP. APP.	01295	LM741CN

REF. DESIG.	PEN-KEM P/N	CLAN./ ASSEM.	DESCRIPTION	MANUF.	MANUF. P/N
U13	*****	0	IC:PREC. COMP.	12040	LM311H
U14	*****	1	IC:DUAL,J-K F/F	C1295	SN7476N
U15	*****	1	IC:4-BIT BINARY COUNTER	C1295	SN7453N
U16	*****	0	IC:QUAD,2-INPUT NAND	C1295	SN7453N
U17	*****	1	IC:QUAD,2-INPUT EXCL.-OR	C1295	SN7466N
U18	*****	0	IC:QUAD,2-INPUT NAND	C1295	SN7466N
U19	*****	1	BOALO ASSY: DIGITAL	PENK	CK0681C3
C1	51C5-CCCC	21	C:FXD CER 0.01 UF	55275	CK0681C3
C2	*****	0	C:FXD CER 0.01 UF	55275	CK0681C3
C3	*****	0	C:FXD CER 0.01 UF	55275	CK0681C3
C4	*****	2	C:FXD TA 1 UF 50 V	56289	CSR13E1C5
C5	*****	0	C:FXD TA 1 UF 50 V	56289	CSR13E1C5
C6	*****	1	C:FXD TA 6.8 UF 35V	56289	CSR13E1C5
C7	*****	0	C:FXD CER 0.01 UF -C770C24 BYPASS	55275	CK0681C3
P1	*****	6	R:FXD COMP 4.7K OHM 5% 1/4W	01121	RCR07G472JS
R2	*****	0	R:FXD COMP 4.7K OHM 5% 1/4W	01121	RCR07G472JS
R3	*****	2	R:FXD COMP 1K OHM 5% 1/4W	01121	RCR07G1C2JS
R4	*****	0	R:FXD COMP 1K OHM 5% 1/4W	01121	RCR07G1C2JS
R5	*****	2	R:FXD COMP 180 OHM 5% 1/4W	01121	RCR07G1E1JS
R6	*****	2	R:FXD COMP 680 OHM 5% 1/4W	01121	RCR07G6E1JS
R7	*****	0	R:FXD COMP 680 OHM 5% 1/4W	01121	RCR07G6E1JS
R8	*****	1	R:FXD COMP 110 OHM 5% 1/4W	01121	RCR07G6E1JS
R9	*****	0	R:FXD COMP 180 OHM 5% 1/4W	01121	RCR07G1E1JS
R10	*****	0	R:FXD COMP 4.7K OHM 5% 1/4W	01121	RCR07G472JS
R11	*****	0	R:FXD COMP 4.7K OHM 5% 1/4W	01121	RCR07G472JS
R12	*****	0	R:FXD COMP 4.7K OHM 5% 1/4W	01121	RCR07G472JS
R13	*****	1	R:NOT USED	01121	RCR07G472JS
R14	*****	0	R:FXD COMP 4.7K OHM 5% 1/4W	01121	RCR07G472JS
R15	*****	1	R:NUT USED	01121	RCR07G472JS
TP7	*****	2	TEST JACK:WHITE:CYLINDRICAL	74970	105-CE51-001
TP8	*****	0	TEST JACK:WHITE:CYLINDRICAL	74970	105-CE51-001
U1	*****	5	IC:4-BIT BINARY COUNTER	C1295	SN7453N
U2	*****	0	IC:4-BIT BINARY COUNTER	C1295	SN7453N
U3	*****	0	IC:4-BIT BINARY COUNTER	C1295	SN7453N
U4	*****	0	IC:4-BIT BINARY COUNTER	C1295	SN7453N
U5	*****	0	IC:4-BIT BINARY COUNTER	C1295	SN7453N
U6	*****	5	IC:QUAD,2 INPUT NAND	C1295	SN7466N
U7	*****	1	IC:READ-OUT DISPLAY, SIGN	C7980	5082-73C4
U8	*****	3	IC:READ-OUT DISPLAY, NUMERICAL	C7980	5082-73C0
U9	*****	0	IC:READ-OUT DISPLAY, NUMERICAL	C7980	5082-73C0
U10	*****	0	IC:READ-OUT DISPLAY, NUMERICAL	C7980	5082-73C0
U11	*****	1	IC:DUAL, D-TYPE F/F	C1295	SN7474N
U12	*****	0	IC:QUAD,2 INPUT NAND	C1295	SN7466N
U13	*****	1	IC:DUAL,2-WIDE 2-INPUT OR-INVERT	C1295	SN7451N
U14	*****	1	IC:DUAL,J-K F/F	C1295	SN7476N
U15	*****	0	IC:QUAD,2-INPUT NAND	C1295	SN7466N
U16	*****	0	IC:QUAD,2-INPUT NAND	C1295	SN7466N
U17	*****	0	IC:QUAD,2-INPUT NAND	C1295	SN7466N
U18	*****	3	IC:SYN UP/DWN COUNTER	C1295	SN7415C
U19	*****	0	IC:SYN UP/DWN COUNTER	C1295	SN7415C

M. DESIG.	REF.	PEN-KEM P/N	QUAN./ ASSEM.	DESCRIPTION	MANUF.	MANUF. P/N
U20		*****	0	IC: SYN UP/DWN COUNTER	C1295	SN7415CN
U21		*****	1	IC: TRIPLE 3-INPUT NAND	C1295	SN741CN
U22		*****	1	IC: QUAD 2-INPUT EXCL.-OR	C1295	SN748CN
X1		*****	1	SOCKET 36 PIN	71279	703-3853-01-0316
		*****	1	BOARD ASSY: SWITCH- MODEL 400 ONLY	PENKM	
C1		*****	1	BOARD ASSY: MOTHER- MODEL 400 ONLY	PENKM	
C2		*****	1	C: FXD DUAL ELECT 10 UF 500VDCM	56289	TVL17C5
C4		*****	1	C: FXD DUAL ELECT 10 UF 450VDCM	56289	TVL2933
C5		*****	2	C: FXD ELECT 4000 UF 15VDCM	56289	TVL1173
C6		*****	0	C: FXD ELECT 4000 UF 15VDCM	56289	TVL1173
CR1		*****	1	C: FXD CER 1000 PF	55275	CK058X1C2
CR2		*****	2	DIODE: SI RECT.	01295	1N40C1
CR3		*****	0	DIODE: SI RECT.	01295	1N40C7
CR4		*****	4	DIODE: SI RECT.	01295	1N40C1
CR5		*****	0	DIODE: SI RECT.	01295	1N40G1
CR6		*****	0	DIODE: SI RECT.	01295	1N40C1
CR7		*****	0	DIODE: SI RECT.	01295	1N40C1
F1		*****	1	DIODE: ZENER 3.3V	01295	1N746
J1		*****	1	MICROFUSE 0.125A	75915	273-125
J5		*****	3	CONN: PC MOUNT J1 THRU J3	71785	252-22-30-240
K1		*****	2	JACK: BANANA J5 THRU J6	74970	108-C5C2-001
L1		*****	1	RELAY: HV REED	54696	M102VX-45
PS1		*****	1	L: CHOKE	81095	C-1X
R1		*****	1	PWR-SUPPLY DUAL 15VDC	33256	M100-15
R2		*****	1	R: FXD MET FLM 7.5K OHM 1% 1/8W	11502	RN60C1C1
R3		*****	1	R: FXD MET FLM 10 OHM 1% 1/8W	11502	RN60C1C0
R4		*****	1	R: FXD MET FLM 1K OHM 1% 1/8W	11502	RN60C1C1
R5		*****	1	R: NOT USED		
R6		*****	1	R: VAR COMP 10K OHM	01121	JAN2CCP1C3UA
R7		*****	1	R: NOT USED		
R8		*****	2	R: FXD MET FLM 100K OHM 1% 1/2W	11502	RN70C1C3
R9		*****	0	R: FXD MET FLM 100K OHM 1% 1/2W	11502	RN70C1C3
R10		*****	1	R: NOT USED		
R11		*****	1	R: NOT USED		
R12		*****	2	R: FXD COMP 100 OHM 5% 1/4W	01121	RCR07G1C1JS
R13		*****	1	R: FXD MET FLM 5.11K OHM 1% 1/8W	11502	RN60C5111
R14		*****	1	R: NOT USED		
R15		*****	5	R: FXD MET FLM 10K OHM 1% 1/8W	11502	RN60C1C2
R16		*****	5	R: VAR COMP 10K OHM	80294	3252N-1C3
R17		*****	0	R: VAR COMP 10K OHM	80294	3252N-1C3
R18		*****	0	R: VAR COMP 10K OHM	80294	3252N-1C3
R19		*****	0	R: FXD MET FLM 5.11K OHM 1% 1/8W	11502	RN60C5111
R20		*****	0	R: FXD MET FLM 10K OHM 1% 1/8W	11502	RN60C1C2
R21		*****	1	R: NOT USED		
R22		*****	6	R: FXD COMP 4.7K OHM 5% 1/4W	01121	RCR07G472JS
R23		*****	0	R: FXD COMP 4.7K OHM 5% 1/4W	01121	RCR07G472JS
R24		*****	0	R: FXD COMP 4.7K OHM 5% 1/4W	01121	RCR07G472JS
R25		*****	0	R: FXD MET FLM 10K OHM 1% 1/8W	11502	RN60C1C2
R26		*****	0	R: FXD MET FLM 10K OHM 1% 1/8W	11502	RN60C1C2
		*****	1	R: FXD MET FLM 33.2K OHM 1% 1/8W	11502	RN60C3322

M. REF. DESIG.	P/N-KEM P/N	QUAN./ ASSEMB.	DESCRIPTION	MANUF.	MANUF. P/N
R27	*****	0	R:FXD COMP 4.7K OHM 5% 1/4W	C1121	RCR07G472JS
R28	*****	0	R:FXD COMP 4.7K OHM 5% 1/4W	01121	RCR07G472JS
R29	*****	0	R:FXD MET FLM 10K OHM 1% 1/8W	11502	RN60C1CC2
R30	*****	1	R:FXD MET FLM 15K OHM 1% 1/8W	11502	RN60C15C2
R31	*****	1	P:FXD MET FLM 3.4K OHM 1% 1/8W	11502	RN60C34C1
R32	*****	0	R:VAR COMP 10K OHM	80294	32524-1C3
R33	*****	1	R:FXD MET FLM 20K OHM 1% 1/8W	11502	RN60C2CC2
R34	*****	1	R:FXD COMP 200K OHM 5% 2W	01121	RCR42G2C4JS
R35	*****	1	R:FXD MET FLM 12.1K OHM 1% 1/8W	11502	RN60C1212
R36	*****	0	R:FXD COMP 4.7K OHM 5% 1/4W	01121	RCR07G472JS
R37	*****	0	R:VAR COMP 10K OHM	80294	32524-1C3
S1	*****	1	SWITCH: PC MOUNT	88818	T8201
SPKR1	*****	1	SPEAKER:2"DIA. 8 OHM	C3508	S2-202
T1	*****	1	X-FORMER HV	08779	PC-12C-35
U1	*****	2	IC:QUAD.2-INPUT NAND	C1295	SN74CCN
L2	*****	0	IC:QUAD.2-INPUT NAND	C1295	SN74CCN
L3	*****	1	IC:LIN CP AMP	01295	LM741CN
XFI	*****	1	MICROFUSE HCLCER	75915	2810C1
C1	51C17-CC00C	1	CHASSIS ASSY:ELECTRONICS	PENKM	CSR13EE65
C2	*****	1	C:FXD TA 6.8 UF	56289	P8292ZM11
F1	*****	1	C:FXD PAPER 0.25 UF	00656	3130C1
F1	*****	1	FUSE.1 AMP SLC-BLC: MODEL 102	75915	313.5CC
R1	*****	1	FUSE.1/2 AMP SLC-BLC: MODEL 102A	75915	WW10C
T1	*****	1	R:VAR WW 10 OHM 5W	71590	RT201
T2	*****	1	POWER TRANSFORMER	STANC	171
U1	*****	1	AUTO TRANSFORMER	83008	LM305K
LAS1	*****	1	IC:5V SUPPLY	12040	133P MODIFIED
MP	51131-CC00C	1	ASSY:LASER	PENKM	
MP	51C3E-C0000	2	SUPPORT:LASER	PENKM	
MP	51132-CC00C	1	ASSY:LASER OPTICS,MODEL 400 ONLY	PENKM	
MP	51134-CC000	1	RIGHT ANGLE DRIVE,MODIFIED	PENKM	
MP	51133-CC00C	1	PRISM:6 HUB :VERT. HEIGHT ACJ.	PENKM	
A1	5112C-CC00C	1	CAM:PRISM	PENKM	
MS1	511C4-CC000	1	SUBASSY:LASER TELESCOPE	PENKM	
MP	51125-CC00C	1	ASSY:MICROSCOPE,MODEL 400	PENKM	
MP	*****	1	MICROSCOPE STAND "SU"	11451	77507
MP	*****	1	EXT. TUBE 15MM	11451	75276
MP	*****	1	OBJECTIVE LENS 20X 1.4 NA	11451	77800
MP	*****	1	OBJECTIVE NOSE PLUGS	11451	77702
PH1	*****	1	BINOULAR HEAD	11451	7775C
MP	*****	1	EYEPIECE 1-PAIR 10X	11451	7785E
MP	*****	1	KETICLE 0.5MP FOR LEFT EYEPIECE	57157	30073
DS1	51C8E-CC000	1	ASSY:GALVO MODULE,MODEL 400	PENKM	
MP	51C77-CC00C	1	ASSY:AUTOMATIC TRANSFER STAGE	PENKM	
MP	*****	1	LAMP:SUBSTAGE	SPARK	L1004
MP	*****	4	LUER CONN. MALE	FAMVL	30826
YP	51C62-CC00C	1	CONNECTOR CLAMP	PENKM	
MP	51C66-CC00C	1	ASSY:CELL, MODEL 400 ONLY	PENKM	
MP	51C67-CC00C	1	CHAMBER:ANGDE	PENKM	

REF. DESIG.	PLAN-KEM P/N	QUAN./ ASSEM.	DESCRIPTION	MANUF.	MANUF. P/N
MP	51068-CC000	1	CHAMBER: CATH.	PENKM	
MP	51069-CC000	1	ELECTRUCDE: ANCCD	PENKM	
MP	51070-CC000	1	ELECTRUCDE: CATHODE	PENKM	
MP	51071-CC000	1	CELL CHANNEL: TCP	PENKM	
MP	51072-CC000	1	CELL CHANNEL: MIDDLE	PENKM	
MP	51073-CC000	1	CELL CHANNEL: BOTTOM	PENKM	
MP	51074-CC000	1	BASE PLATE: DELRIN	PENKM	
MP	51075-CC000	2	PLUG: BRASS	PENKM	
MP	51076-CC000	1	PRESSURE PLATE	PENKM	
MP	*****	2	G-RING 1/4 ID 1/200	07060	2-202
MP	*****	2	G-RING 1/16 ID 1/1800	07060	2-022
MP	*****	2	JACK: TIP	83330	124
MP	*****	2	CONN: LUER MALE	FAMVL	30826
MP	*****	1	PIN: S-5	WBERG	52-15
MP	51136-CC000	1	FILTER: SUBSTAGE ILLUMINATION	PENKM	
MP	51056-CC000	1	HOLD DOWN BRACKET	PENKM	
MP	*****	1	SUBSTAGE ILLUMINATOR	77911	77507
MP	*****	1	LINE CURD	16428	17258
MP	*****	1	T: TAPPED	08779	0F112
MP	51044-40000	1	ASSY: INSTRUMENT CASE	PENKM	
MP	51044-40000	1	COVER: FIBREGLOSS	STF8G	
A1	51151-CC000	1	ACCESSORIES: MDEL400	PENKM	
A2	51063-CC000	1	ASSY: THERMISTOR	PENKM	
A3	51139-CC000	1	ASSY: PUMP, BULB W HOSE AND FITTING	PENKM	
A4	51141-CC000	1	ASSY: TUBING 7-3 FOOT LENGTHS	PENKM	
A5	*****	1	ASSY: SYRINGE- 50 ML	PENKM	
A5	51140-CC000	1	ASSY: DRAIN 18" PVC WITH FITTING	PENKM	
A5	*****	3	ADAPTER: SYRINGE	THOMA	8960-D2C
A6	51152-CC000	1	TEST CULLOID	PENKM	
A7	51153-CC000	1	CELL CLEANER	PENKM	
A8	51138-CC000	1	MANUAL: OPERATING MODEL 400	PENKM	
A8MP	*****	1	CIVIDERS		
A8MP	*****	1	BINULER: 3 RING	FAMVL	16801
MP	*****	1	STOPPER: LUER		
MP	*****	1	CLEANER: ELECTRODE, TWINKLE	FAMVL	86505
MP	*****	2	HOSE TEFLON : 6 INCH- LUER FITTINGS	FAMVL	
MP	*****	1	COVER: MICRSCCPE	11451	
MP	*****	1	NOT USED		
MP	51056-CC000	1	ASSY: AUTOMATIC TRANSFER MODULE	PENKM	
MP	51055-CC000	1	MANIFOLD: MAIN	PENKM	
MP	51103-CC000	1	PANEL: FRONT MCD	PENKM	
MP	51115-CC000	1	CASE: MOD BUD	PENKM	
MP	51123-CC000	1	BRACKET: HOSE	PENKM	
MP	*****	1	VALVE: 4WAY DIST	FAMVL	86414
MP	*****	1	VALVE: 4WAY 2ADJ	FAMVL	86410
S1	*****	1	SWITCH: POWER	09353	7101-J4-ZQE-2
M1	*****	1	LAMP: INDICATOR	55263	1919
MP	*****	1	MOTOR-GEARBOX	BARNA	7543-50
MP	*****	1	PUMP HEAD	BARNA	7017-20
XFI	*****	1	HOLDER: FUSE	75915	345001



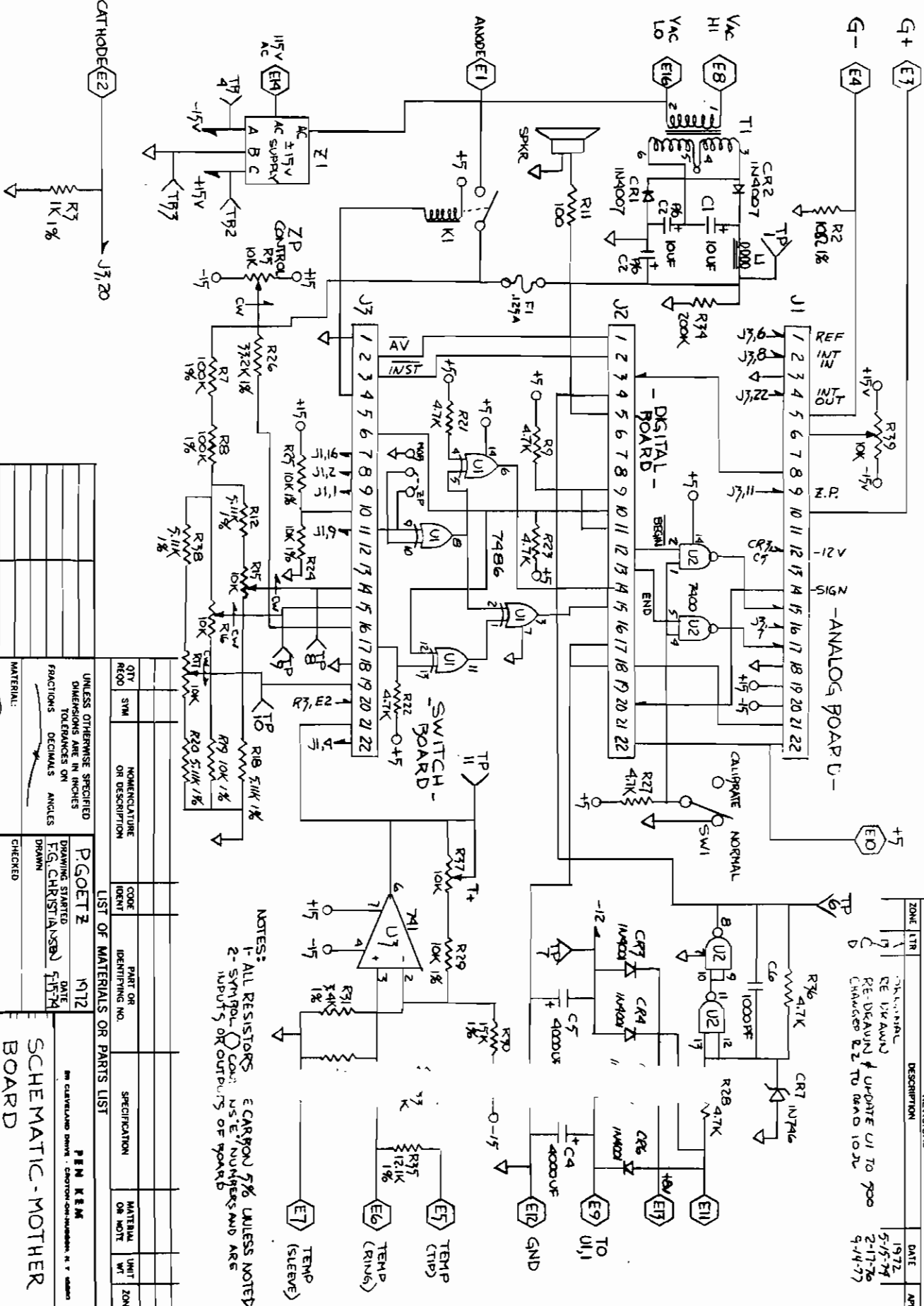
M. REF. DESIG.	PEN-KEM P/N	QUAN./ ASSEM.	DESCRIPTION	MANUF.	MANUF. P/N
F1	*****	1	FUSE:SLC BLC .75 AMP (220 V)	75915	313.75C
F1	*****	1	FUSE:SLC BLC 1.5 AMP (115 V)	75915	31301.5
T1	*****	1	TRANSFORMER:TAPPED	08779	0F112
MP	*****	16	NUTS:TEFLON TFE	GENVL	5-1-125-2
MP	*****	16	FERRULE:TEFLCN	GENVL	6-1-C62-2
MP	*****	7	CONN:MALE LUER	FANVL	30826
MP	*****	2	TERMINAL:TEFLCN	CARLC	003-5761
AP	*****	2	JUMPER:TERMINAL	KULKA	600-J
MP	*****	1	TUBING:TFE .125 ID -10.5 FT	GENVL	.125X.016 WALL
MP	*****	8	FEET:PLASTIC	8333C	2183
MP	*****	2	FITTING:BULKHEAD	GENVL	13-6
MP	*****	2	CLAMP:HOSE -NAPA-BELKAMP	NAPAB	4-454C
MP	*****	1	PIN:MALE GUIDE	00779	2003E5-2
MP	*****	1	PIN:FEMALE GUIDE	00779	20C35C-2
MP	*****	2	CATCH:LOCKING SPRING	00779	201922-1
MP	*****	3	CONTACT:MALE CRIMP	00779	66103-3
MP	*****	14	TERMINAL RING	00779	3188E
MP	*****	1	LINE COND:MOGULE	16428	1725CC
MP	*****	1	MISC. PARTS	PENKM	
	*****	1	MODEL 400: COMPLETE SYSTEM	PENKM	

# MANUFACTURERS CODE LIST

00656 AEROVOX CORP, 740 BELLEVILLE AVE, NEW BEDFORD, MASS 02741  
 00779 AMP INC, 155 PARK ST, ELIZABETHTOWN, PA 17022  
 01121 ALLEN-BRADLEY CO, 1201 2ND ST, S MILWAUKEE, WIS 53204  
 01295 TEXAS INSTRUMENTS INC, 13500 N CENTRAL EXPRESSWAY, DALLAS, TEXAS 75231  
 02660 AMPHENOL CONNECTOR, DIV, 2801 S 25TH AVE, BROADVIEW, ILL 60153  
 03508 GE, SEMI-CONDUCTOR PRODUCTS DEPT, ELECTRONICS PARK, SYRACUSE, NY 13201  
 04713 MOTOROLA, SEMICONDUCTOR PRODUCTS DIV, PHOENIX AZ  
 05668 COLE PALMER, 7425 N OAK PARK AVE, CHICAGO, ILL 60648  
 06383 PANDUIT CORP, 17301 RIDGELAND AVE, TINLEY PARK, ILL 60477  
 07060 C.E. CONOVER, 333 PASSAIC AVE, FAIRFIELD, NJ 07006  
 07980 HEWLETT-PACKARD, GREEN POND RD, ROCKAWAY, NJ 07866  
 08779 SIGNAL TRANSFORMER, 1 JUNIUS ST, BROOKLIN, NY 11212  
 09023 CORNELL-DUBILIER ELECTRONICS, DALRYMPLE ST, SANFORD, NC 27330  
 09353 C&K COMPONENTS INC, 103 MORSE ST, WATERTOWN, MASS 02172  
 11451 NIKON INC., INSTRUMENT DIV., 623 STEWART AVE, GARDEN CITY, NY 11530  
 11502 TRW ELECTRONICS COMPONENTS, IRC BOONE DIV, BOONE, NC  
 12040 NATIONAL SEMI-CONDUCTOR CORP, PO BOX 443, COMMERCE GR, DANBURY, CT 06810  
 14674 CORNING GLASS WORKS, CORNING, NY  
 16428 BELDON ELECTRONIC DIV, PO BOX 1100, RICHMOND, IND 47374  
 18324 SIGNETICS CORP, 811 E ARGUE AVE, SUNNYVALE, CA 94086  
 21033 SPECTRA PHYSICS INC, 1250 W MIDDLEFIELD RD, MOUNTAIN VIEW, CA 94042  
 24353 KLINGER SCIENTIFIC CORP, 8345 PARSONS BLVD, JAMACA, NY 11432  
 24595 BUD RADIO CORP, 870 NORTH 20TH ST, COLUMBUS, OHIO 43219  
 33256 HYBRID SYSTEM CORP, 87 2ND AVE, BURLINGTON, MASS 01803  
 35643 LEITZ OPTO-METRIC TOOLS, INC, ROCKLEIGH IND CT, ROCKLEIGH, NJ 07647  
 49956 RAYTHEON CO, 141 SPRING ST, LEXINGTON, MASS 02173  
 56289 SPRAGUE ELECTRIC CO, NORTH ADAMS, MASS  
 60437 TOWER MANUFACTURING J.H. (IRON WORKS), 145 PINE ST, PROVIDENCE, RI 02903  
 71279 CAMBRIDGE THERMIONIC CORP, 445 CONCORD AVE, CAMBRIDGE, MASS 02138  
 71590 CENTRALAB ELECTRONICS, 5757 N GREEN BAY AVE, MILWAUKEE, WIS 53201  
 71785 CINCH MFG CO, H B JONES DIV, 1026 S HOMAN AVE, CHICAGO, ILL 60634  
 72136 ELMENCO, WILLIMANTIC, CONN 06226  
 72653 G.C. ELECTRONICS, DIV OF HYDROMETALS INC, 400 S WYMAN ST, ROCKFORD, ILL 61101  
 72928 GUDEMAN CORP, 340 W HURON ST, CHICAGO, ILL 60610  
 74970 E.F. JOHNSON CO, 299 10TH AVE SW, WASECA, MINN 56093  
 75915 LITTLEFUSE INC, 800 E NORTHWEST HWY, DES PLAINES, ILL 60016  
 79963 ZIERICK MFG CO, RADIO CIRCLE, MT KISCO, NY 10549  
 80223 U.T.C., 150 VARICK ST, NYC, NY 10013  
 80294 BURNS INC, 1200 COLUMBIA AVE, RIVERSIDE, CA 92507  
 81095 TRIAD-UTRAD, DIV OF LITTON SYSTEMS, VENICE, CA  
 82389 SWITCHCRAFT, 5555 ELSTON AVE, CHICAGO, ILL 60630  
 83008 STACO INC, 2240 E 3RD ST, DAYTON, OHIO 45403  
 83330 H.F. SMITH INC, 812 SNEDIKER AVE, BROOKLYN, NY 11207  
 88818 SINGER CO, KEARFOOT DIV, MACBRIDE AVE, LITTLE FALLS, NJ 07424  
 91637 DALE ELECTRONICS, COLUMBUS DIV, 1376 28TH AVE, COLUMBUS, NEB 68601  
 91929 HUNNEYWELL INC, MICRO-SWITCH DIV, CHICAGO & SPRING STS, FREEPORT, ILL 61032  
 92194 ALPHA (WIRE CORP), 711 LIEGERSWOOD AVE, ELIZABETH, NJ 07207  
 94696 MAGNACRAFT ELECTRIC CO, 5575 W LYNCH AVE, CHICAGO ILL 60630  
 95263 LEECRAFT MFG CO INC, 21-16 44TH RD, LONG ISLAND CITY, NY 11101  
 95275 VITRAMON INC, BOX 544, BRIDGEPORT, CONN 06601  
 97197 EDMUND SCIENTIFIC, 300 EDSCORP BLDG, BARRINGTON, NJ 08007  
 97794 YELLOW SPRINGS INSTRUMENTS, BOX 279, YELLOW SPRINGS, OHIO 45387  
 98291 SEAELECTRO CORP, 225 HOYT ST, MAMARONECK, NY 10544  
 99813 JAN HARDWARE MFG CO, 47-27 36ST, LI CITY, NY 11101  
 ACTPA ACTIVE & PASSIVE CO, 6 AERIAL WAY, SYOSSET, N.Y. 11791  
 ANGAR ANGAR SCIENTIFIC, 131 HARRISON AVE, ROSELAND, NJ 07068

BARNA BARNANT CORP., P.O. BOX 510, BARRINGTON, ILL 60010  
BLOCK BLOCKSOM  
BRANS BRANSON INSTRUMENTS CO., PROGRESS DRIVE, STAMFORD, CONN. 06904  
CARLC CARLAC, 75 ORVILLE DRIVE, BOHEMIA, N.Y. 11716  
GCELE G.C. ELECTRONICS CO., 400 S. WYMAN, ROCKFORD, ILL. 61101  
GENVL GENERAL VALVE CO. 110 RT 10, BOX 272, E HANOVER, NJ 07936  
GENSC GENERAL SCANNING INC, 80 COLIDGE HILL RD, WATERTOWN, MASS 02172  
GRIFF GRIFFITH PLASTICS, 1027, CALIF. DRIVE, BURLINGAME, CA. 94010  
HAMVL HAMILTON VALVES CO, PO 7500, RENO, NA 89502  
KULKA KULKA ELECTRIC CORP, MT VERNON, NY 10551  
MODPL MODERN PLASTICS, 678 HOWARD ST, BRIDGEPORT, CONN 06601  
PENKM PEN KEM, 211 CLEVELAND DR, CROTON-ON-HUDSON, NY 10520  
PRECL PRECISION CELLS, 560 S. BROADWAY, HICKSVILLE, N.Y. 11801  
S.O.S  
SPARK A.C. SPARK, DIV. GEN. MOTORS  
STANC STANCOR DIV, % ESSEX INT'L, 3501 W ADDISON ST, CHICAGO ILL  
TUFTS LAWRENCE TUFTS CO INC, WOODSIDE AVE, BRIARCLIFF MNR, NY 10510  
WBERG W.M. BERG INC, 449 OCEAN AVE, E ROCKAWAY, NY 11518

REVISIONS			DATE	APPROVED
ZONE	TR	DESCRIPTION		
1	1	ORIGINAL	1972	
2	2	RE-DESIGNED & UPDATE U1 TO 700	5-15-74	
3	3	RE-DESIGNED & UPDATE U1 TO 700	2-17-76	
4	4	CHANGED R22 TO 100K	9-14-77	



CATHODE E2

J3, 20

K1

Z1

AC ±15V

AC SUPPLY

A B C

TR2

TR7

R7

1K 1%

J3, 20

K1

Z1

AC ±15V

AC SUPPLY

A B C

TR2

TR7

R7

1K 1%

J3, 20

K1

Z1

AC ±15V

AC SUPPLY

A B C

TR2

TR7

R7

1K 1%

J3, 20

K1

Z1

AC ±15V

AC SUPPLY

A B C

TR2

TR7

R7

1K 1%

J3, 20

K1

Z1

AC ±15V

AC SUPPLY

A B C

TR2

TR7

R7

1K 1%

J3, 20

K1

Z1

AC ±15V

AC SUPPLY

A B C

TR2

TR7

R7

1K 1%

J3, 20

K1

Z1

AC ±15V

AC SUPPLY

A B C

TR2

TR7

R7

1K 1%

J3, 20

K1

Z1

AC ±15V

AC SUPPLY

A B C

TR2

TR7

R7

1K 1%

J3, 20

K1

Z1

AC ±15V

AC SUPPLY

A B C

TR2

TR7

R7

1K 1%

J3, 20

K1

Z1

AC ±15V

AC SUPPLY

A B C

TR2

TR7

R7

1K 1%

J3, 20

K1

Z1

AC ±15V

AC SUPPLY

A B C

TR2

TR7

R7

1K 1%

J3, 20

K1

Z1

AC ±15V

AC SUPPLY

A B C

TR2

TR7

R7

1K 1%

J3, 20

K1

Z1

AC ±15V

AC SUPPLY

A B C

TR2

TR7

R7

1K 1%

J3, 20

K1

Z1

AC ±15V

AC SUPPLY

A B C

TR2

TR7

R7

1K 1%

J3, 20

K1

Z1

AC ±15V

AC SUPPLY

A B C

TR2

TR7

R7

1K 1%

J3, 20

K1

Z1

AC ±15V

AC SUPPLY

A B C

TR2

TR7

R7

1K 1%

J3, 20

K1

Z1

AC ±15V

AC SUPPLY

A B C

TR2

TR7

R7

1K 1%

J3, 20

K1

Z1

AC ±15V

AC SUPPLY

A B C

TR2

TR7

R7

1K 1%

J3, 20

K1

Z1

AC ±15V

AC SUPPLY

A B C

TR2

TR7

R7

1K 1%

J3, 20

K1

Z1

AC ±15V

AC SUPPLY

A B C

TR2

TR7

R7

1K 1%

J3, 20

K1

Z1

AC ±15V

AC SUPPLY

A B C

TR2

TR7

R7

1K 1%

J3, 20

K1

Z1

AC ±15V

AC SUPPLY

A B C

TR2

TR7

R7

1K 1%

J3, 20

K1

Z1

AC ±15V

AC SUPPLY

A B C

TR2

TR7

R7

1K 1%

J3, 20

K1

Z1

AC ±15V

AC SUPPLY

A B C

TR2

TR7

R7

1K 1%

J3, 20

K1

Z1

AC ±15V

AC SUPPLY

A B C

TR2

TR7

R7

1K 1%

J3, 20

K1

Z1

AC ±15V

AC SUPPLY

A B C

TR2

TR7

R7

1K 1%

J3, 20

K1

Z1

AC ±15V

AC SUPPLY

A B C

TR2

TR7

R7

1K 1%

J3, 20

K1

Z1

AC ±15V

AC SUPPLY

A B C

TR2

TR7

R7

1K 1%

J3, 20

K1

Z1

AC ±15V

AC SUPPLY

A B C

TR2

TR7

R7

1K 1%

J3, 20

K1

Z1

AC ±15V

AC SUPPLY

A B C

TR2

TR7

R7

1K 1%

J3, 20

K1

Z1

AC ±15V

AC SUPPLY

A B C

TR2

TR7

R7

1K 1%

J3, 20

K1

Z1

AC ±15V

AC SUPPLY

A B C

TR2

TR7

R7

1K 1%

J3, 20

K1

Z1

AC ±15V

AC SUPPLY

A B C

TR2

TR7

R7

1K 1%

J3, 20

K1

Z1

AC ±15V

AC SUPPLY

A B C

TR2

TR7

R7

1K 1%

J3, 20

K1

Z1

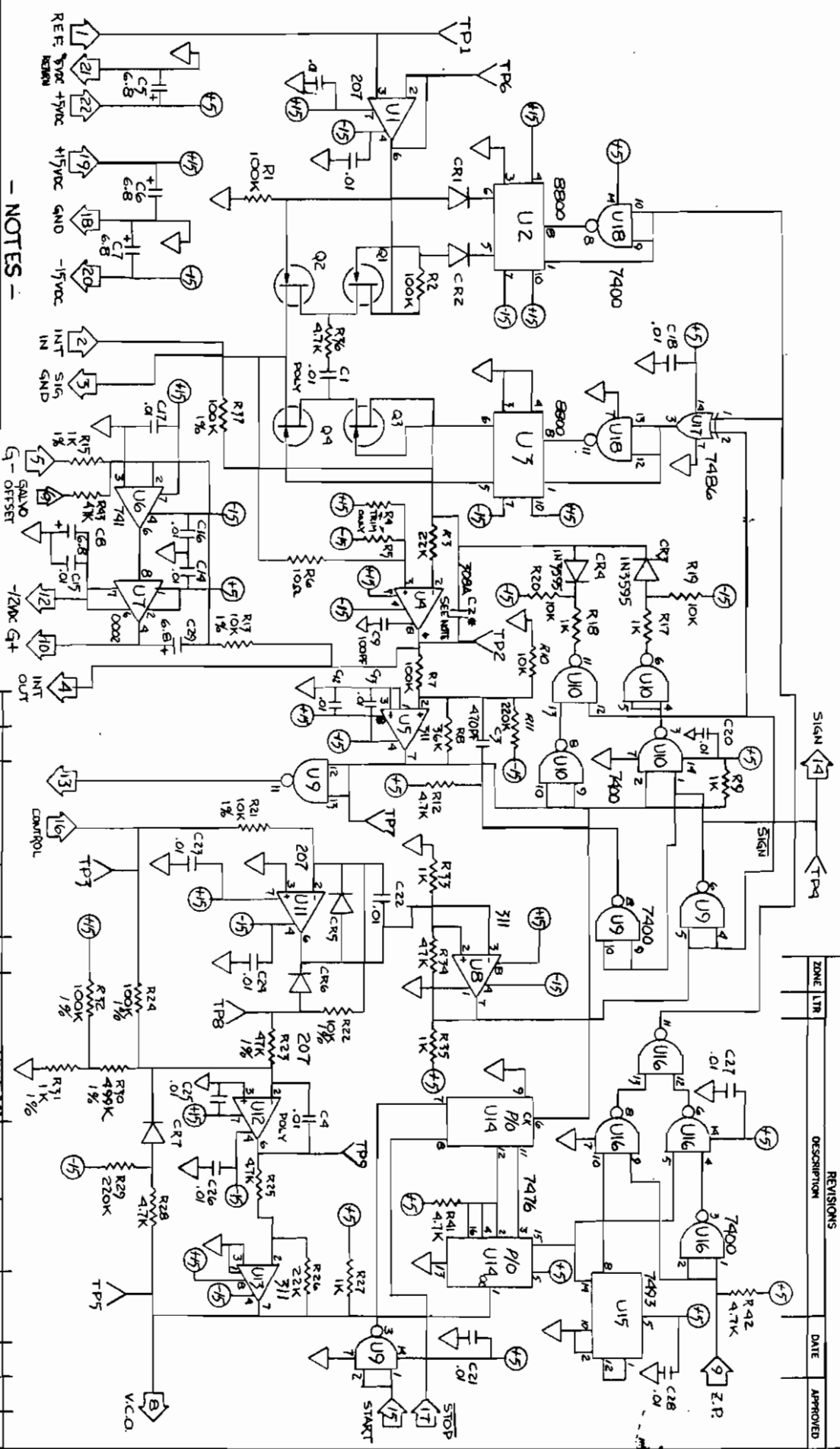
AC ±15V

AC SUPPLY




A B C

TR2



TR7



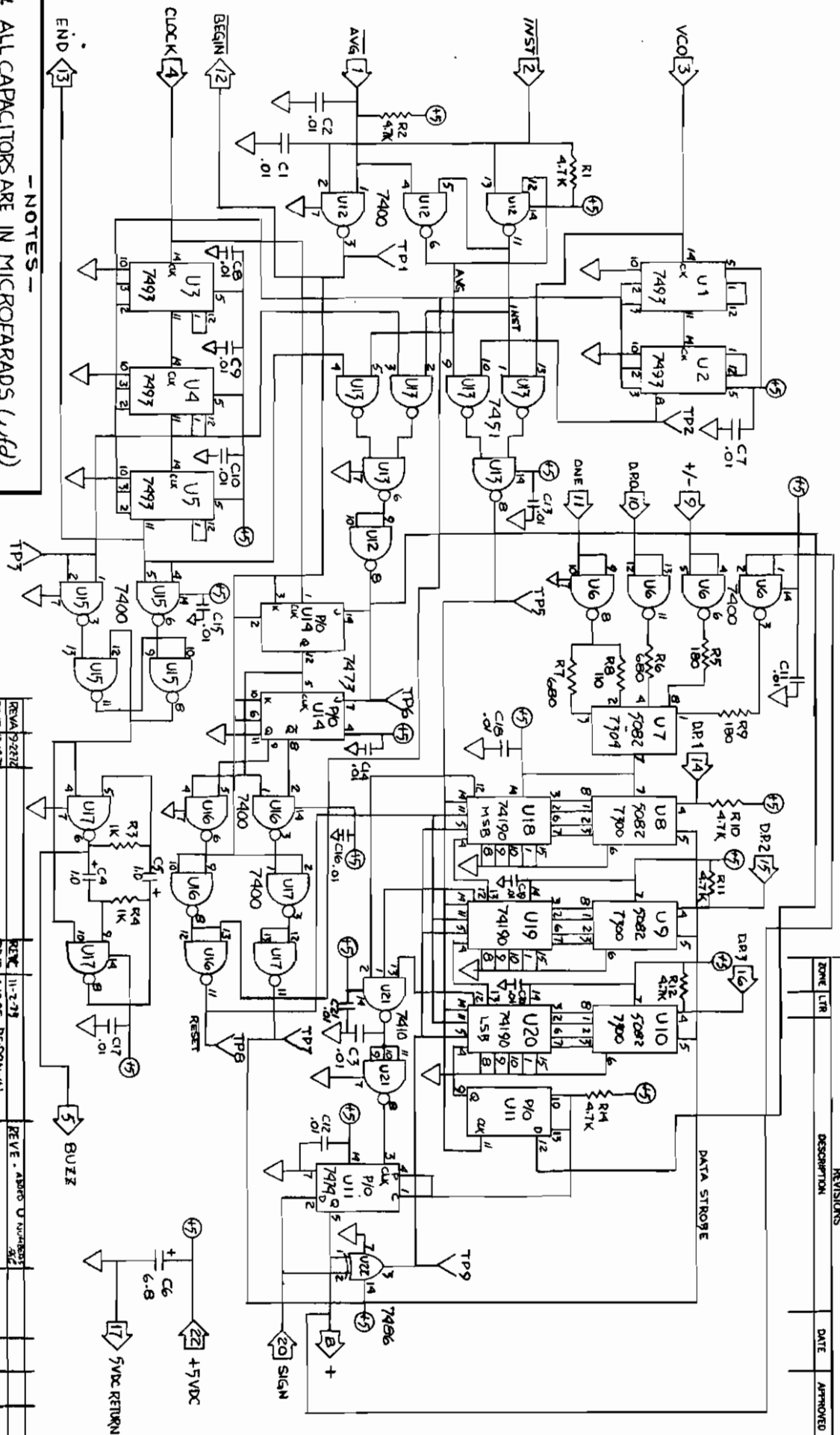
## - NOTES -

- 1. ALL RESISTORS ARE 5% CARBON, UNLESS NOTED
- 2. ALL CAPACITORS ARE IN MICROFARADS (ufd)
- 3. ALL DIODES ARE IN 914, UNLESS NOTED
- 4. ALL TRANSISTORS ARE 2N4857
- \*5. CAPACITOR C2 - BOARD P/N 51001-000 = 5.0ufd ONLY  
BOARD P/N 51001-400 = 2.5ufd ONLY
- 6. SYMBOL -  = INDICATES CONNECTOR PIN NUMBER  
\$ DIRECTION OF SIGNAL FLOW
- 7. SYMBOL -  = INDICATES DEVICE CONNECTION  
TO POWER SOURCE
- 8. SYMBOL -  = INDICATES DEVICE CONNECTION  
TO POWER RETURN BUSS

[illegible]



UNLESS OTHERWISE SPECIFIED DIMENSIONS ARE IN INCHES TOLERANCES ON FRACTIONS      DECIMALS      ANGLES	P. GOETZ	7-72
DRAWING STARTED BY E. G. CHRISTIANSEN 4-18-72	CHECKED	DATE
DRAWN	ENGR	
MATERIAL:		
		
FINISH		
		

P E N K E M	
RM QUARTERMASTER PRINTS - CROFTON-OR-AMERICAN, N. Y. 10040	
SCHEMATIC DIAGRAM	
ANALOG BOARD	
SIZE	CODE IDENT NO.
C	51004
SCALE	REV G
	SHEET



- NOTES -**
1. ALL CAPACITORS ARE IN MICROFARADS ( $\mu f$ )
  2. ALL RESISTORS ARE IN OHMS UNLESS NOTED
  3. SYMBOL - [D] = INDICATES CONNECTOR PIN NUMBER  
                   $f^{\circ}$  DIRECTION OF SIGNAL FLOW.
  4. SYMBOL - ⊕ = INDICATES DEVICE CONNECTION  
                     TO +5VDC POWER BUSS
  5. SYMBOL ∇ = INDICATES DEVICE CONNECTION  
                     TO 5VDC RETURN BUSS
  6. MICRO-CIRCUIT PIN LAYOUT-AS VIEWED FROM  
COMPONENT SIDE :     pin1(9)                  pin8(6)

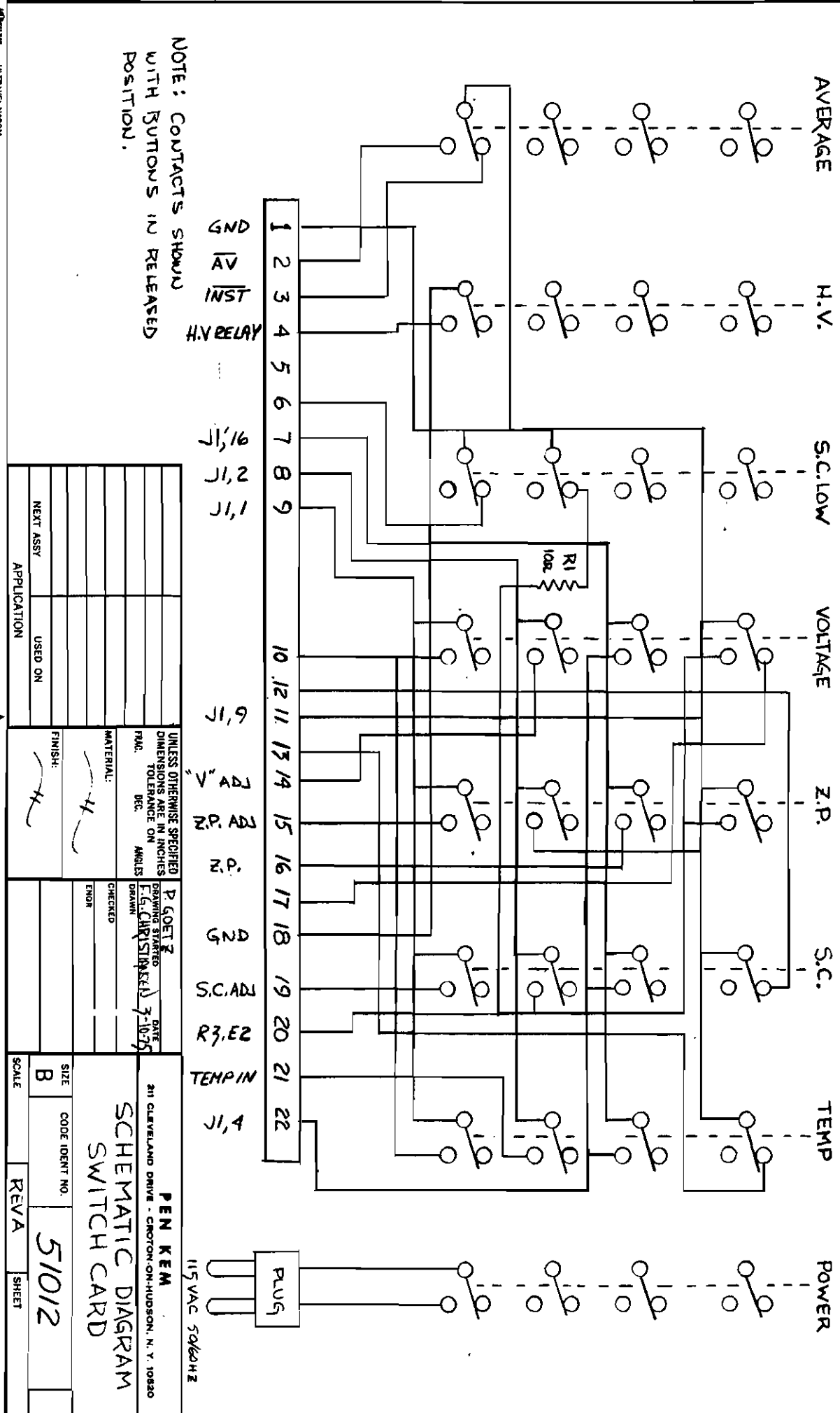
[illegible]

<p>FINISH:</p> 	<p>MATERIAL:</p> 
<p>UNLESS OTHERWISE SPECIFIED DIMENSIONS ARE IN INCHES TOLERANCES ON</p>	<p>FRACTIONS DECIMALS ANGLES</p>

P. GOETZ	9/22/77
DEAWMA, PART D	DATE
F.S. CHRYSLER 800	4/11/77
DEAWMA	
CHECKED	
ENGR	

PEN KEM		80 CALVIN AND GROVE - CROFTON-OR-FARMINGTON, N. Y. 12055	
SCHEMATIC DIAGRAM			
DIGITAL BOARD			
SIZE	CODE	IDENT NO.	
C			51008
SCALE		REV E	SHEET 1 OF 1

REVISIONS			
ZONE	LTR	DESCRIPTION	DATE
REV A	REPLACED	3-10-75	JAC



NOTE: CONTACTS SHOWN WITH BUTTONS IN RELEASED POSITION.

UNLESS OTHERWISE SPECIFIED DIMENSIONS ARE IN INCHES TOLERANCE ON FRACTIONS DECIMALS ANGLES		P. GOETZ DRAWING STARTED E.G. CHRISTENSEN DATE 3-10-75		PEN KEM 211 CLEVELAND DRIVE - CROTON-ON-HUDSON, N. Y. 10820	
MATERIAL:		CHECKED		SCHEMATIC DIAGRAM SWITCH CARD	
FINISH:		ENDR		CODE IDENT NO. 51012	
NEXT ASSY		USED ON		SCALE B	
APPLICATION				REV A SHEET	

ULTRAVEL M8800  
BOSTON, MASS 02111  
MADE IN U.S.A.

SIZE	CODE	IDENT NO.	51020
C			
SCALE		REVA	SHEET